

Performance of Multi-Phase Passive Control Systems in Steel Structures

by

Basima O. Abdulrahman

A thesis submitted to the Graduate Faculty of
Auburn University
in partial fulfillment of the
requirements for the Degree of
Master of Science

Auburn, Alabama
December 13th, 2014

Keywords: multi-phase system, seismic, design, analysis,
gap element, buckling-restrained brace (BRB)

Copyright 2014 by Basima O. Abdulrahman

Approved by

Justin D. Marshall, Chair, Associate Professor of Civil Engineering
Mary L. Hughes, Lecturer of Civil Engineering
James S. Davidson, Professor of Civil Engineering

Abstract

Earthquake resistant buildings can experience significant damage during an event. A multi-phase passive control system (MPCS) was developed to reduce structural damage, repair costs, and downtime of buildings subjected to large earthquakes by limiting the main damage to the replaceable elements. Previous research investigated multi-phase behavior in single degree of freedom (SDOF) systems to identify the factors affecting structural response. An overall improvement has been detected by the multi-phase system when compared to a baseline system consisting of a dual lateral force resisting system.

In this study, the multi-phase system was implemented in a multi degree of freedom (MDOF) model. The multi-phase behavior is created by adding a gap element with multilinear elastic properties to a dual system that consists of a moment frame and buckling-restrained braced frame. The gap element has a lock-out mechanism that creates a transition phase when the slip displacement is reached. After the gap locks out, the buckling restrained braces (BRB) will become effective. The transition phase created by the gap allows the buckling restrained braces (BRBs) to yield before the moment frame because the BRBs are replaceable and easier to replace.

Dynamic response history analyses of 3-story and 6-story steel frames were performed for a suite of scaled ground motions. The comparison between the multi-phase systems and the baseline systems was based on the story drift, story accelerations, moment frame plastic hinge rotation, and cumulative BRB ductility response. Superior behavior was achieved by the multi-phase system on certain aspects.

Acknowledgment

I would like to express my gratitude to my supervisor, Dr. Justin Marshall, whose expertise, understanding, and patience, added considerably to my graduate experience. I appreciate his vast knowledge, skill, and assistance in writing the thesis. I would like to thank the rest of my faculty committee, Dr. Mary Hughes and Dr. James Davidson for the assistance they provided at all levels. Appreciation also goes out to Zhongliang Xie for his technical assistance and the time he devoted helping in Perform 3D modeling.

A very special thanks goes out to my family for the support they provided me through my entire life. Without their encouragement I would not have reached this point. I am also grateful to my friends; their guidance and friendship was vital to me. You helped me work my way during my time in Auburn.

Finally, I would also like to thank all my fellow graduate students, the faculty members, and staff in the Civil Engineering Department for their assistance, cooperation, and experience; they really made my stay in Auburn one I'll always remember.

Table of Contents

Abstract.....	ii
Acknowledgment.....	iv
List of Tables.....	ix
List of Figures.....	x
Chapter 1: Introduction.....	1
1.1 Defining the Problem.....	1
1.2 The Proposed Solution.....	2
1.3 Scope and Approach.....	3
1.4 Thesis Organization.....	4
Chapter 2: Background and Literature Review.....	6
2.1 Introduction.....	6
2.2 Seismic Isolation.....	9
2.2.1 Elastomeric Bearings.....	10
2.2.2 Lead Rubber Bearings (LRB).....	11
2.2.3 Friction Pendulum Systems (FPS).....	11
2.2.4 The Double Concave Friction Pendulum (DCFP).....	12

2.2.5 Triple Friction Pendulum (TFP)	13
2.2.6 Combined Elastomeric and Sliding Bearings	14
2.2.7 Sliding Bearings with Restoring Force	15
2.3 Passive Energy Dissipation Systems	16
2.3.1 Metallic Dampers	16
2.3.2 Friction Dampers	21
2.3.3 Viscoelastic Solid Dampers	25
2.3.4 Viscoelastic or Viscous Fluid Dampers	25
2.3.5 Tuned Mass Dampers	27
2.3.6 Tuned Liquid Dampers	28
2.3.7 Smart Materials	29
2.4 Semi-active and Active Systems	30
2.4.1 Active Bracing Systems (ABS)	32
2.4.2 Active Mass Dampers	35
2.4.3 Variable Stiffness and Damping Systems	36
2.5 Combination of Structural Control Systems	38
2.6 Summary	50
Chapter 3: Parametric Study of Multi-Phase Systems	52
3.1 Introduction	52
3.2 Prototype Buildings	53

3.3 Seismic Design.....	54
3.3.1 Local Seismicity.....	54
3.3.2 Equivalent Lateral Force (ELF) Procedure.....	55
3.4 Scaled Ground Motions	56
3.5 System Configurations.....	58
3.5.1 Moment Frame and Braced Frame Strength Ratios.....	58
3.5.2 Gap Sizes	59
3.5.3 Hazard Levels	60
3.6 Baseline Systems	61
3.7 System Combinations	62
3.8 Summary.....	64
Chapter 4: Structure Design and Modeling	65
4.1 Introduction.....	65
4.2 Prototype Design Procedure	65
4.2.1 Moment Frame Elements Design Approach.....	67
4.2.2 BRB Elements Design Approach.....	68
4.2.3 Moment Frame Connections Design	69
4.3 Drift Check.....	69
4.4 Final Prototype Building.....	70
4.5 Finite Element Modeling	73

4.5.1 Moment Frame Elements Modeling	73
4.5.2 BRB Elements Modeling	75
4.5.3 Gap Element Modeling	76
4.5.4 Moment Frame Connections Modeling	77
4.5.5 Inherent Damping	79
4.6 Summary	80
Chapter 5: Analysis of Results and Data Presentation.....	81
5.1 Introduction.....	81
5.2 Comparison to Baseline Systems.....	81
5.3 Effect of Acceleration Spikes	96
5.4 Summary	99
Chapter 6: Summary and Conclusions.....	101
6.1 Summary	101
6.2 Conclusions.....	103
6.3 Recommendations.....	104
References.....	108
Appendix A: Selected Design Calculations.....	116
Appendix B: Analysis Results of Perform 3D.....	176

List of Tables

Table 2-1: Seismic Resisting System Descriptions and Abbreviations (Marshall 2008) .	44
Table 2-2: Multi-Phase Systems and Abbreviations (Rawlinson 2011).....	48
Table 3-1: Scaled Earthquake Records.....	57
Table 4-1: The First and Second Mode Periods of Different Prototypes	80
Table 5-1: 3-Story Building Systems Indices	93
Table 5-2: 6-Story Building Systems Indices	94

List of Figures

Figure 2-1: A visualization of performance-based earthquake engineering (Moehle and Deierlein 2004)	7
Figure 2-2: Behavior of Building Structure with Base Isolation System (Symans 2009)	10
Figure 2-3: Elastomeric Bearings (Erkal, Tezcan and Laefer 2011)	11
Figure 2-4: - (a) Main components of the FPS bearing and FPS device movement; (b) and (c) motion of the pendulum and the FPS device, respectively (Esteves 2010).....	12
Figure 2-5: Cross Section of DCFP Bearing at Various Stages of Motion (Fenz and Constantinou 2009).....	13
Figure 2-6: Cross Section of the TFP Bearing (Fadi and Constantinou 2009).....	14
Figure 2-7: Combined Elastomeric and Sliding Bearings (Trelleborg 2010).....	15
Figure 2-8: The behavior of ADAS damper during earthquake (all dimensions in centimeter) (Alehashem, Keyhani and Pourmohammad 2008).....	17
Figure 2-9: The behavior of TADAS damper during earthquake (all dimensions in centimeter) (Alehashem, Keyhani and Pourmohammad 2008).....	17
Figure 2-10: Buckling-Restrained Braces Configuration (Calado, et al. n.d.)	18
Figure 2-11: Summary of construction, hysteretic behavior, physical models, advantages, and disadvantages of passive energy dissipation devices for seismic protection applications (Symans, et al. 2008)	19
Figure 2-12: (a) Schematic diagram of typical shear-link and (b) arrangement of shear-link in shear-link brace frame system (SLBF) (Rai, Annam and Pradhan 2013).	20
Figure 2-13: (a) Portion of building and its tributary loading area of the prototype considered for the model and (b) cross-sectional view of the frame under consideration (Rai, Annam and Pradhan 2013)	21
Figure 2-14: Typical Slotted Bolted Connection (SBC) (Marshall 2008).....	22

Figure 2-15: Friction Damping System: (a) Device Scheme (b) Location in Braced Frame (Colajanni and Papia 1995).....	23
Figure 2-16: Force-Displacement Cycle for FDBS (Colajanni and Papia 1995)	24
Figure 2-17: Longitudinal Cross Section of a Fluid Damper (a) Damper with an Accumulator (b) Damper with a Run-Through Rod (Hwang 2002).....	26
Figure 2-18: Hysteresis Loop of Dampers with Pure Viscous and Viscoelastic Behavior (Hwang 2002)	27
Figure 2-19: Tuned mass damper in the Taipei 101 skyscraper in Taiwan (Woodford 2013).....	28
Figure 2-20: TLD on the top of One Rincon Hill in San Francisco (TechBlog 2008).....	29
Figure 2-21: Block diagram of structural control systems: (a) passive control system, (b) active control system and (c) semi-active control system. (Symans and Constantinou 1999).....	31
Figure 2-22: Configuration of Active Bracing System (Reinhorn, et al. 1992)	33
Figure 2-23: Block Diagram of Control System (Reinhorn, et al. 1992)	34
Figure 2-24: Details of First Story Active Braces (Reinhorn, et al. 1992).....	35
Figure 2-25: Schematic Diagram of AVSD Control Device (Tan, Zhou and Yan 2004)	37
Figure 2-26: Three-building connected system (Palacios-Quinonero, et al. 2011)	39
Figure 2-27: General view of the building being isolated and location of isolators (Leblouba 2007).....	40
Figure 2-28: The Different Combinations Considered (Leblouba 2007)	41
Figure 2-29: Simple Schematic of HPCD (Marshall 2008).....	42
Figure 2-30: High Damping Rubber Sandwich Damper (Marshall 2008)	43
Figure 2-31: Diagram of Hybrid Energy Dissipation Systems (Marshall 2008).....	44
Figure 2-32: DBE Residual Displacements with Non-hybrid Systems (LA) (Marshall 2008).....	45
Figure 2-33: DBE Residual Displacements with Hybrid HDRD Systems (LA) (Marshall 2008).....	46

Figure 2-34: System Combinations (Rawlinson 2011).....	47
Figure 2-35: System Arrangement Comparison (Rawlinson 2011)	50
Figure 3-1: Plans of Three-Story and Six-Story Buildings (Sabelli 2001).....	53
Figure 3-2: Design Response Spectrum for Los Angeles, CA from USGS	55
Figure 3-3: System Arrangements	62
Figure 4-1: 2-D Frame Configuration.....	67
Figure 4-2: BRB Backbone Curve.....	69
Figure 4-3: The Final Prototypes of the 3-Story Steel Frames: (a) 40M60B System (b) 50M50B System (c) 60M40B System	71
Figure 4-4: The Final Prototypes of the 6-Story Steel Frames: (a) 40M60B System (b) 50M50B System (c) 60M40B System	73
Figure 4-5: FEMA Frame Component (a) Basic Components for Chord Rotation Model (b) Implementation of Chord Rotation Model (CSI 2006).....	74
Figure 4-6: System Arrangement.....	75
Figure 4-7: BRB Backbone Curve.....	76
Figure 4-8: Gap Backbone Curve	77
Figure 4-9: Model for Panel Zone Component (CSI 2006).....	78
Figure 4-10: Distortion in Connection Panel Zone (CSI 2006).....	78
Figure 4-11: Force-Deformation Relationship for the Krawinkler Model (Charney and Marshall 2006).....	79
Figure 5-1: 3-Story_40M60B_Gap0.45% with Baseline System.....	83
Figure 5-2: 3-Story_40M60B_Gap0.30% with Baseline System.....	84
Figure 5-3: 3-Story_40M60B_Gap0.15% with Baseline System.....	85
Figure 5-4: 6-Story_40M60B_Gap0.45% with Baseline System.....	88
Figure 5-5: 6-Story_40M60B_Gap0.30% with Baseline System.....	89

Figure 5-6: 6-Story_40M60B_Gap0.15% with Baseline System.....	90
Figure 5-7: Roof Accelerations of Multi-Phase System and Baseline System.....	97
Figure 5-8: 1 st Floor Gap Forces and Displacements.....	97
Figure 5-9: 1 st Floor Gap Displacements versus Nodal Accelerations	98
Figure 5-10: 1 st Floor Gap Forces versus Nodal Accelerations	99
Figure 6-1: Combined Effect of Damping Device with Gap Element.....	105
Figure B-1: 3-Story_50M50B_Gap0.45% with Baseline System	177
Figure B-2: 3-Story_50M50B_Gap0.30% with Baseline System	178
Figure B-3: 3-Story_50M50B_Gap0.15% with Baseline System	179
Figure B-4: 3-Story_60M40B_Gap0.45% with Baseline System	180
Figure B-5: 3-Story_60M40B_Gap0.30% with Baseline System	181
Figure B-6: 3-Story_60M40B_Gap0.15% with Baseline System	182
Figure B-7: 6-Story_50M50B_Gap0.45% with Baseline System	183
Figure B-8: 6-Story_50M50B_Gap0.30% with Baseline System	184
Figure B-9: 6-Story_50M50B_Gap0.15% with Baseline System	185
Figure B-10: 6-Story_60M40B_Gap0.45% with Baseline System	186
Figure B-11: 6-Story_60M40B_Gap0.30% with Baseline System	187
Figure B-12: 6-Story_60M40B_Gap0.15% with Baseline System	188

Chapter 1: Introduction

1.1 Defining the Problem

In the past, structures were designed to resist small lateral loads by elastic behavior. During moderate to high earthquakes, building codes were intended mainly to provide life safety by preventing the building from collapsing. However, the design for life safety offered by current codes is fundamental but not sufficient. The seismic risk has increased in recent major earthquakes and the damage caused is far from being economic. In order to reduce structural damage and repair costs after severe earthquakes, a need for a design that controls structural and nonstructural damage is required. The key to achieving this is to develop a new design methodology, performance-based seismic design, and new structural systems.

Performance-based earthquake engineering aims to enhance the seismic performance of buildings in many aspects by using new design methodologies coupled with innovative structural elements, systems, and technologies to control inelastic deformation demands. Seismic control systems were developed by using different methods such as seismic isolation, passive energy dampers, and semi-active and active control systems. These systems control the vibrations on the structure by dissipating the energy in different ways. However, each seismic control device has strengths and weaknesses. A new approach is required to eliminate the system weaknesses and take advantage of all the benefits of energy dissipation devices.

1.2 The Proposed Solution

A multi-phase passive control device was developed by combining two types of passive control devices in one system in order to offset the weaknesses of each system and improve the overall structural performance. In this research, multi-phase behavior was created by adding a gap element with multilinear elastic properties to a dual system that consists of a special moment frame and buckling restrained braced frame. The gap element was built in a way so that it will lock out when the frame reaches a certain displacement. The lateral load resistance will be shifted from the moment frame to the braced frame once the limit displacement is reached. The transition phase created by the gap allows the buckling restrained braces (BRBs) to yield before the moment frame because BRBs are replaceable and easier to replace.

In order to understand the overall behavior of multi-phase systems, different system combinations involving various gap sizes, moment frame and braced frame strength ratios, building heights, and earthquake levels were considered in this research. The analysis results of multi-phase system combinations were compared to their corresponding baseline systems to identify the benefits and important parameters. The baseline systems consist of the same dual system used in the multi-phase systems without the addition of the gap elements.

1.3 Scope and Approach

A single degree of freedom (SDOF) study was previously conducted to understand the fundamental behavior of the multi-phase system and to provide the ground work for a multi degree of freedom (MDOF) study. The MDOF study added valuable insights into the performance of the multi-phase system as it seeks to eliminate the uncertainties of the SDOF study. For that reason, 3-story and 6-story steel frames were designed for lateral loads effect. The design procedure followed the AISC Seismic Provisions for Structural Steel Buildings (AISC 2005) and ASCE Standard 7-10 (ASCE 2010) design codes along with the Computers and Structures, Inc. program SAP 2000 (CSI 2012). The finite element modeling and response history analysis criteria were developed using Perform 3D (CSI 2011).

The response of the multi-phase system has been studied using nonlinear dynamic analysis with scaled ground motions from various site conditions. Different parameters have been selected to examine the moment frame and braced frame ductility responses. Reduction of story drifts as well as reduction of system acceleration was highly desirable. The ideal multi-phase system combination is identified by comparing various system combinations with the baseline systems.

1.4 Thesis Organization

Chapter 1 gives the introduction to this research by defining the problem, introducing the proposed solution, and discussing the scope of work and the approach used during this research.

Chapter 2 includes an extensive literature review designed to develop an understanding of the previous research on lateral resisting and passive control systems in order to enable a thorough understanding of the conceptual changes and improvements undertaken in this study. Also, a brief discussion of the SDOF research is included and the groundwork for the MDOF study is specified.

Chapter 3 presents an overview on the prototype buildings and the selected lateral force resisting systems. The seismic design is discussed for the prototype buildings. An illustration of the system arrangements of the multi-phase system and the baseline system is presented. The system combinations involved in this study are also outlined in this chapter.

Chapter 4 details the design procedure and finite element modeling of the moment frame and braced frame components of the prototype buildings. The model configuration is displayed and clarified.

Chapter 5 provides a broad analysis by involving all system combinations across three different earthquake levels to identify the best system performance. The nonlinear dynamic response history analysis results are presented and discussed.

Chapter 6 summarizes the research and provides recommendations for future studies.

Chapter 2: Background and Literature Review

2.1 Introduction

Structures located in seismically active zones must be designed to resist earthquake loads along with gravity loads. At first, structures were designed to resist small lateral loads simply by their elastic behavior. During moderate to high earthquakes, structures were permitted to experience damage but not collapse, providing life safety (Hwang 2002). The design for life safety offered by current codes is fundamental but not sufficient. Consequences of recent earthquakes exhibited high costs due to damage of structures that were designed to provide life safety. This design procedure has uncertainties regarding seismic demand and capacity of the structure. A need for a design that controls structural and nonstructural damage is required. Therefore, performance-based seismic design has been established. The idea of performance-based seismic design is that the building performance targets a certain level of stress, load, displacement, limit state, or damage state (Ghobarah 2001).

The performance-based earthquake engineering procedure involves assessments and design methods that will lead to the best seismic risk decision-making. Figure 2-1 shows the visualization of a problem by using assessments and design procedures, where a building subjected to earthquake-induced lateral forces is damaged due to nonlinearity. Correlations have been made between structural responses such as inter-story drifts, member deformations, and member forces with performance-oriented descriptions such

as Immediate Occupancy, Life Safety and Collapse Prevention. As a result, some limitations have been identified regarding seismic design as indicated by Moehle and Deierlein (2004).

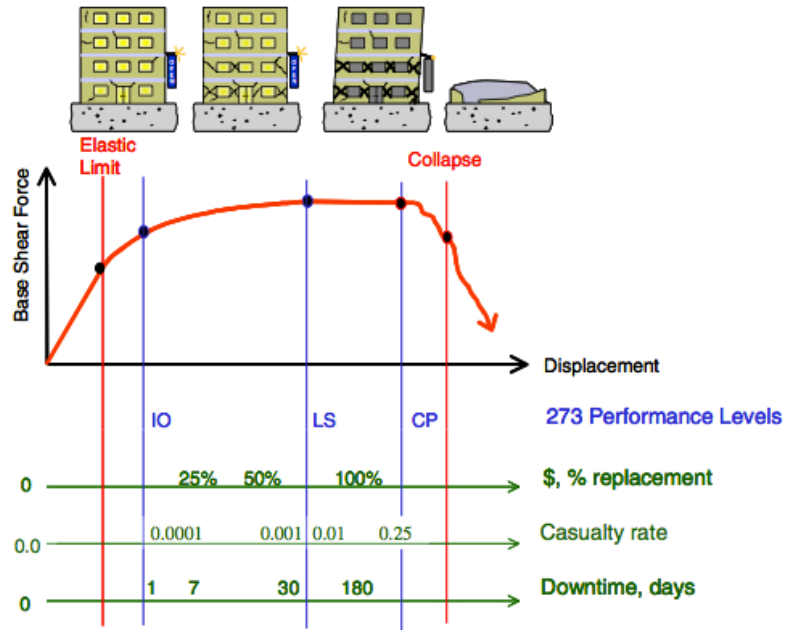


Figure 2-1: A visualization of performance-based earthquake engineering (Moehle and Deierlein 2004)

In June 2000, the Japanese seismic design code for buildings adopted the performance-based structural engineering framework. This allowed the use of new structural elements, systems, and technologies that developed by structural engineers in order to satisfy the performance objectives of the code. The revision came after the 1995 Hyogoken-nanbu earthquake that caused enormous loss in human lives and buildings,

which led scientists and engineers to develop performance-based engineering to assure high safety levels of buildings during earthquakes (Midorikawa, et al. 2001).

Structural systems can significantly enhance the seismic performance of buildings by controlling inelastic deformation demands on the lateral load resisting system. As specified by Constantinou, Soong and Dargush (1998), modern structural control systems can be divided into three main groups:

- Seismic Isolation

- ❖ Elastomeric Bearings
- ❖ Lead Rubber Bearings
- ❖ Sliding Friction Pendulum Systems
- ❖ The Double Concave Friction Pendulum
- ❖ Triple Friction Pendulum
- ❖ Combined Elastomeric and Sliding Bearings
- ❖ Sliding Bearings with Restoring Force

- Passive Energy Dissipation Systems

- ❖ Metallic Dampers
- ❖ Friction Dampers
- ❖ Viscoelastic Solid Dampers
- ❖ Viscoelastic or Viscous Fluid Dampers
- ❖ Tuned Mass Dampers
- ❖ Tuned Liquid Dampers

- ❖ Smart Materials
- Semi-active and Active Systems
 - ❖ Active Bracing Systems
 - ❖ Active Mass Dampers
 - ❖ Variable Stiffness and Damping Systems

In order to understand the different mechanisms and behaviors of each structural control system, a brief description is provided in the following sections.

2.2 Seismic Isolation

In recent years, seismic or base isolation became a very popular method to protect buildings from earthquake forces by isolating the base foundation and the structure. The main purpose of base isolation is to lower the fundamental frequency of structural vibration under the major earthquake frequency limit. Also, it dissipates lateral forces transmitted to the system during a seismic event (Tongaokar and Jangid 1998). In Figure 2-2, a visual comparison of responses exhibited by a conventional structure and an isolated structure is presented. The former is facing inter-story drifts and amplified accelerations at upper floor levels, while the latter has deformation at the base level and uniform accelerations over the height of the structure (Symans 2009). This system is suitable for low- to mid-height buildings, especially important once due to its high cost (Chopra 2007).

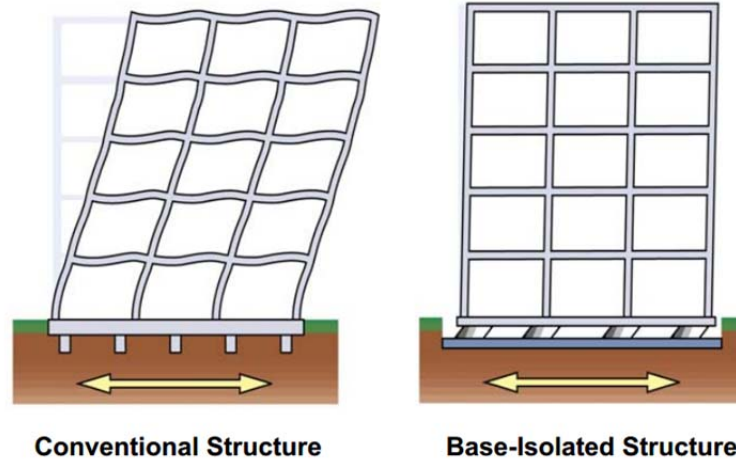


Figure 2-2: Behavior of Building Structure with Base Isolation System (Symans 2009)

2.2.1 Elastomeric Bearings

This system is considered one of the basic systems used in base isolation engineering. It consists of high density rubber layers bonded to intermediate steel plates. The steel plates act as an absorber of the earthquake forces (see Figure 2- 3 a). These layers have a low horizontal stiffness (shear stiffness) that isolates the structure from the earthquake horizontal ground motions, thus decreasing the inelastic deformations of the structure. The vertical stiffness of the elastomeric bearings is provided by the close spacing of the steel plates. A steel cover might be provided on the top, bottom, and sides of the bearings to facilitate its attachment to the structure (Sabu 2006).

2.2.2 Lead Rubber Bearings (LRB)

Lead rubber bearings are a type of base isolation system used to enhance the seismic performance of buildings and bridges during earthquakes. Theoretically, a lead rubber bearing (LRB) differs from an elastomeric bearing through the addition of a lead core located in the center as shown in Figure 2-3 (b). Hysteretic damping, lead bearing capacity, and a re-centering force are characteristics offered by the LRB, which makes it convenient to construct (Robinson and Tucker 1977).

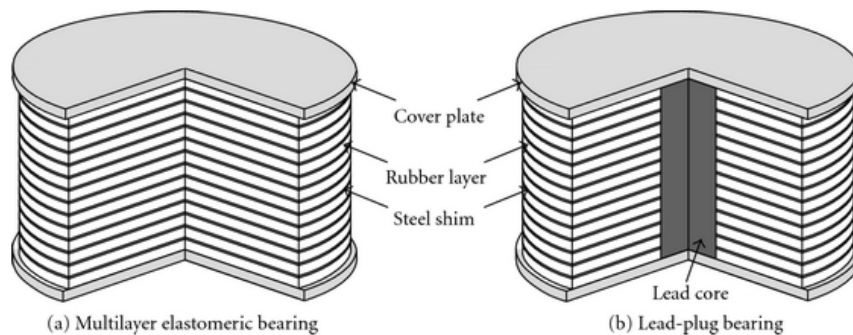


Figure 2-3: Elastomeric Bearings (Erkal, Tezcan and Laefer 2011)

2.2.3 Friction Pendulum Systems (FPS)

The Friction Pendulum System (FPS) is a sliding seismic isolation bearing widely used in the United States because of its effectiveness for a wide range of excitation frequencies. As specified by Esteves (2010), “The FPS Bearings are constituted by two sliding parts. One of them contains an articulated chrome extremity, coated with Teflon or another composite material with a low and high capability of bearing that slides on the

concave polished surface (spherical) that constitutes the second part.” When a structure with a friction pendulum base isolation experiences motion resulting from a seismic load, it returns to its position due to its own weight and the round shape of the device’s sliding surface. This mechanism is similar to a pendulum working mechanism as shown in Figure 2-4 (Esteves 2010).

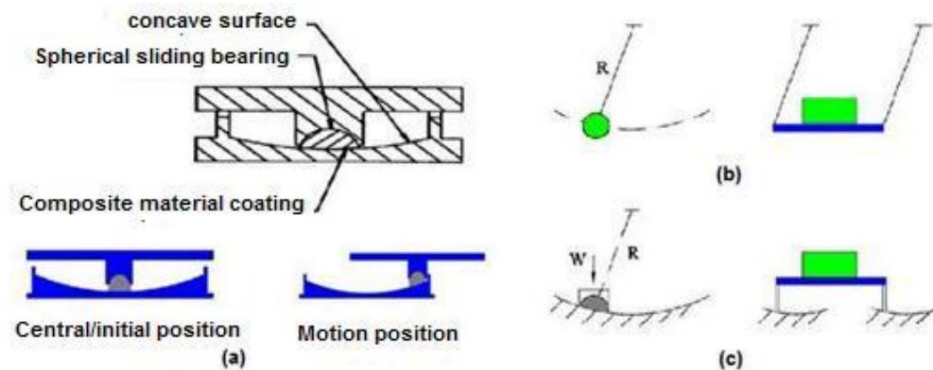


Figure 2-4: - (a) Main components of the FPS bearing and FPS device movement; (b) and (c) motion of the pendulum and the FPS device, respectively (Esteves 2010)

2.2.4 The Double Concave Friction Pendulum (DCFP)

The Double Concave Friction Pendulum (DCFP) is a friction pendulum system with two sliding surfaces. The two surfaces can have different friction coefficients and radii of curvature to provide flexibility when optimizing the performance. The DCFP can tolerate large displacements compared to a FPS of similar dimensions. Figure 2-5 shows the DCFP bearing behavior at different displacement levels (Fenz and Constantinou 2009).

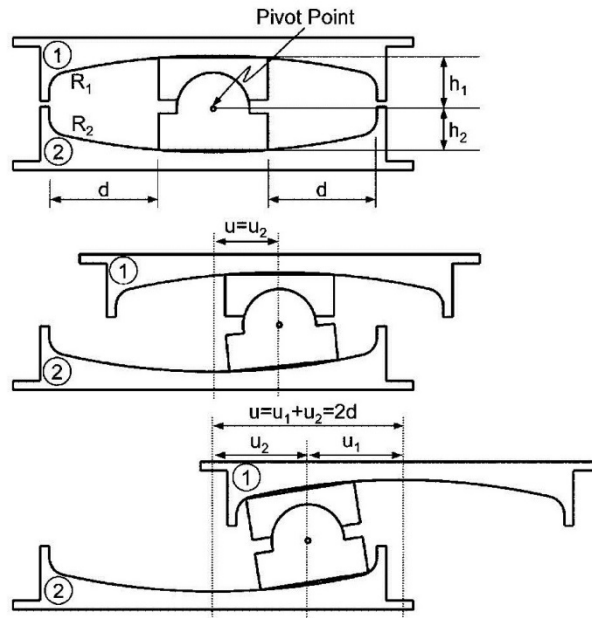


Figure 2-5: Cross Section of DCFP Bearing at Various Stages of Motion (Fenz and Constantinou 2009).

2.2.5 Triple Friction Pendulum (TFP)

The Triple Friction Pendulum (TFP) is a friction pendulum isolator where sliding takes place in three sliding surfaces as seen in Figure 2-6. Different friction coefficients and curvature radii of the sliding surfaces can be used as in the DCFP bearings. When compared to friction pendulum isolators, TFP isolators are found beneficial in reducing the displacement demands as well as the forces and accelerations in structural systems (Fadi and Constantinou 2009).

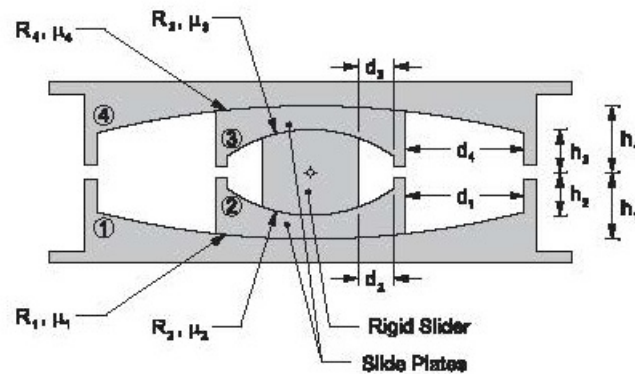


Figure 2-6: Cross Section of the TFP Bearing (Fadi and Constantinou 2009).

2.2.6 Combined Elastomeric and Sliding Bearings

This system is a combination of two isolation system categories. The first is elastomeric bearings such as the high damping rubber bearing system (HDRB) and lead rubber bearing system (LRB), and the second is sliding bearings such as the friction pendulum system (FPS) and sliding bearing system without recentering (Leblouba 2007). The sliding bearing system allows horizontal movement of the structure beyond the shear capacity limit in addition to the elastomeric system characteristics that were previously discussed (See Figure 2-7) (Trelleborg 2010).



Figure 2-7: Combined Elastomeric and Sliding Bearings (Trelleborg 2010)

2.2.7 Sliding Bearings with Restoring Force

Using a sliding bearing system along with a restoring force system is found to be a very effective technique for reducing the seismic reaction of a structure (Krishnamoorthy 2008). The sliding bearing system provides the structure flexibility to move horizontally which results in a good performance under significant earthquake motions. But a freely sliding structure will also have large permanent displacements that need to be controlled (Constantinou, Mokha and Reinhorn 1991). Combining a restoring force system with a sliding bearing controls the structural seismic response by reducing the residual displacements and sliding. Besides, it helps in restoring the original position of the structure at the end of the seismic event (Krishnamoorthy 2008). For that, the combination of these two systems will lead to better structural performance during an earthquake.

2.3 Passive Energy Dissipation Systems

The main function of a passive energy dissipation system is to reduce damage to the frame. This is done by reducing the inelastic energy dissipation demand of the frame system by absorbing a portion of the seismic energy. The energy absorption mechanism results from either converting the kinetic energy to heat or transferring energy to different modes of vibration. This results in a decrease of inter-story drifts as well as nonstructural damage. Additionally, these systems can reduce the ductility demands on the structural components by decreasing the accelerations and the shear forces (Sadek, et al. 1996). Passive energy dissipation systems are ideal for design because they do not need an external power source in addition to the low maintenance costs (Spencer Jr. and Nagarajaiah 2003).

2.3.1 Metallic Dampers

Metallic dampers are typically made of steel. These devices are designed to deform inelastically during an earthquake by absorbing some of the seismic energy transmitted to the structure. Examples of metallic dampers are: buckling-restrained braces (BRB), added damping and stiffness (ADAS) dampers, and triangular added damping and stiffness (TADAS) dampers (Symans, et al. 2008). Figures 2-8 and 2-9 illustrate the behavior of the ADAS and TADAS dampers during an earthquake, where the upper end of the damper is moving relative to the lower end due to inter-story drifts. The yielding of

the dampers' metallic plates due to this movement provides energy dissipation to the system (Alehashem, Keyhani and Pourmohammad 2008).

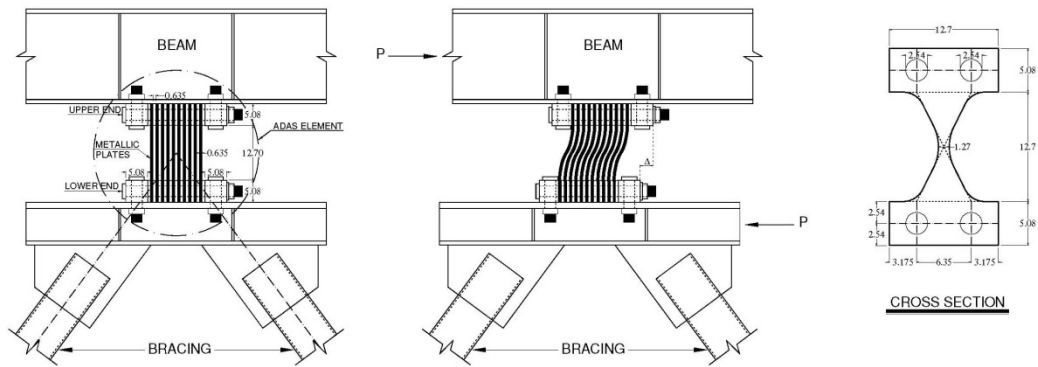


Figure 2-8: The behavior of ADAS damper during earthquake (all dimensions in centimeter) (Alehashem, Keyhani and Pourmohammad 2008)

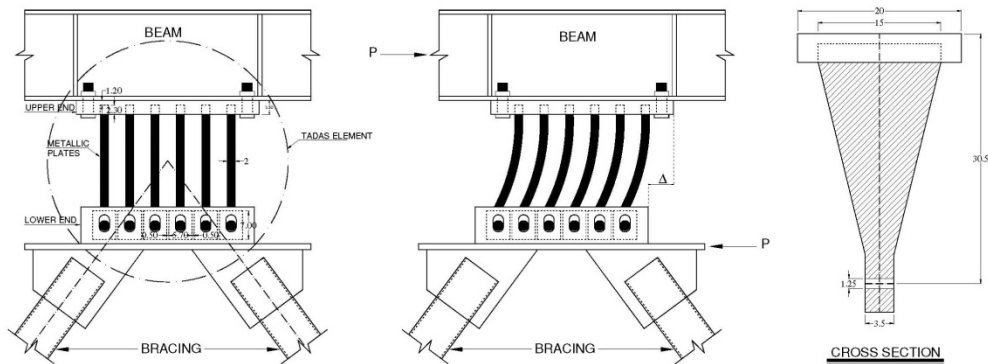
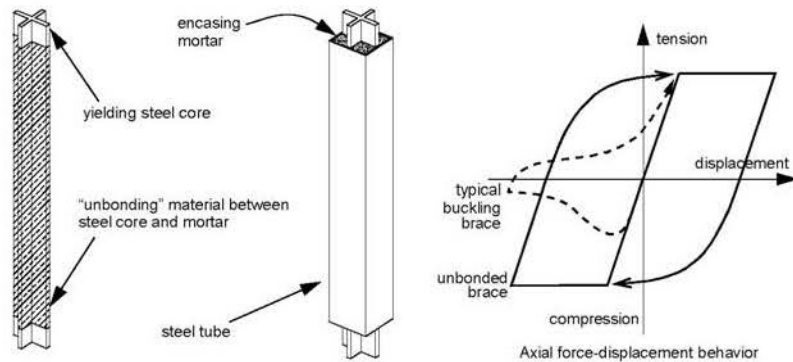


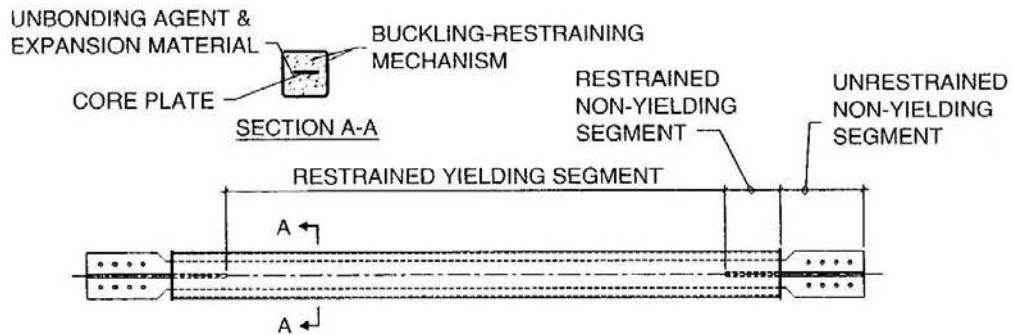
Figure 2-9: The behavior of TADAS damper during earthquake (all dimensions in centimeter) (Alehashem, Keyhani and Pourmohammad 2008)

A buckling restrained brace (BRB), as defined by Calado, et al., “is a bracing member consisting of a steel core plate or another section encased in a concrete-filled steel tube over its length” (see Figure 2-10 a). An example of a typical BRB is presented

in Figure 2-10 (b) which shows the different components that the brace consists of (Calado, et al.).



(a) Buckling-restrained unbonded steel brace



(b) Components of typical BRB

Figure 2-10: Buckling-Restrained Braces Configuration (Calado, et al. n.d.)

BRBs are tension-compression braces with hysteretic behavior. These braces have the ability to dissipate energy by yielding in tension and compression by resisting axial loads in the steel core and resisting buckling through the steel casing (UC 2011). See Figure 2-11 for more details on metallic dampers.

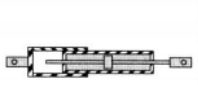

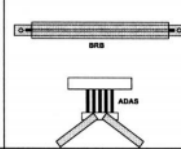

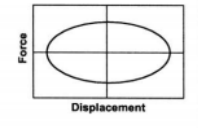
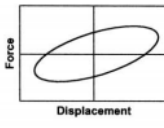
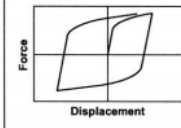
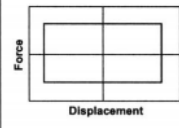
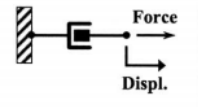
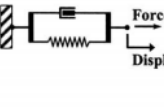
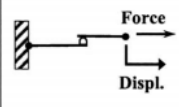
	Viscous Fluid Damper	Viscoelastic Solid Damper	Metallic Damper	Friction Damper
Basic Construction				
Idealized Hysteretic Behavior				
Idealized Physical Model			Idealized Model Not Available	
Advantages	<ul style="list-style-type: none"> - Activated at low displacements - Minimal restoring force - For linear damper, modeling of damper is simplified. - Properties largely frequency and temperature-independent - Proven record of performance in military applications 	<ul style="list-style-type: none"> - Activated at low displacements - Provides restoring force - Linear behavior, therefore simplified modeling of damper 	<ul style="list-style-type: none"> - Stable hysteretic behavior - Long-term reliability - Insensitivity to ambient temperature - Materials and behavior familiar to practicing engineers 	<ul style="list-style-type: none"> - Large energy dissipation per cycle - Insensitivity to ambient temperature
Disadvantages	<ul style="list-style-type: none"> - Possible fluid seal leakage (reliability concern) 	<ul style="list-style-type: none"> - Limited deformation capacity - Properties are frequency and temperature-dependent - Possible debonding and tearing of VE material (reliability concern) 	<ul style="list-style-type: none"> - Device damaged after earthquake; may require replacement - Nonlinear behavior; may require nonlinear analysis 	<ul style="list-style-type: none"> - Sliding interface conditions may change with time (reliability concern) - Strongly nonlinear behavior; may excite higher modes and require nonlinear analysis - Permanent displacements if no restoring force mechanism provided

Figure 2-11: Summary of construction, hysteretic behavior, physical models, advantages, and disadvantages of passive energy dissipation devices for seismic protection applications (Symans, et al. 2008)

Another example of metallic dampers is the aluminum shear-link. A study established by Rai, Annam and Pradhan (2013) had investigated the behavior of an

ordinary chevron braced frame (OCBF) after adding aluminum shear-links to it as seen in Figure 2-12. The study showed that the seismic response of the system was improved remarkably as the base shear was reduced after being subjected to a series of scaled Taft ground motion with increasing severity. Since aluminum is a low yielding alloy metal, which is very ductile in shear yielding and can sustain large inelastic deformations without tearing or buckling, it was found to be excellent for producing the I-shaped shear-links that were used in the system (Rai, Annam and Pradhan 2013).

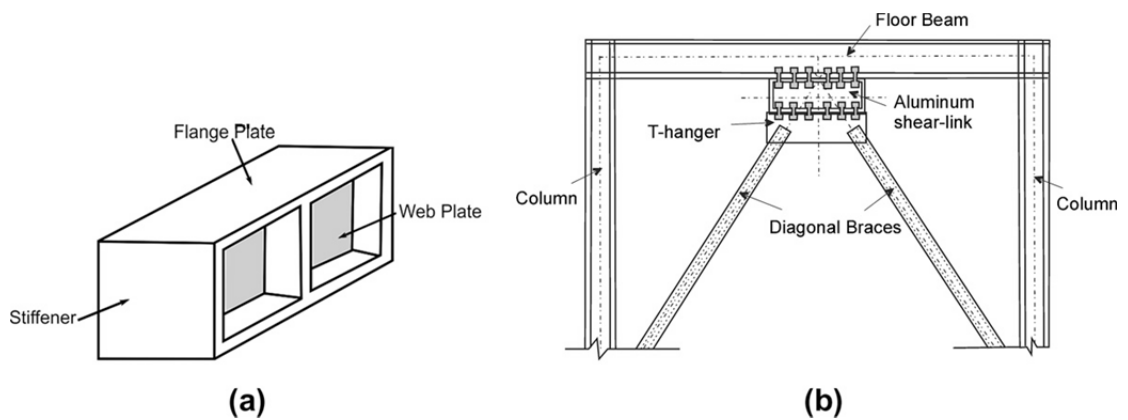


Figure 2-12: (a) Schematic diagram of typical shear-link and (b) arrangement of shear-link in shear-link brace frame system (SLBF) (Rai, Annam and Pradhan 2013)

A prototype of the two-story building is presented in Figure 2-13 where six braced bays are used in the N-S direction to provide lateral resistance. The frames in the middle bay were designed as shear-link braced frames (SLBFs) while the other interior frames were designed to carry gravity loads only. The SLBF system components were

designed to follow the capacity design approach in which the frame does not yield until the dampers get their ultimate shear stress (Rai, Annam and Pradhan 2013).

During ground shaking, the damper or the aluminum shear-link will yield in shear providing massive energy dissipation through its inelastic deformation. Moreover, the enormous amount of aluminum alloy's strain-hardening will influence the shear-links to carry more loads after the first yield and will let the shear-links in the other stories participate in lateral load resistance. Therefore, the inelasticity will extend to neighboring bays and stories until it covers the whole structure. This makes the aluminum shear-link suitable for new and existing structures (Rai, Annam and Pradhan 2013).

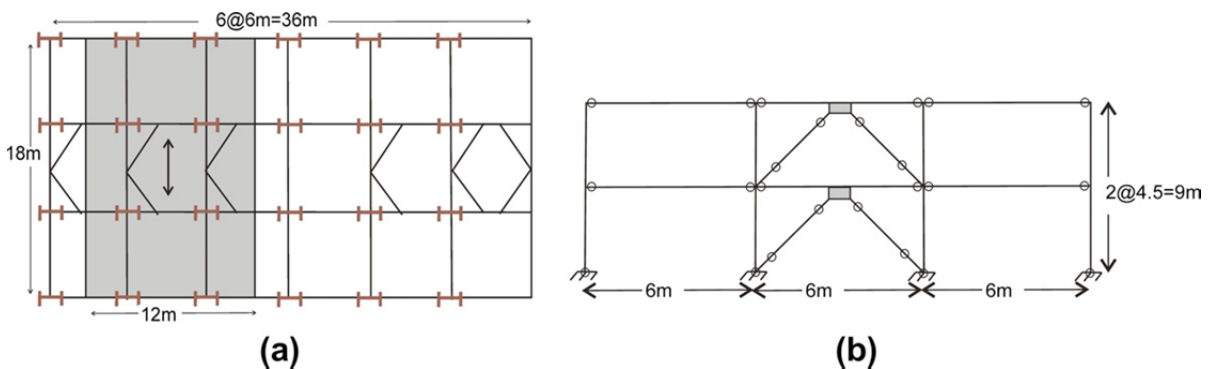


Figure 2-13: (a) Portion of building and its tributary loading area of the prototype considered for the model and (b) cross-sectional view of the frame under consideration (Rai, Annam and Pradhan 2013)

2.3.2 Friction Dampers

Mechanical engineers have used the concept of the friction damper to control machines and automobiles motions for centuries, which inspired the development of

friction damper device. This device can be used for low-rise buildings, concrete shearwalls, braced steel/concrete frames, and clad-frame construction and is preferred for being economic and easy to manufacture (Pall and Pall 1998). A friction damper is a passive control device that dissipates energy through the friction between two surfaces. It consists of a series of steel plates clamped together using high strength steel bolts as shown in Figure 2-11. These plates have a predetermined friction force that should be reached in order to allow the plates to slip. The slip force is based on the clamping force and the coefficient of friction (Symans, et al. 2008).

A simple model of a friction damper is illustrated in Figure 2-14; this model is called the slotted bolted connection (SBC). The center and the outer plates are allowed to slip with respect to each other using the slotted bolt holes. The bolts provide the clamping force. The energy dissipation comes from heat build-up due to friction (Marshall 2008).

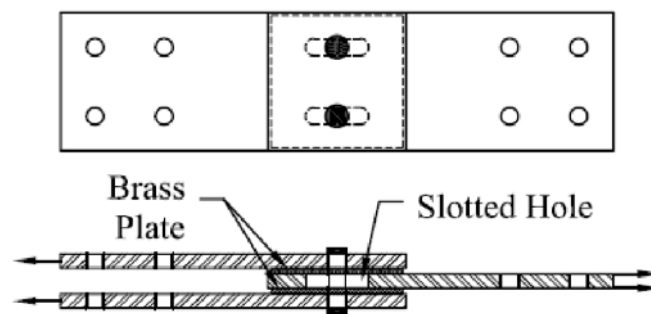


Figure 2-14: Typical Slotted Bolted Connection (SBC) (Marshall 2008)

A study was made by Colajanni and Papia (1995) for two different bracing systems: a friction damped bracing system (FDBS) and an ordinary cross-bracing system (CBS). This study investigated the seismic response of the FDBS and the CBS by analyzing the behavior of frames with the designated bracing systems. The results proved the practicality of using the FDBS, which showed a better performance in reducing the seismic forces when compared to the CBS (Colajanni and Papia 1995).

The FDBS is made by coupling a bracing system with a friction damping system. The system consists of four hinged links organized in a quadrilateral shape hinged at the joints, as displayed in Figure 2-15 (a), with two diagonal links that are connected to external diagonal braces. Each diagonal link has two separate parts inside the quadrilateral region. These parts are partially superimposed by a friction brake joint placed at the center of the device (Colajanni and Papia 1995).

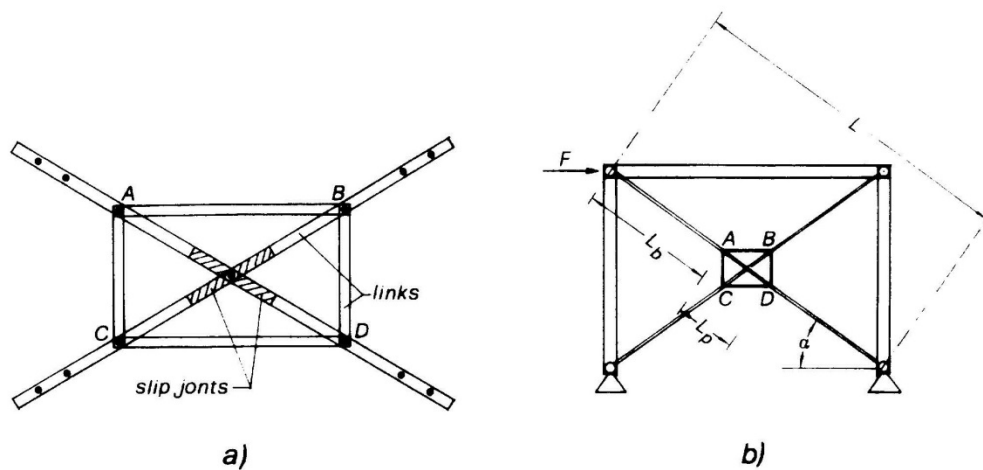


Figure 2-15: Friction Damping System: (a) Device Scheme (b) Location in Braced Frame (Colajanni and Papia 1995)

2.3.3 Viscoelastic Solid Dampers

A viscoelastic solid damper is another type of passive control device used as a means of energy dissipation. The typical viscoelastic damper is comprised of viscoelastic layers bonded with steel plates as shown in Figure 2-11. It can be installed in the structure within a chevron or diagonal bracing. The energy dissipation is produced by the deformation of the viscoelastic layers as the damper's ends displace with respect to each other, resulting in heat development. These dampers are velocity and displacement dependent owing to their viscoelastic nature. The behavior of the dampers depends on vibration frequency, strain levels and temperature (Symans, et al. 2008).

2.3.4 Viscoelastic or Viscous Fluid Dampers

Due to the long successful history of fluid damper application in the military, there was a rapid jump in its implementation. These devices have been well-developed and applied to civil structures as passive control energy dissipaters against seismic and wind loads (Symans, et al. 2008). Figure 2-17 (a) and (b) show two types of fluid dampers consisting of a hollow cylinder that has a stainless steel piston with an orifice head. The cylinder is filled with a viscous fluid (e.g. silicon oil). The difference between these two dampers is that one of them has an accumulator and the other has a run-through rod (Hwang 2002). During a seismic event, the piston rod and the piston head will stroke, forcing the fluid to flow into the openings around or through the piston head. A very high pressure will be created on the upstream side and a low one on the downstream side. The

difference in pressure will produce very large forces that resist the damper motion. Also, due to the high velocity flow of the fluid, friction between fluid particles and the piston head will occur, causing energy dissipation in a form of heat. More details are shown in Figure 2-11 about the advantages and disadvantages of this type of damper (Symans, et al. 2008).

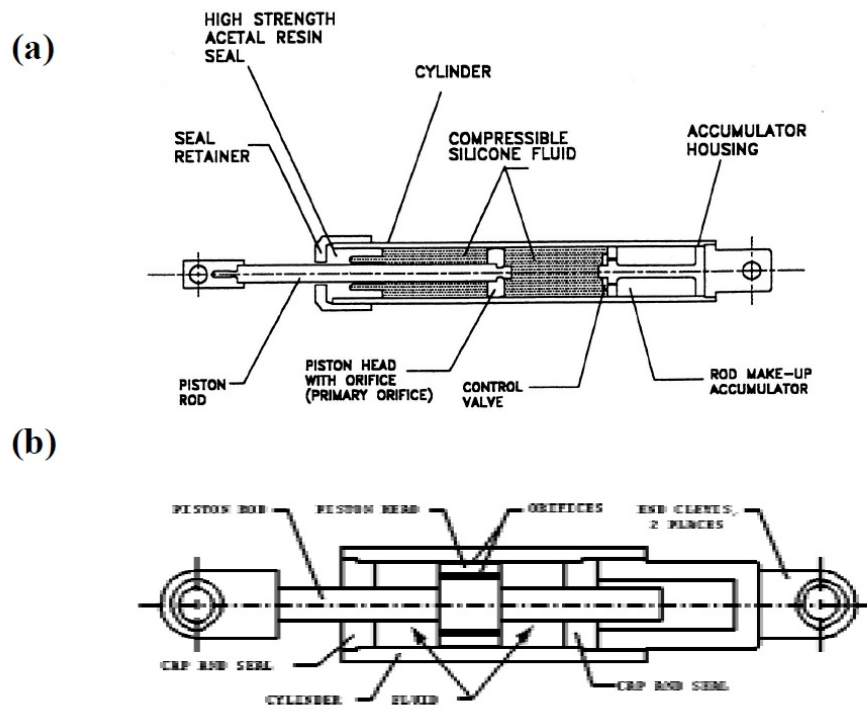


Figure 2-17: Longitudinal Cross Section of a Fluid Damper (a) Damper with an Accumulator (b) Damper with a Run-Through Rod (Hwang 2002)

Pure viscous behavior, as shown in Figure 2-18 (a), occurs when the damper force and the velocity remain in phase. However, in high frequency motions, the hysteresis loop will turn into viscoelastic behavior as shown in Figure 2-18 (b), because of the

restoring force development, which is in phase with displacement rather than velocity (Hwang 2002).

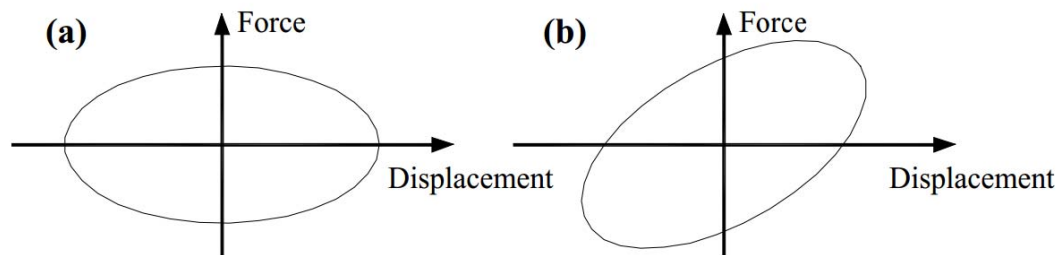


Figure 2-18: Hysteresis Loop of Dampers with Pure Viscous and Viscoelastic Behavior (Hwang 2002)

2.3.5 Tuned Mass Dampers

In 1909, the tuned mass damper (TMD) concept was used for the first time to reduce ships' motions and ships' hull vibrations (Connor 2002). During the years, many studies have been made in order to improve the performance of the device. The TMD is a device that can be attached to the structure by a spring and a damping element to control vibration problems. It will be activated when the structure is excited by a frequency close to the natural frequency (resonance), where the TMD is tuned to vibrate. The damper's inertia force that acts on the structure is the source of energy dissipation (Connor 2002). These devices are mostly used in structures that tend to excite severely in one of their mode shapes under dynamic loads, like tall and slender free-standing structures such as bridges, pylons of bridges, chimneys, TV towers...etc (Stroscher). Taipei 101, otherwise known as the Taipei World Financial Center, located in Taipei, Taiwan, has the world's

largest tuned mass damper (see Figure 2-19). It is designed as a pendulum suspended from the 92nd to the 87th floor and weighs 730 tons. During strong gusts, the pendulum will sway in order to offset the movements in the tower and acts as an energy dissipater (Kourakis 2007).

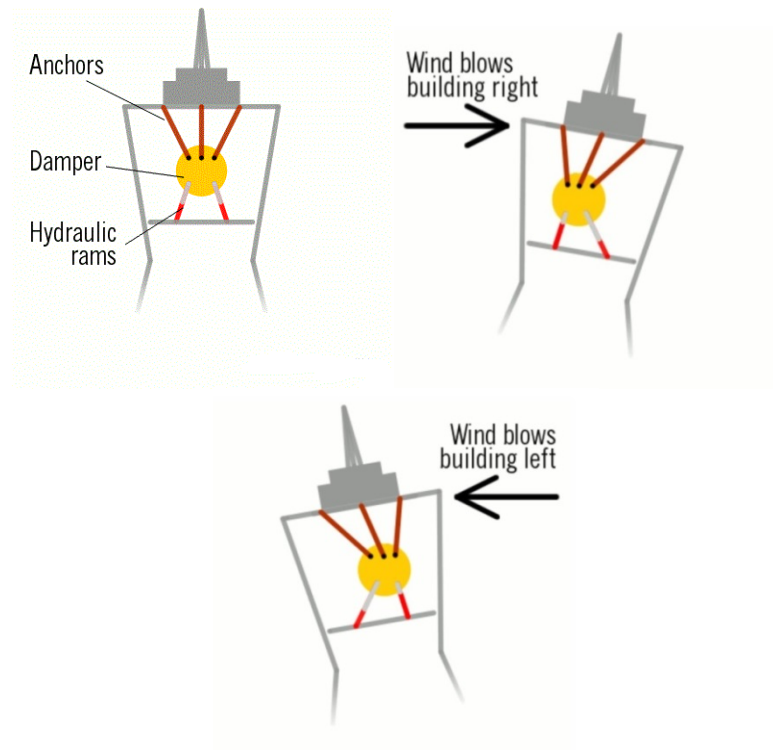


Figure 2-19: Tuned mass damper in the Taipei 101 skyscraper in Taiwan (Woodford 2013)

2.3.6 Tuned Liquid Dampers

A Tuned Liquid Damper (TLD) is a form of a tuned mass damper (TMD) but the mass is replaced by a liquid, usually water. These dampers control vibrations on the structure by absorbing energy through the liquid sloshing motion. The energy can be

absorbed in different ways such as the inherent friction of the liquid, the friction between the liquid and the wall surfaces, the friction of the floating particles, or the particles collision. TLDs are very economical due to its low initial cost and limited maintenance. Also, these devices are desired for many other advantages, for instance, frequency tuning simplicity, extensive vibration amplitude, ability to be installed in existing buildings, and efficiency in very low amplitude vibrations (Tamura, et al. 1995). Figure 2-20 shows the TLD located on the top of One Rincon Hill in San Francisco. This damper consists of a giant storage tank full of water with a capacity of approximately 100,000 gallons (TechBlog 2008).

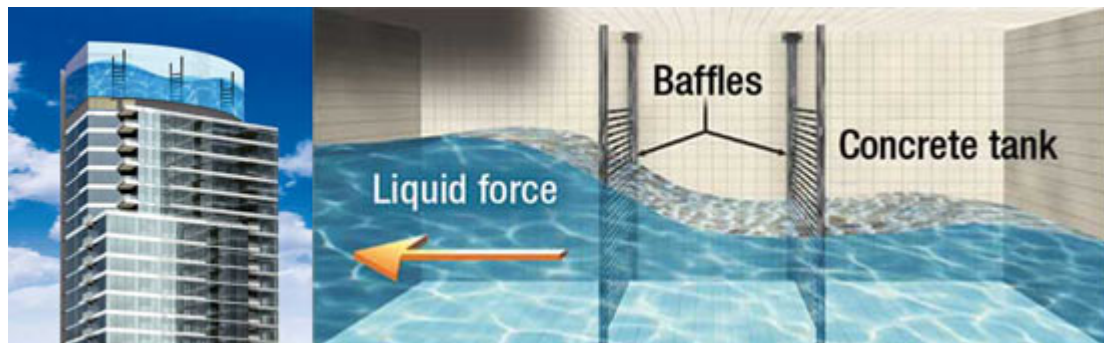


Figure 2-20: TLD on the top of One Rincon Hill in San Francisco (TechBlog 2008)

2.3.7 Smart Materials

New materials have been developed in civil engineering to provide better performance for structures under natural hazards. These materials have been called smart materials for their ability to sense an external stimulus such as stress, pressure,

temperature change, magnetic field, etc. and respond to it accordingly. Smart materials might be made of metals or alloys, polymers, ceramics or composites (Sreekala , Muthumani and Nagesh 2011). Examples of smart materials are shape memory alloys (SMA). SMA refers to the capability of some alloys (e.g. Ni – Ti, Cu – Al – Zn etc.) to withstand large displacements and to recover their initial conditions with no residual deformations (Muthumani and Sreekala 2002). The application of SMA is described by Choi, et al. (2010) where superplastic SMA bars have been used in steel structures to develop rotational performance at beam-column connections. Also, SMAs have been used in reinforced concrete structures in order to improve the ductility at the hinges in columns and beam-column connections. These applications have improved the performance of these structures significantly during seismic events (Choi, et al. 2010).

2.4 Semi-active and Active Systems

Recently, active and semi-active control systems have drawn attention as means of structural protection against wind and earthquake loads. As defined by Soong and Spencer (2000), active and semi-active control systems are “force delivery devices integrated with real-time processing evaluators/controllers and sensors within the structure.” These systems improve structural performance by working instantaneously with the hazard excitation (Soong and Spencer 2000). Active control systems need a large external power source in order to operate electrohydraulic or electromechanical actuators. The actuators provide the structure with control forces, which are developed based on the

structure's response measured by sensors. On the other hand, semi-active control systems need a smaller power source, a battery for example, to develop control forces by utilizing the structure movement. The development of the control forces is the same as in active control systems. A block diagram is shown in Figure 2-21 to simulate the mechanism of each system (Symans and Constantinou 1999). There are many different active and semi-active devices, but only few have been selected, to show the differences compared to passive control devices.

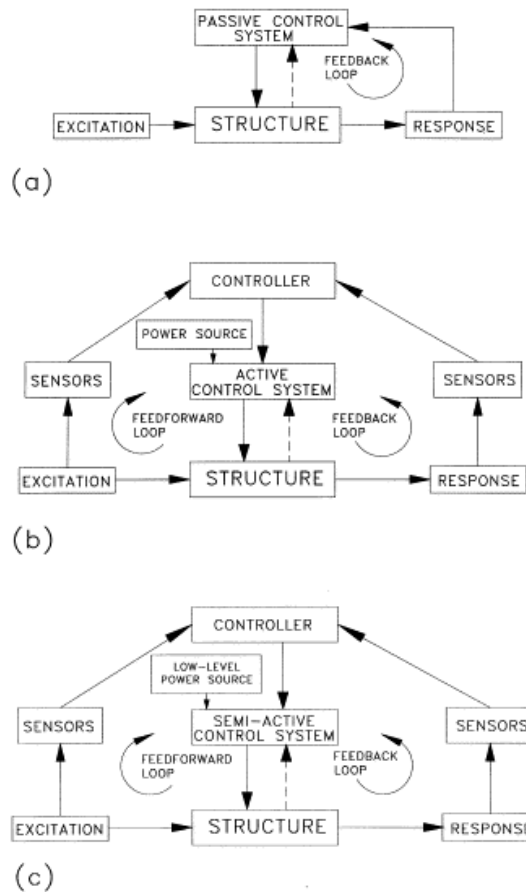


Figure 2-21: Block diagram of structural control systems: (a) passive control system, (b) active control system and (c) semi-active control system. (Symans and Constantinou 1999)

2.4.1 Active Bracing Systems (ABS)

Active bracing systems are considered one of the most studied active control systems in earthquake engineering. They involve a set of prestressed tendons or braces attached to the structure. Electrohydraulic servomechanisms are used to control the forces on these elements. Because prestressed tendons or braces are already part of the structural building, this system has become favored, especially in strengthening existing structures. A test was held in Tokyo, Japan to verify the performance of ABS. Figure 2-22 demonstrates a symmetric two-bay six-story building that has solid diagonal tube braces at the first story connected to it after the construction was completed. These tube braces are designed as ABS with the details presented in Figure 2-24. The longitudinal expansion and contraction of the braces are controlled by hydraulic servocontrolled actuators, which are implanted between the braces, building an internal part of the control system. Other parts used in the system, as shown in Figure 2-23, a hydraulic power supply, an analog and digital controller, and analog sensors. The test of the developed system works as an invaluable experience through the development of the active control systems and it can be used as a resource for future studies (Reinhorn, et al. 1992).

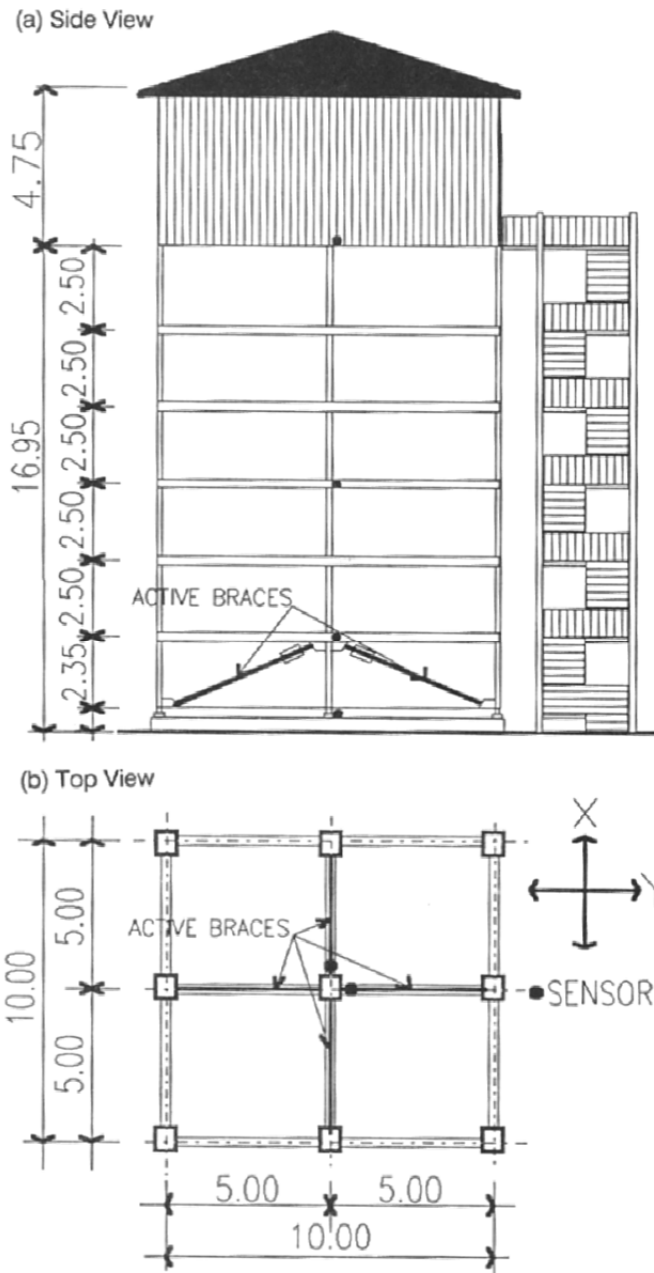


Figure 2-22: Configuration of Active Bracing System (Reinhorn, et al. 1992)

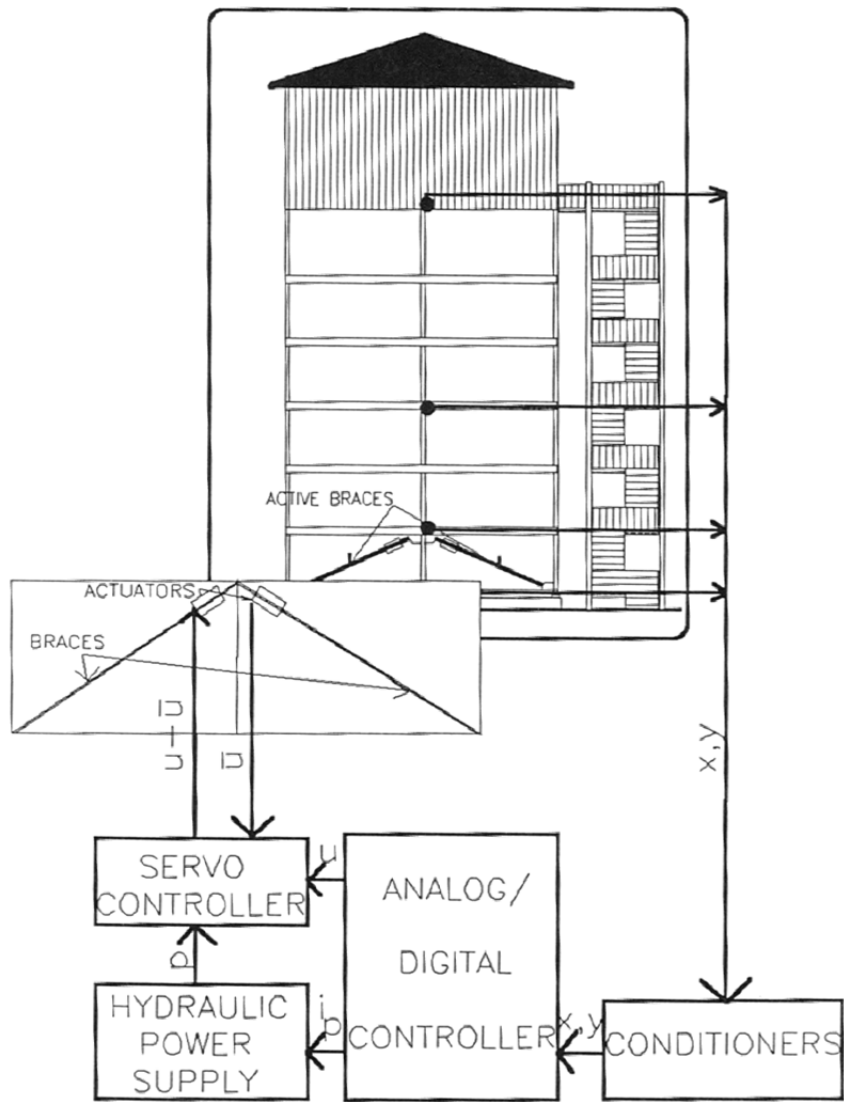


Figure 2-23: Block Diagram of Control System (Reinhorn, et al. 1992)

consumes little energy.” The AMD absorbs energy by generating control forces through accelerating and decelerating auxiliary masses that provided by the actuator. During this process, cyclic energy is added to the structural system and extracted again, resulting in larger energy. This process provides damping to the structure as the resulting energy will be dissipated in the device itself (Scheller and Starossek 2011).

2.4.3 Variable Stiffness and Damping Systems

Many studies have been made to improve vibration control systems. Providing variable damping for these systems was a big concern for many researchers who sought to reduce the motion on the structure by using passive, semi-active, and active control systems. Yet, these studies showed a difficulty in reducing the vibration below the natural frequency level with variable dampers only. On another hand, some studies have been made using a variable stiffness system along with a variable damper system. The results of these studies have exhibited an improvement in vibration control systems when compared to systems with variable damper and fixed stiffness (Liu, et al. 2005). Tan, Zhou and Yan (2004), proposed a new semi-active variable stiffness and damping (AVSD) system; they suggested adding supplemental damping to an active variable stiffness system (AVS). The new AVSD system consists of a tube filled with hydraulic oil, which connects two hydraulic cylinder-piston systems with an on-off valve. The damping and the stiffness are provided by including dampers and bracings in the device as shown in Figure 2-25. During the event, the valve will be locked and unlocked

simultaneously with the movement of the building, producing two working conditions. First, when the valve is locked, it will prevent the oil in the cylinders from flowing freely and the bracings will deliver more stiffness to the structure. The second condition will start once the valve is unlocked, where supplemental damping is produced due to the free movement of the oil between the hydraulic cylinders. As a result, the AVSD system is found to be very reliable in dissipating energy during earthquakes by altering rigidity or damping at every control interval (Tan, Zhou and Yan 2004).

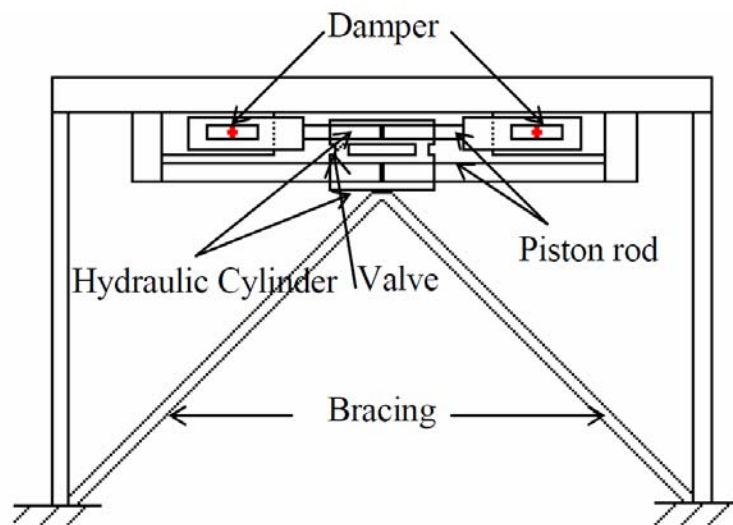


Figure 2-25: Schematic Diagram of AVSD Control Device (Tan, Zhou and Yan 2004)

2.5 Combination of Structural Control Systems

Adopting a performance-based design concept improved the performance of structures subjected to seismic and wind loads. Using a single structural control system can enhance the structural resistance by reducing the inertia forces and inter-story drifts to an acceptable level. The problem is that each structural system has a weakness. In order to get a better performance and overcome the weakness of the system, a combination of structural control systems have been investigated in recent studies.

A combination of passive, active, and semi-active control systems could be used for structural protection. In a study made by Palacios-Quinonero, et al. (2011), a passive-active control approach was used for three adjacent buildings to diminish their seismic response and to prevent inter-building pounding. The passive control system consists of a set of damping devices that work as inter-building link elements, as shown in Figure 2-26. The active control system consists of local devices implemented in the buildings in which superior seismic protection is needed. This approach was tested by numerical simulations in order to check the behavior of the system. The results have shown a significant reduction in the story drifts and elimination of inter-building pounding (Palacios-Quinonero, et al. 2011).

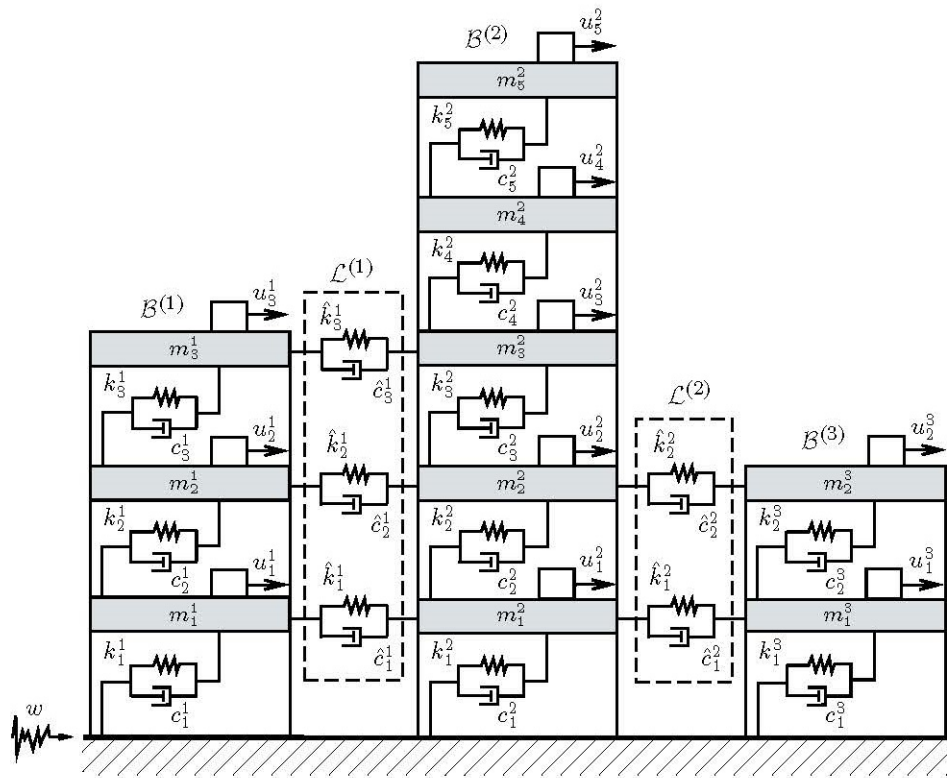


Figure 2-26: Three-building connected system (Palacios-Quinonero, et al. 2011)

Leblouba (2007) has tested combinations of the most used isolation systems, which are the high damping rubber bearing system (HDRB), the lead rubber bearing system (LRBs), and the friction pendulum system (FPS). Figure 2-27 demonstrates a three-story reinforced concrete building with a base isolation scheme that combines two of the systems mentioned before.

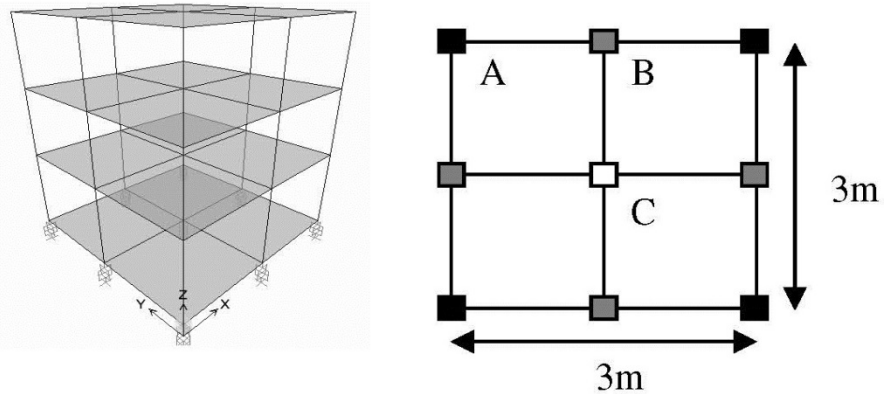


Figure 2-27: General view of the building being isolated and location of isolators (Leblouba 2007)

Six different combinations of base isolation systems were investigated as displayed in Figure 2-28. A nonlinear time history analysis was performed to evaluate each combination and to determine the best response. It was concluded that using LRBs and HDRB give almost the same amount of isolation. Also, combining the FPS with LRBs and HDRB reduced the base shear and increased the displacement. However, it appeared that using HDRB isolation decreases the cost remarkably compared to LRBs. It was shown that the combining a FPS with HDRB in structural isolation provides better performance compared to other combinations and reduces the total cost of the isolation system (Leblouba 2007).

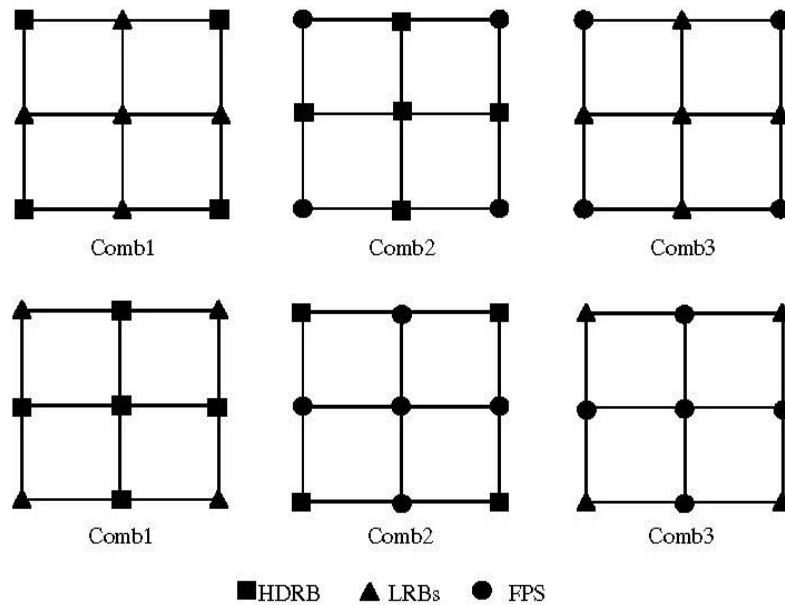


Figure 2-28: The Different Combinations Considered (Leblouba 2007)

A study was made by Marshall (2008) in which two typical passive control devices (a buckling restrained brace and a damper) were combined in a way such that the advantages of the two devices are increased and the disadvantages are eliminated. The new system was called the hybrid passive control device (HPCD). Two phases were considered during the development of the HPCD. In the first phase, a high-damping rubber sandwich damper was used to create a viscoelastic behavior for the system at this stage. It was selected due to the simplicity of the damper production and the design of the lock-out method. The second phase employed a metallic yielding device through a buckling restrained brace (BRB). This device was picked because of its ductility and popularity in lateral load resistance. Figure 2-29 demonstrate a simple representation of

the hybrid passive control device (HPCD) without the lockout mechanism of the high-damping rubber sandwich damper (Marshall 2008).

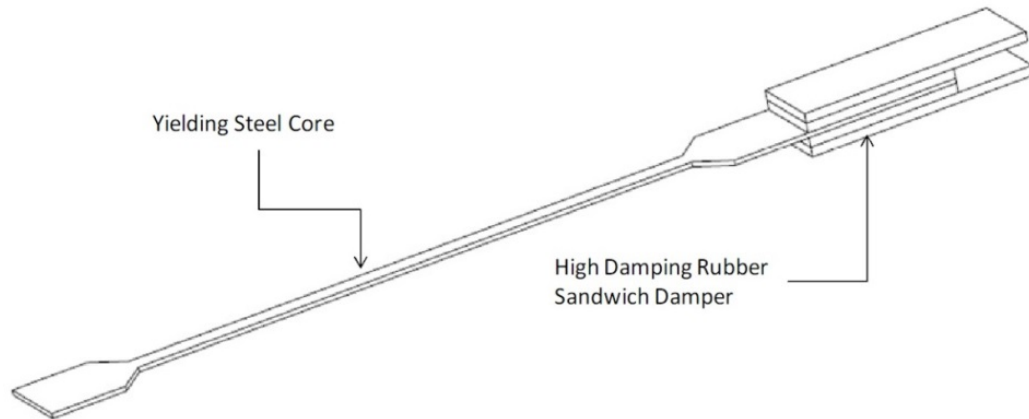


Figure 2-29: Simple Schematic of HPCD (Marshall 2008)

In order to transmit forces to the BRB, a simple lock-out mechanism was chosen to develop a smooth transition by using the slotted bolt holes concept with rubber pads bonded into the edge of the slots in the exterior steel plates, as displayed in Figure 2-30 (Marshall 2008).

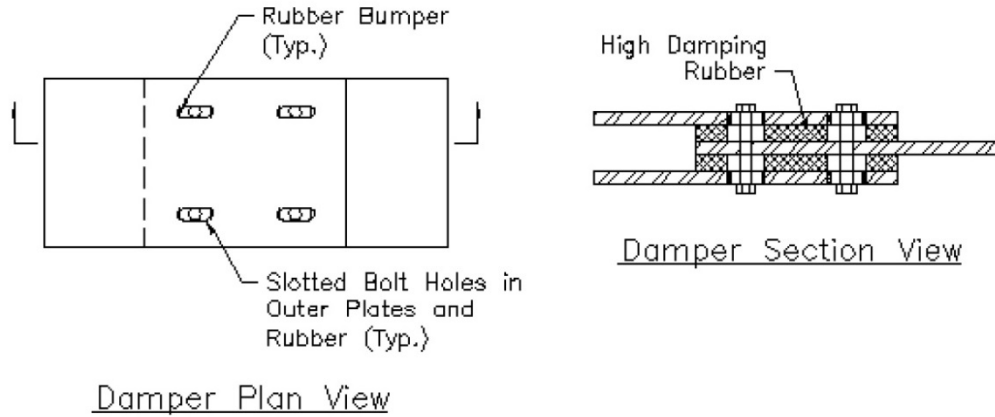
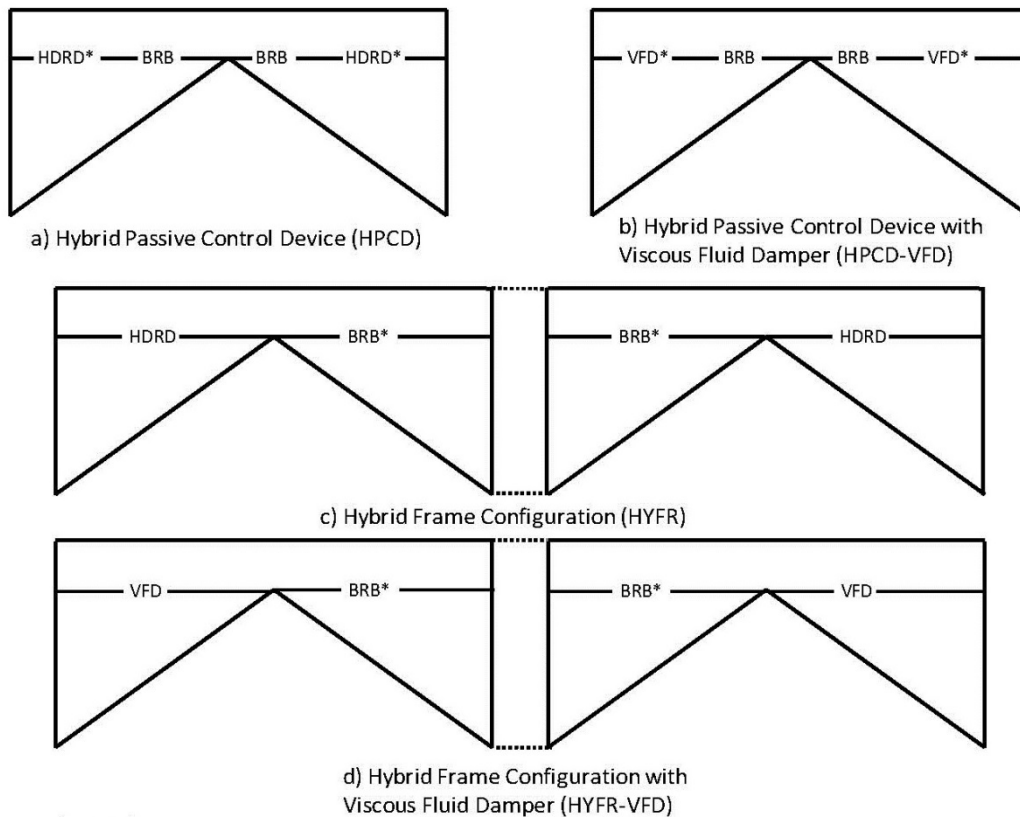


Figure 2-30: High Damping Rubber Sandwich Damper (Marshall 2008)

Nonlinear dynamic response history analysis was completed using the Computers and Structures, Inc. (CSI 2009) program SAP 2000 to compare the performance of a steel moment frame connected to different hybrid damping systems with a bare steel moment frame and a moment frame coupling typical passive control systems. Several configurations of hybrid systems were considered in this study; their arrangements are exhibited in Figure 2-31 by simplified diagrams. Table 2-1 explains the abbreviations and gives a short description of each system used in this study. These systems were applied to a 9-story building designed for conditions in Los Angeles and Charleston (Marshall 2008).

Table 2-1: Seismic Resisting System Descriptions and Abbreviations (Marshall 2008)

SMRF	Fully Code Compliant Special Steel Moment Resisting Frame (LA9 or CHA9)
BRBF	Reduced Strength SMRF with Buckling Restrained Braces
HDRD	Reduced Strength SMRF with High Damping Rubber Dampers
VFD	Reduced Strength SMRF with Viscous Fluid Damper
HPCD	Reduced Strength SMRF with Hybrid Passive Control Device
HYFR	Reduced Strength SMRF with Hybrid Frame Configuration
HPCD-VFD	Reduced Strength SMRF with Hybrid Passive Control Device Using a Viscous Fluid Damper
HYFR-VFD	Reduced Strength SMRF with Hybrid Frame Configuration Using a Viscous Fluid Damper



Legend:

HDRD – High Damping Rubber Damper VFD – Viscous Fluid Damper
 BRB – Buckling Restrained Brace

Note – An “*” denotes the element with a locking mechanism.

Figure 2-31: Diagram of Hybrid Energy Dissipation Systems (Marshall 2008)

The residual displacements along the height of the Los Angeles structure are shown in Figure 2-32 for the non-hybrid systems at the design basis earthquake (DBE) level. Each system shows a different residual drift at the end of the earthquake, and the LA9 or the SMRF structure displayed the worst behavior. Figure 2-33 shows the residual displacements along the height of the same structure for hybrid systems with rubber dampers at DBE level. A significant reduction in the residual drifts took place in all hybrid systems compared to the non-hybrid ones (Marshall 2008).

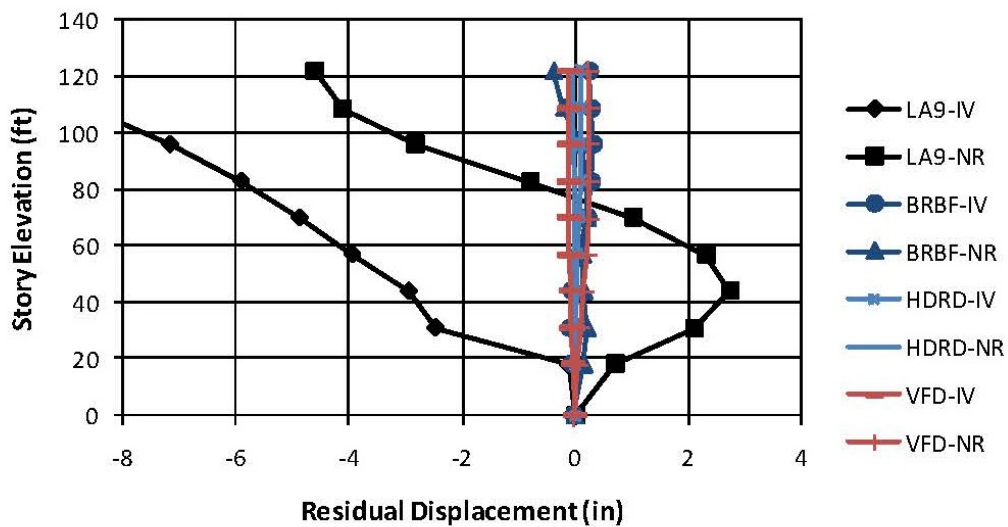


Figure 2-32: DBE Residual Displacements with Non-hybrid Systems (LA) (Marshall 2008)

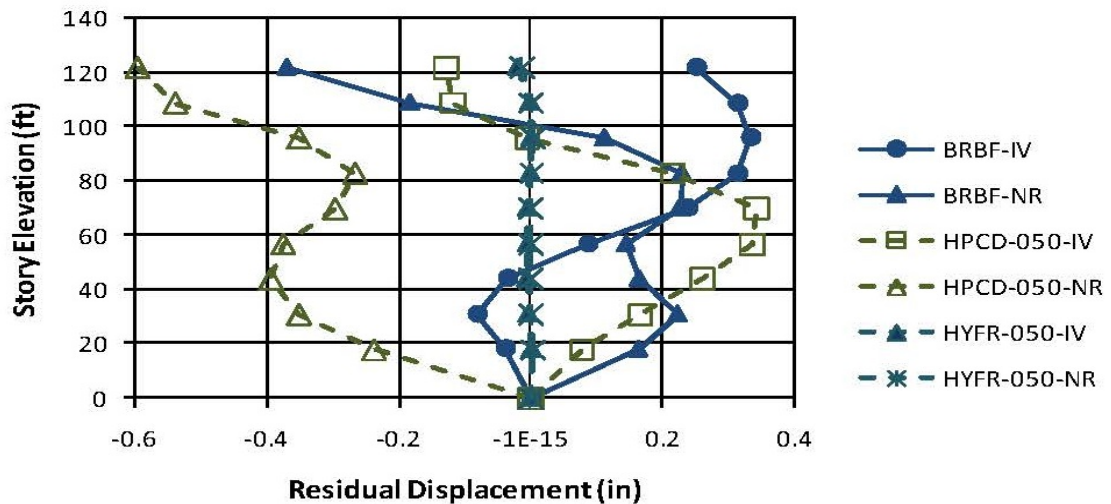


Figure 2-33: DBE Residual Displacements with Hybrid HDRD Systems (LA) (Marshall 2008)

The analysis results showed a noticeable drop in the seismic response when hybrid devices were used. Each hybrid configuration helped in reducing some aspect of structural seismic response. The transition between the first and the second phase in the device was also demonstrated, creating what is called a multi-phase behavior. However, this study was limited, and more research about hybrid devices was needed. A single degree of freedom (SDOF) research was suggested in order to closely study the effect of some variables such as initial gap size, added damping, and the BRB-to-SMRF strength ratio (Marshall 2008).

Subsequently, a SDOF study was conducted by Rawlinson (2011), with the intention of investigating the effect of combining different variables with the multi-phase control systems. Viscous fluid dampers (VFD) and viscoelastic dampers (VED) were

considered in this research as the velocity dependent device. Buckling restrained braces (BRBs) were used to provide hysteresis behavior and energy dissipation in the system. A number of factors were involved in this study: damping device, hysteretic device, system arrangement, the strength ratio of BRB-to-SMRF, seismic hazard, natural period, and transition gap size. Figure 2-34 shows the combinations involving all the variables that were considered in Rawlinson’s (2011) research. The multi-phase system abbreviations are detailed in Table 2-2 (Rawlinson 2011).

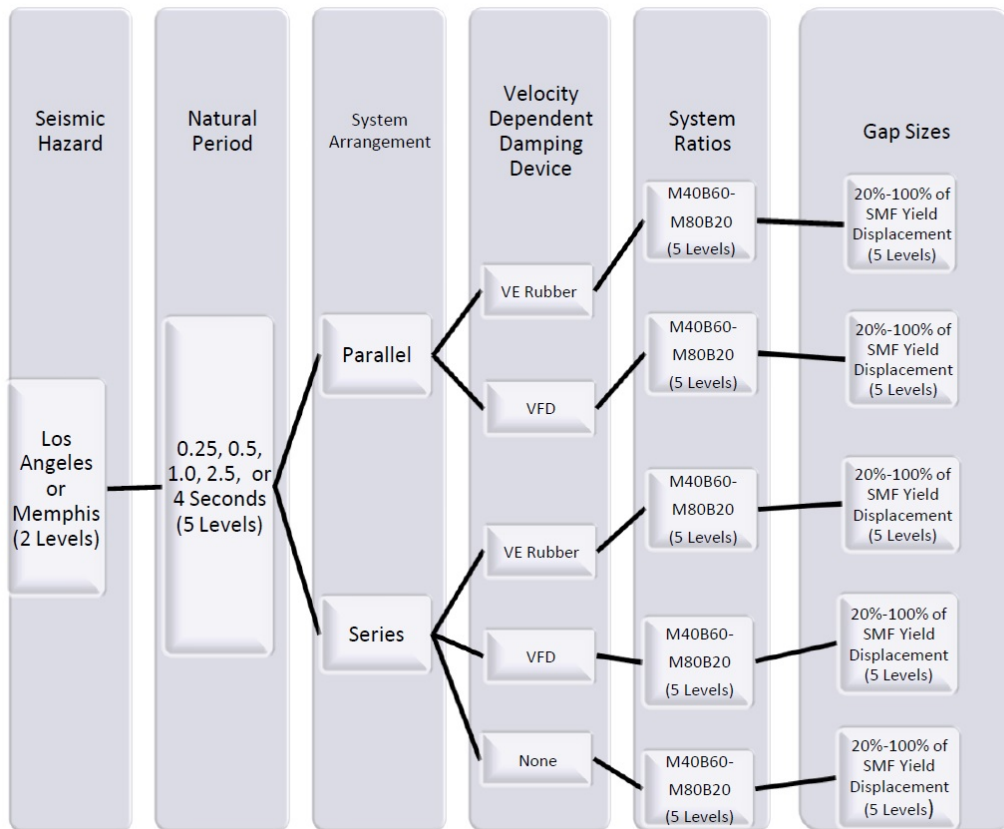


Figure 2-34: System Combinations (Rawlinson 2011)

Table 2-2: Multi-Phase Systems and Abbreviations (Rawlinson 2011)

Abbreviation	System Description
HPCD	Special moment frame with a multi-phase passive control device utilizing a BRB and high-damping rubber sandwich damper
HPCD-VFD	Special moment frame with a multi-phase passive control device utilizing a BRB and linear viscous fluid damper
HPCD-None	Special moment frame with a multi-phase passive control device with no damper
HYFR	Special moment frame with a multi-phase frame configuration utilizing an BRB and compressed elastomeric device
HYFR-VFD	Special moment frame with a multi-phase frame configuration utilizing a BRB and viscous fluid damper

The systems were modeled by using SAP 2000 (CSI 2009). A preliminary analysis was established for the SDOF models in both locations under selected ground motions to limit the research to a smaller scope. Then, a full factorial analysis was completed by comparing the structural responses of the remaining systems to narrow down the study so that a multi-degree of freedom (MDOF) study could be conducted in the future with an acceptable range of values. The full factorial analysis was accomplished by comparing the responses of the multi-phase systems to their equivalent baseline systems in order to identify the system with the best performance. Also, responses of multi-phase control systems with different natural periods, arrangements, strength ratios, and gap sizes were compared together to determine the combination that showed the best response. The selected baseline systems were composite of a special moment frame and a braced frame in a dual frame (Rawlinson 2011).

A final comparison was established for the four best multi-phase systems as presented in Figure 2-35. The four systems showed similar behavior in the moment frame yielding response and the brace ductility response. Some variances were exhibited in the acceleration and base shear responses. The acceleration spikes and residual deformations were also analyzed. The acceleration spikes did not have a great impact on the system responses. Different values of residual deformations were exhibited in the best performing systems and the HYFR system had the lowest values. In brief, the multi-phase systems showed benefits over the baseline systems, except in the moment frame ductility. The poor moment frame ductility issue can be solved by increasing the damping ratio. A MDOF research was suggested by Rawlinson (2011) in order to fully understand the multi-phase system responses with more realistic results (Rawlinson 2011).

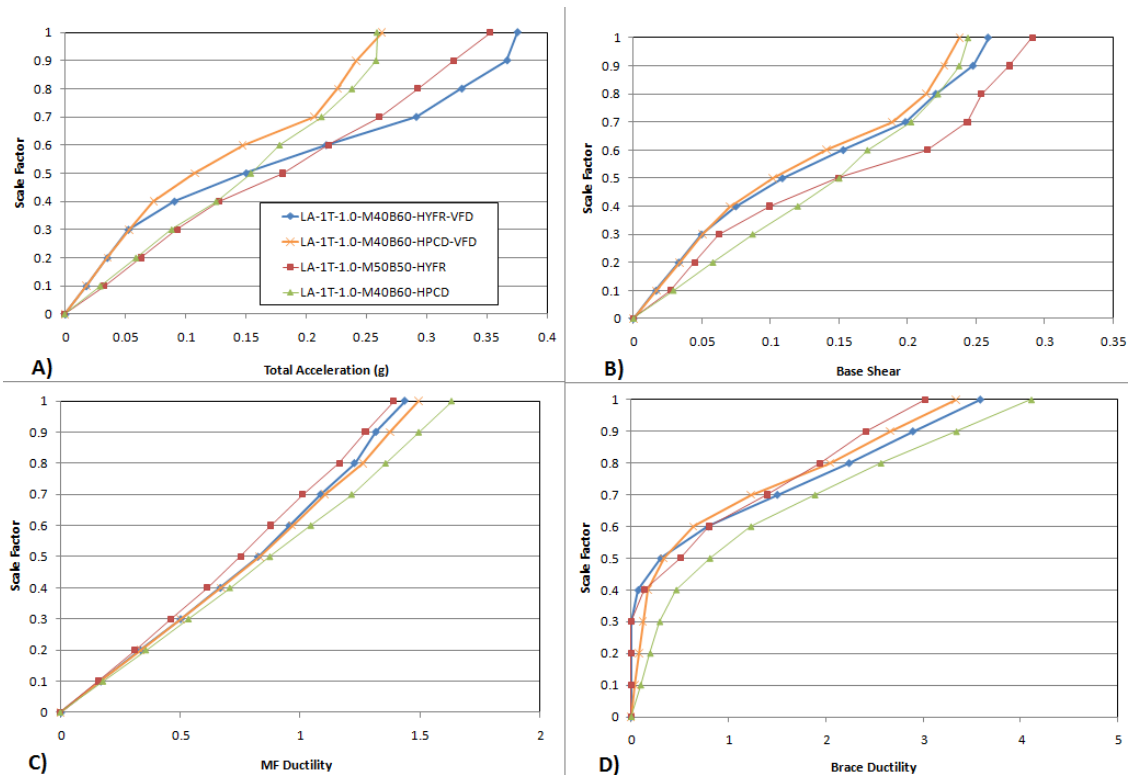


Figure 2-35: System Arrangement Comparison (Rawlinson 2011)

2.6 Summary

Establishment of performance-based seismic design has improved the structural response significantly. A selection of different types of structural control systems that fulfill this concept were briefly discussed within the literature in order to provide a general idea about their mechanisms and behavior under lateral loads. Combined structural systems developed by previous studies were also outlined. These systems demonstrated better performance by offsetting the weaknesses in the structure. A multi-phase control system mechanism is adopted by some of the combined structural systems. The advantages of the multi-phase systems are clearly presented in this chapter.

Previous studies built a solid groundwork for the MDOF study. The variables and the system combinations that affected the responses in the SDOF systems were considered in this research. The best system will be determined in the following chapters in an effort to achieve the ultimate structural performance.

Chapter 3: Parametric Study of Multi-Phase Systems

3.1 Introduction

It was necessary to develop a full understanding of the previous research in order to enable a thorough understanding of conceptual changes and improvements undertaken as part of this study. The background and terminology necessary for reader understanding was provided in Chapter 2. Also, a brief discussion of the SDOF research was presented and the groundwork for the MDOF study was defined. In this chapter, the factors that were involved in this study are described. The process of selecting the effective factors was based on the results of the SDOF study by Rawlinson (2011). The variables that showed a significant impact were adopted for this research and the ones with small or no impact were eliminated.

Since this research is about determining the effect of multi-phase passive control systems on the responses of a MDOF model, a realistic design was needed to demonstrate a real life structure. An overview on the prototype buildings and their lateral force resisting systems is presented in this chapter. These buildings will be supplemented by gap elements. The gap elements will be designed to lock out once the frame reaches the displacement limit to activate the buckling restrained braces (BRBs). The BRBs will be allowed to yield before the moment frame for structural protection.

3.2 Prototype Buildings

A series of three- and six-story steel braced frame buildings were considered for analysis. Both structures have the same geometry as in the 2000 NEHRP Professional Fellowship Report in which the SAC model building design criteria was followed (Sabelli 2001). The two buildings are office-type occupancy with Risk Category II and are located on a site class D soil in downtown Los Angeles. Building weights were adopted from the 2000 NEHRP Professional Fellowship Report and are listed in Appendix A. The plan view and the configurations of the chevron braces used in the braced bays of these buildings are shown in Figure 3-1.

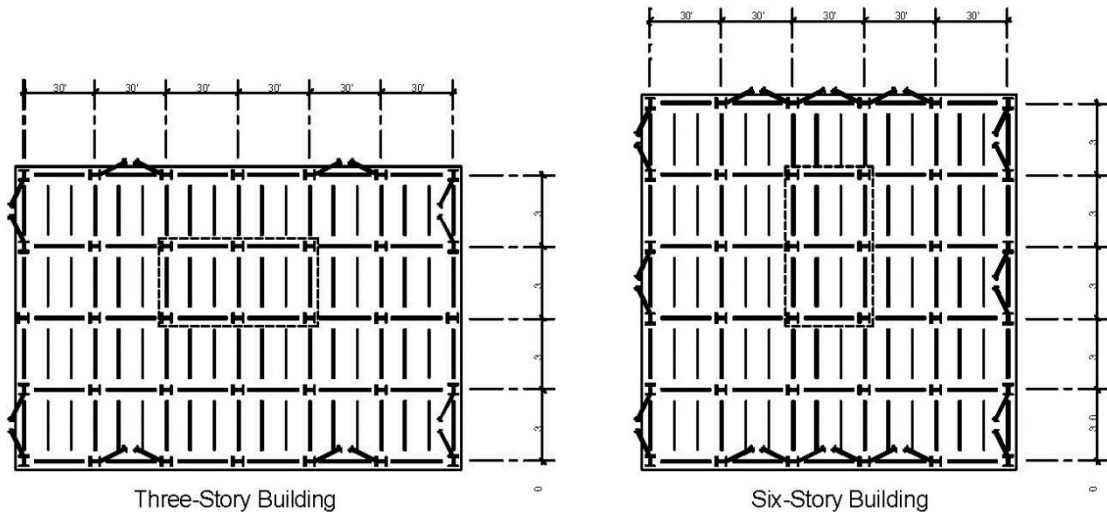


Figure 3-1: Plans of Three-Story and Six-Story Buildings (Sabelli 2001)

The three-story building has a typical story height of 13-foot. The dimensions of the building plan are 124 feet by 184 feet, consisting of 30-foot by 30-foot bays with a

small penthouse (30-foot by 60-foot) at the top of the building. The six-story building has an 18-foot height at the first story and 13-foot height for the other stories. The plan dimensions of the six-story building are 154 feet by 154 feet. The dimensions of the bays and the penthouse are the same as in the three-story building. The braced bays at each side of the two buildings are responsible for the seismic resistance.

3.3 Seismic Design

3.3.1 Local Seismicity

As stated previously, the prototype structures are located in Los Angeles, CA where the latitude and longitude are 34.05 and -118.24. The spectral acceleration values were obtained directly by using the U.S. Seismic Design Maps, which are available in the United States Geological Survey's (USGS) Earthquake Hazards Program web site.¹ The short period, S_s , and the 1 s period, S_1 , accelerations reported by the program are 2.423 g and 0.849 g, respectively. The spectral response acceleration parameters for the short period, S_{MS} , and the 1 s period, S_{M1} , of site class D are equal to 2.423 g and 1.273. These values were multiplied by 2/3 to find the design spectral acceleration parameters, which are 1.615 g for the short period, S_{DS} , and 0.849 g for the 1 s period, S_{D1} . Based on these values, the Seismic Design Category (SDC) of the structures is found as SDC D according to Tables 11.6-1 and 11.6-2 in ASCE 7-10 (ASCE 2010). Figure 3-2 shows the design response spectra for Los Angeles, CA from the U.S. Seismic Design Maps results.

¹ <http://earthquake.usgs.gov/designmaps/us/application.php>

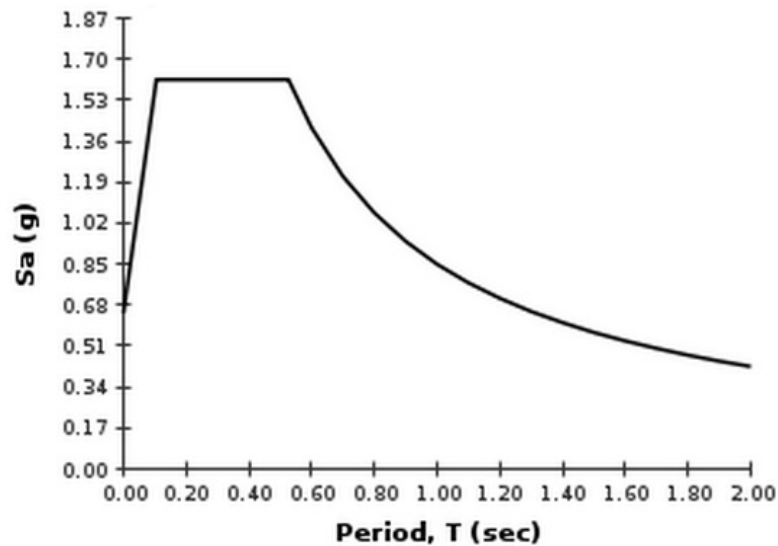


Figure 3-2: Design Response Spectrum for Los Angeles, CA from USGS

3.3.2 Equivalent Lateral Force (ELF) Procedure

The design for lateral loads was established based on the current provisions of ASCE 7-10 (ASCE 2010). The Equivalent Lateral Force (ELF) procedure was used in order to develop the loads that were used for strength requirements. Steel buckling-restrained braced frames were selected for both directions where the Response Modification Coefficient, R , equals 8, System Overstrength Factor, Ω_0 , equals 2.5, and Deflection Amplification Factor, C_d , equals 5. By using equation 12.8-7 of ASCE 7-10, the approximate fundamental period, T_a , was calculated. The approximate periods of the three-story and the six-story buildings are equal to 0.468 s and 0.825 s. The maximum periods are found by multiplying the approximate periods by the Upper Limit Coefficient, C_u , from Table 12.8-1 in ASCE 7-10. C_u was found to be 1.4 for both

buildings. Thus, the upper limit periods for strength calculations are equal to 0.655 s and 1.155 s for the three- and the six-story buildings respectively.

The total base shear, V_x , was calculated using equation 12.8-13 in order to develop the lateral seismic forces, F_x , which were found through equation 12.8-11 where V_x is multiplied by the vertical distribution factor, C_{vx} , of each story. The total base shear, V_x , was found as 1177 kip for the three-story building and 1510 kip for the six-story building.

3.4 Scaled Ground Motions

Eleven ground motions have been selected based on magnitude, source type, site class, and distance from source. The magnitudes of the ground motions ranged between 6.53 to 7.62 Mw. This suite includes far and near field earthquakes. The records were scaled so the geometric mean of the records did not go below the Maximum Considered Earthquake (MCE) spectrum over the range including the important modes to the structure. The MCE scale factors are scaled down to represent the Design (2/3) and Service level (1/4) earthquake. Each ground motion has two scale factors, one for the three-story building and the other for the six-story building. These motions are applied to the models during the response history analysis to determine the reliability, energy dissipation capability, and damping characteristics of multi-phase device. Details of the ground motions are listed in Table 3-1.

Table 3-1: Scaled Earthquake Records

Event	Year	Station Name	Direction	Magnitude	Duration (s)	Time step (s)	3-Story Scale Factor	6-Story Scale Factor
Northridge, CA	1994	Beverly Hills-Mulholland	MUL009	6.69	29.94	0.01	2.15	1.41
Duzce, Turkey	1999	Bolu	BOL090	7.14	55.89	0.01	1.82	1.24
Kobe, Japan	1995	Nishi-Akashi	NIS090	6.90	40.99	0.01	2.96	2.80
Kocaeli, Turkey	1999	Duzce	DZC270	7.51	27.20	0.005	3.46	2.36
Loma Prieta, CA	1989	Capitola	CAP000	6.93	39.97	0.005	2.06	2.21
Chi-Chi, Taiwan	1999	CHY101	CHY101-N	7.62	90.00	0.005	2.91	1.52
San Fernando, CA	1971	LA-Hollywood Stor	PEL090	6.61	27.94	0.01	4.00	4.00
Irpinia, Italy	1980	Sturno	STU270	6.89	39.35	0.0024	3.40	3.84
Imperial Valley, CA	1979	Bonds Corner	BCR140	6.53	37.60	0.005	1.42	2.70
Loma Prieta, CA	1989	Corralitos	CLS000	6.93	39.95	0.005	1.68	2.19
Chi-Chi, Taiwan	1999	TCU084	TCU084-E	7.62	90.00	0.005	1.18	0.63

3.5 System Configurations

As previously mentioned, the variables and the system combinations that affected the responses in the SDOF systems were considered in this research. In the following sections, the values of these variables and the possible combinations are discussed in more detail.

3.5.1 Moment Frame and Braced Frame Strength Ratios

Five stiffness ratios were selected by Rawlinson (2011) where the lateral forces were split between the moment frame and the buckling restrained braced frame in the dual system. The ratios were M40B60, M50B50, M60B40, M70B30, and M80B20. The first number refers to the moment frame (MF) strength ratio and the second one refers to the braced frame (BF) strength ratio. Only three system ratios were used in the full factorial analysis: M40B60, M50B50, and M60B40 (Rawlinson 2011).

In this study, the moment frame and braced frame strength ratios were assumed to be the same as in the full factorial analysis of the SDOF study. These system ratios were selected due to their high moment frame ductility performance as compared to the other system ratios. These ratios are applied to the steel buckling-restrained braced frames selected for the two buildings. Three cases of each building are considered to determine what the best system ratio is for a multi-phase system. This is developed by dividing the lateral seismic forces between the moment frame and the braced frame based on these

ratios (see Appendix A). More details regarding this will be discussed in the modelling section of Chapter 4.

3.5.2 Gap Sizes

Gap elements are used to improve the performance of the system by creating a more flexible structure initially that experiences lower forces and will not yield in smaller earthquakes. The gap elements have a lock out mechanism that creates a transition phase where the lateral load resistance is shifted from the moment frame to the BRBs. The BRB will remain ineffective until the gap locks to allow the building to be more flexible initially. By knowing that the BRB yields at about 0.5% story drift and the moment frame yields at around 1% story drift, the gap is designed to prevent the moment frame from yielding prior to the BRB yielding. To achieve this, the gap size plus the BRB yield deformation must be less than 1% story drift.

In this study, different values of gap sizes have been used than were used for the SDOF study. The gap sizes were selected to be equivalent to 0.45%, 0.30%, and 0.15% of the story height to determine the effect of various moment frame ductility levels on multi-phase system performance. Accordingly, the gap size values of the three-story building are found to be 0.7 in, 0.47 in and 0.23 in. The six-story building has different gap size for the first story than for the other stories due to different story heights. For that, 0.97 in gap size is used for the first story and 0.7 in gap size is used for the other stories

in the 0.45% case. A 0.65 in gap size was used for the first story and a 0.47 in gap size was used for the other stories in the 0.30% case. The third case is the 0.15% of the story height gap size, which equals to 0.32 in for the first story and 0.23 in for the other stories. The initial stiffness of all the gaps was chosen as 0.5 kip/in. One difference between the SDOF and MDOF study is that no supplemental energy dissipation is included in the MDOF model during the initial phase.

3.5.3 Hazard Levels

The selected prototype buildings were analyzed with a nonlinear response history analysis for three hazard levels. The eleven ground motions stated in section 3.4 were scaled at each hazard level. The hazard levels represent the percent probability of ground motion exceedance in 50 years. The Maximum Considered Earthquake (MCE) hazard level refers to a 2% probability of exceedance in 50 years, which is taken as a 100% of the ground motions. The 10% probability of exceedance is known as the Design Basis Earthquake (DBE) level which is 2/3 of the MCE ground motions. The third hazard level is the Service Level Earthquake (SLE) that has a 50% probability of exceedance in 50 years. The SLE hazard level scale factor was calculated using custom return periods based on the ASCE 41-13 maps of the United States Geological Survey's (USGS) Earthquake Hazards Program web site. The ratio of SLE was approximate to 1/4 of the MCE ground motions. In other words, the selected scale factors for MCE, DBE, and SLE hazard levels were 1.0, 2/3, and 1/4 in that order.

3.6 Baseline Systems

The baseline system consists of a dual lateral force resisting system with a moment frame and BRBs. A buckling restrained braced frame (BRBF) system was used as the baseline system to assess the multi-phase system behavior. A BRBF system was chosen due to its advantageous properties and popularity when compared to other lateral load resisting systems. This system has a remarkable seismic response owing to its symmetric hysteresis curves, high ductility ($R=8$), large drift capacity and better tolerance to fatigue loading (Asgarian and Shokrgozar 2009). In this research, the multi-phase systems have the same elements as the baseline system except for the addition of the lock-out mechanism provided by the gap element, which was not included in the baseline system. Figure 3-3 illustrates a simplified configuration of both systems, showing the spring types employed within the systems and their arrangement in the braced bay. The multilinear plastic spring was used to represent the BRB element and the multilinear elastic spring represents the gap element.

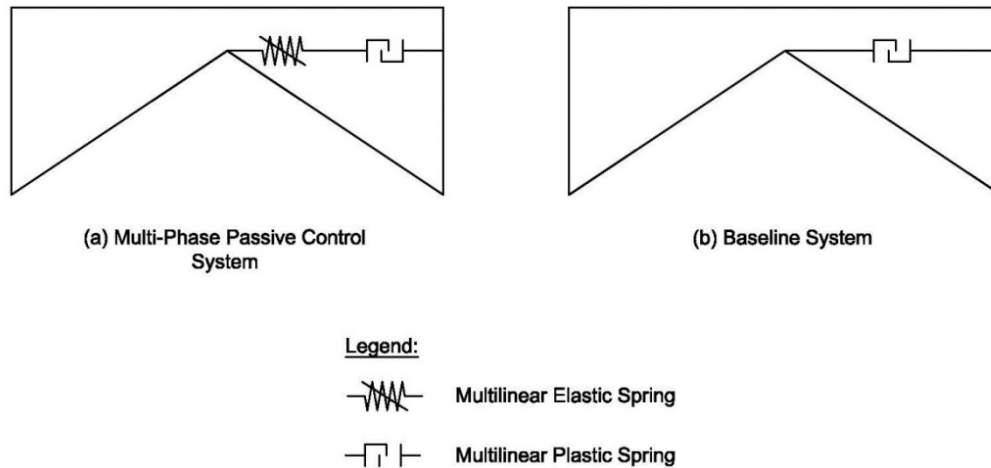


Figure 3-3: System Arrangements

3.7 System Combinations

The variables that will be involved in the system analyses were indicated earlier. The combinations of these variables provide a total of 72 models. Each model contains eleven ground motions as mentioned before. Figure 3-4 shows the system combinations for the considered variables. Results from the analyses of these systems should be sufficient to signify the potential and important parameters of multi-phase systems for enhancing the seismic response.

The identification of different system combinations in the following chapters were based on the given variables. For example, if a three-story building with a 40:60 moment frame and braced frame strength ratio and gap size equaling 0.45% of story height is subjected to ground motions scaled at the Maximum Considered Earthquake (MCE)

hazard level, the name of the system combination will be (3story_40M60B_Gap0.45%_MCE).

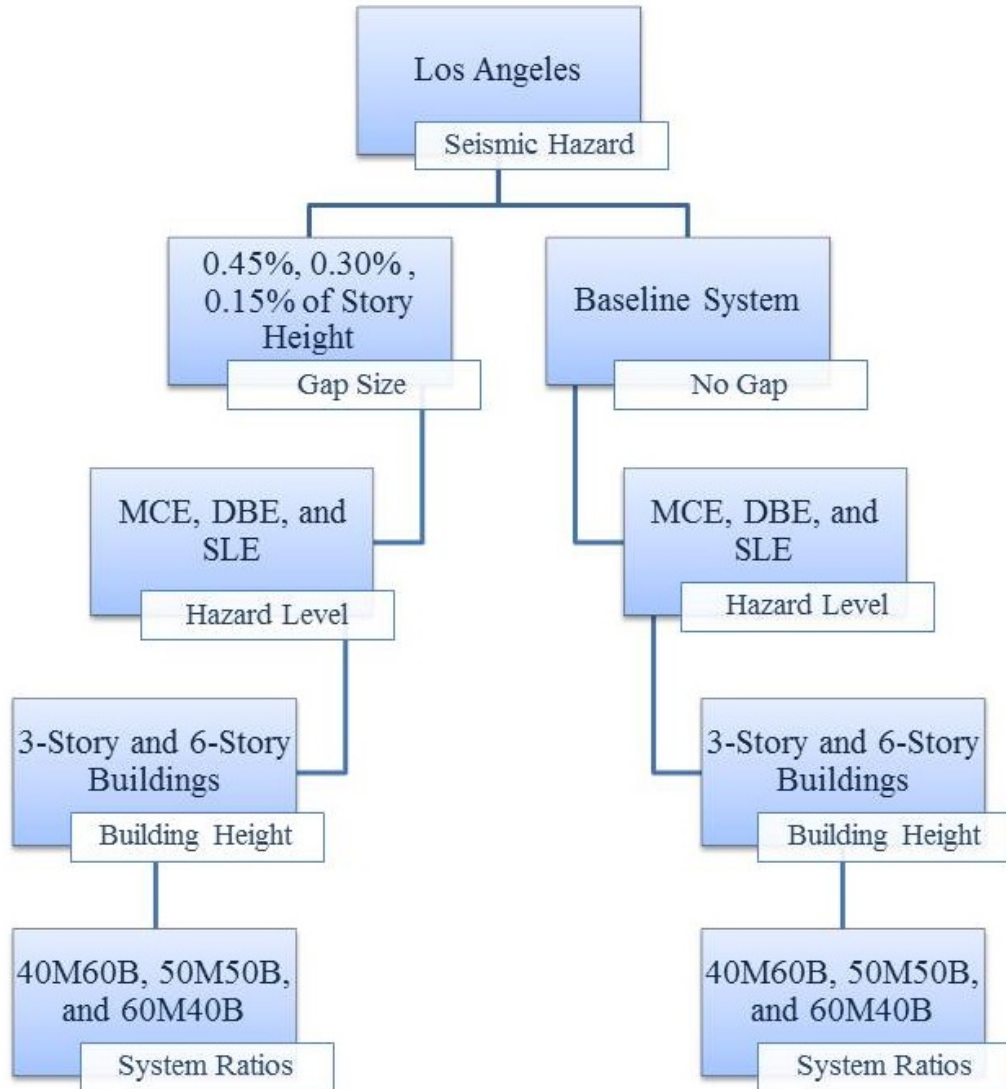


Figure 3-4: System Combinations

3.8 Summary

This chapter has discussed the parametric development and study plan. The proposed prototype buildings and their details were described. The factors involved in the analysis were listed in this chapter. Moment frame and braced frame strength ratios were chosen as 40M60B, 50M50B, and 60M40B, which are adopted from the SDOF study. The gap sizes were selected to be 0.45%, 0.30%, and 0.15% of the story height. Three seismic hazard levels were used in this study with scale factors of 1.0, 2/3, and 1/4 to account for earthquakes with various probabilities of exceedance in a span of 50 years. The building height factor was added to the analysis to determine its effect on the multi-phase device functionality. Subsequently, the design and modeling of the multi-phase and baseline systems will be discussed in detail.

Chapter 4: Structure Design and Modeling

4.1 Introduction

The analysis of a MDOF system with multi-phase control device will not be nearly as straightforward as for a SDOF system. A different response might be attributed to a certain system parameter in a MDOF system compared to a SDOF system due to the complexity of the behavior involved with the former.

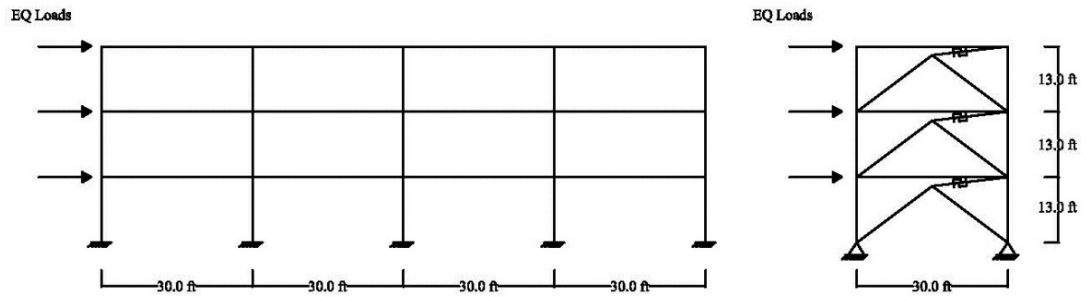
At this point, a detailed design for the prototype buildings' components is required. The capacity design method is followed in proportioning various components. The codes used for design are the AISC Seismic Provisions for Structural Steel Buildings (AISC 2005) and ASCE Standard 7-10 (ASCE 2010) along with the computer program SAP2000 (CSI 2012) for design check determinations. Also, this chapter goes through the finite element modeling process. For a reliable correlation with the prototype, it is necessary that the model has adequate simulation of the various system components. Perform 3D (CSI 2011) has been used for modeling the prototype buildings after finishing the design checks.

4.2 Prototype Design Procedure

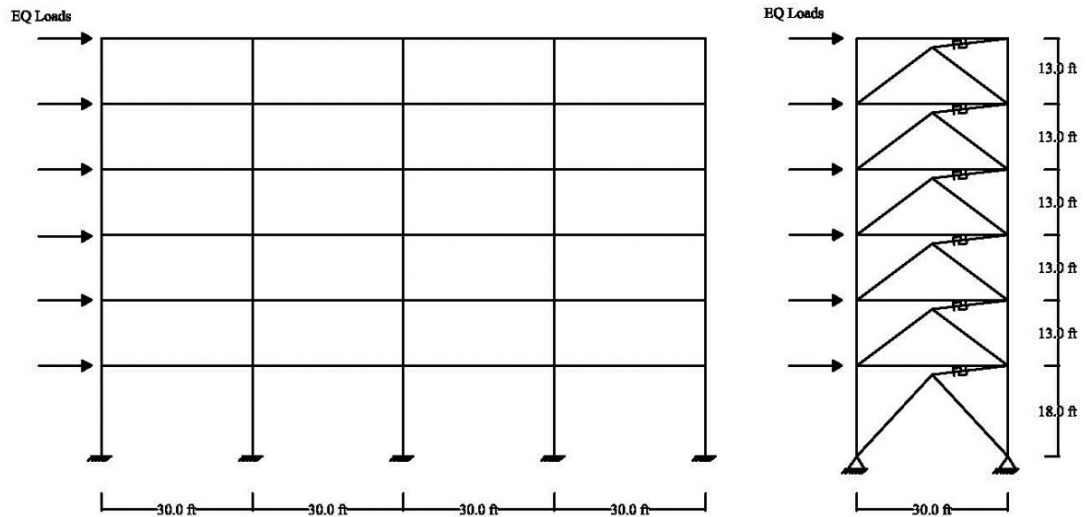
The three- and six-story buildings have been designed under the effect of the lateral loads in addition to the gravity loads (dead and live loads). The gravity loads were

assumed to be large for a safer design. A distributed dead load of 100 psf and a 50 psf live load are used for the two buildings. The amount of the applied earthquake loads differ based on the moment frame and BRBF strength ratio. From ASCE 7-10 (ASCE 2010), the load combination (1.2DL+1.0LL+1.0EQ) was used. The yield stress, f_y , of the steel elements was taken as 50 ksi for frame members and 40 ksi for BRBs with a modulus of elasticity, E , equals 29,000 ksi.

For design check determinations, a 2-D frame was created for each building by using SAP 2000 (CSI 2012). The 2-D frame basically consists of a 4-bay moment frame with a 1-bay braced frame where each of them is subjected to a certain amount of EQ loads based on the system ratios. Figure 4-1 shows the configuration of the 2-D frames for the three- and six-story buildings during the design stage.



Moment Frame and Braced Frame Configuration for the Three-Story Building



Moment Frame and Braced Frame Configuration for the Six-Story Building

Figure 4-1: 2-D Frame Configuration

4.2.1 Moment Frame Elements Design Approach

The design of the beams and columns was completed by using the interaction equations H1-1a and H1-1b from the AISC Steel Construction Manual (AISC 2005), in

which the selected steel section must satisfy the ratio boundary of the required strength to the capacity. The strong-column-weak-beam criterion was fulfilled according to the AISC Seismic Provisions (AISC 2005) for all joints. The strength of the column was required to go 20% above the beam strength for a more conservative design. More details on the design process are in Appendix A.

4.2.2 BRB Elements Design Approach

A multilinear plastic link element was used for the BRB and it is assumed to be located at one side of the chevron brace as seen in Figure 4-1. The backbone curve of the BRB was generated using the strength, area and stiffness values by assuming that the BRB is diagonal and the effective length is 50% of the total length. The criterion of the strain hardening is 3% of the elastic slope. Also, the compression force, P_{yc} , is used as 107% of the tension force, P_{yt} . Figure 4-2 details the behavior of the BRB backbone curve at the design stage.

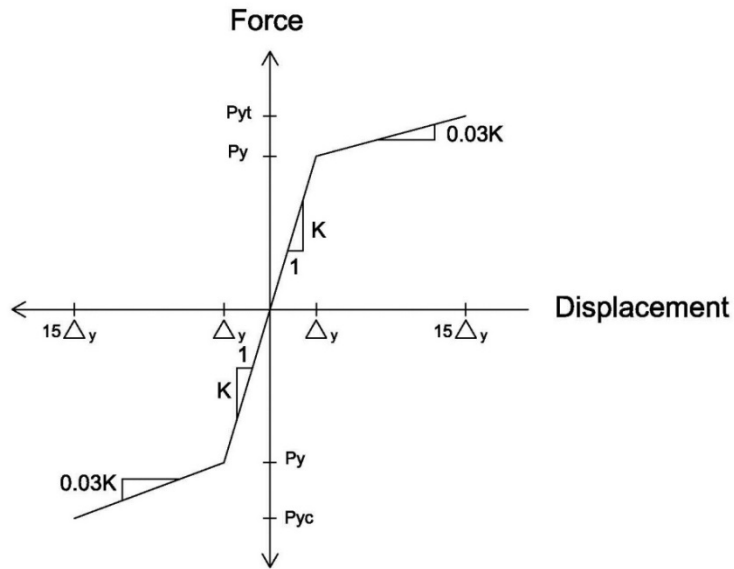


Figure 4-2: BRB Backbone Curve

4.2.3 Moment Frame Connections Design

The design of the connection was completed in accordance with the AISC Seismic Design Manual (AISC 2005). This involves checking the adequacy of the web thickness of the column at the connection as well as calculating the doubler plate thickness that need to be added to the column web.

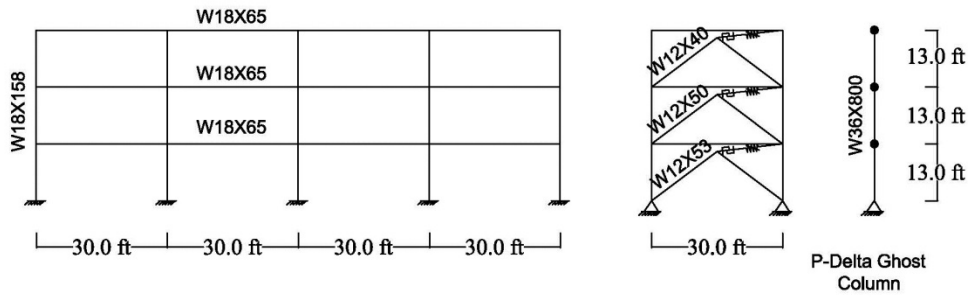
4.3 Drift Check

The story drift is defined as “the difference of the deflections at the centers of mass at the top and bottom of the story under consideration” as stated in section 12.8.6 of

the ASCE 7-10 (ASCE 2010). And the allowable story drift, Δ_a , according to the seismic design requirements in the ASCE 7-10 is given in Table 12.12-1 as $(0.02 \cdot h_{sx})$, where h_{sx} is the story height. In order to check the building's design, the inter-story drifts of the models were investigated. The peak drifts were 0.482 in, 0.542 in, and 0.588 in for the 40M60B, 50M50B, and 60M40B system ratios of the 3-story building, respectively, and 0.543 in, 0.585 in, and 0.625 in for the 40M60B, 50M50B, and 60M40B system ratios of the 6-story building, respectively, which are within the allowable limit.

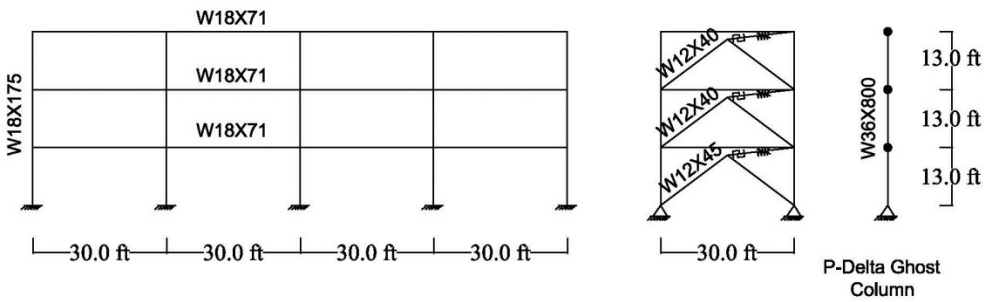
4.4 Final Prototype Building

To simulate and predict aspects of system behavior, p-delta effect was taken into consideration in order to get more realistic and accurate results. For this reason, a ghost column was employed in each building and constrained to the rest of the building. Truss elements were used for the ghost column and they are designed not to have axial deformations. The gravity dead and live loads tributary to the lateral system but not the modeled frame were assigned on the nodes of the ghost column. Figures 4-3 through 4-4 display the final design of the buildings.



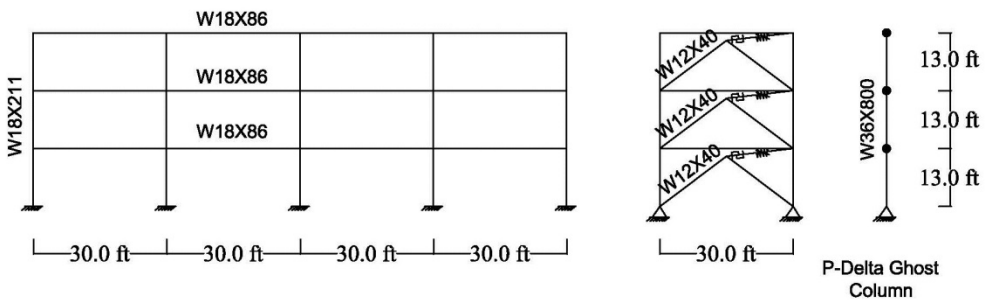
3-Story Building with 40M60B System Ratio

(a)



3-Story Building with 50M50B System Ratio

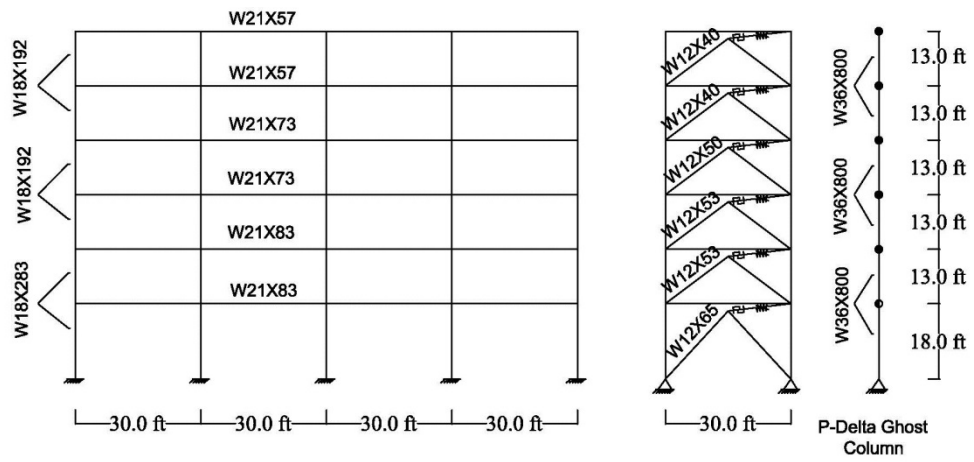
(b)



3-Story Building with 60M40B System Ratio

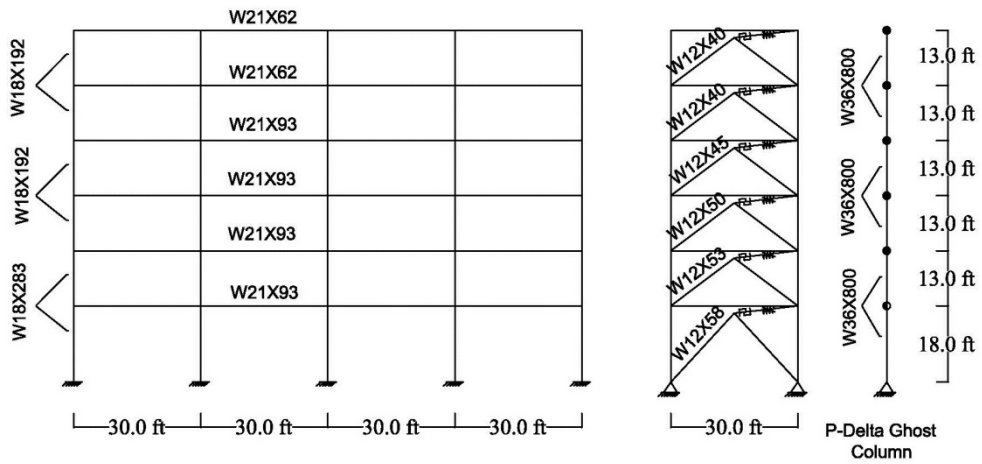
(c)

Figure 4-3: The Final Prototypes of the 3-Story Steel Frames: (a) 40M60B System (b) 50M50B System (c) 60M40B System



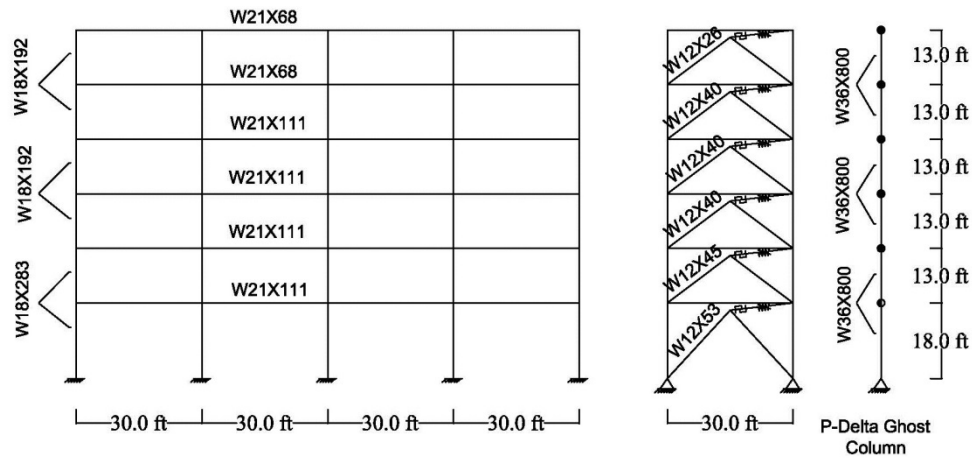
6-Story Building with 40M60B System Ratio

(a)



6-Story Building with 50M50B System Ratio

(b)



6-Story Building with 60M40B System Ratio

(c)

Figure 4-4: The Final Prototypes of the 6-Story Steel Frames: (a) 40M60B System (b) 50M50B System (c) 60M40B System

4.5 Finite Element Modeling

4.5.1 Moment Frame Elements Modeling

The prototypes shown in Figures 4-3 through 4-4 are modeled in Perform 3D V5.0. (CSI 2011). The steel moment frame elements in the moment and braced frames were modeled using FEMA steel sections with inelastic properties. There are different ways to model inelastic behavior in beams and columns. The simplest is to use the "FEMA Beam" and "FEMA Column" models which are chord rotation models that consider the member as a whole and require specifying the relationship between end moment and end rotation. These types are explicitly discussed in FEMA 356 (FEMA-356 2000) and their deformation capacities are provided. Figure 4-5 (a) shows a Perform

Frame Compound component for the chord rotation model. A proportioning length of 50% was used for each component. Perform uses the chord rotation model in Figure 4-5 (a) and converts it to the one in Figure 4-5 (b), where the FEMA component is automatically divided into a rigid-plastic hinge component and an elastic beam component. The chord rotation model assumes the yielding occurs only at the ends of the element. The steps for modeling FEMA steel column and beam are essentially the same (CSI 2006). In Perform 3D (CSI 2011), releases are treated as components. These components were used in the braced frame beams and columns for bending releases and inelastic modeling.

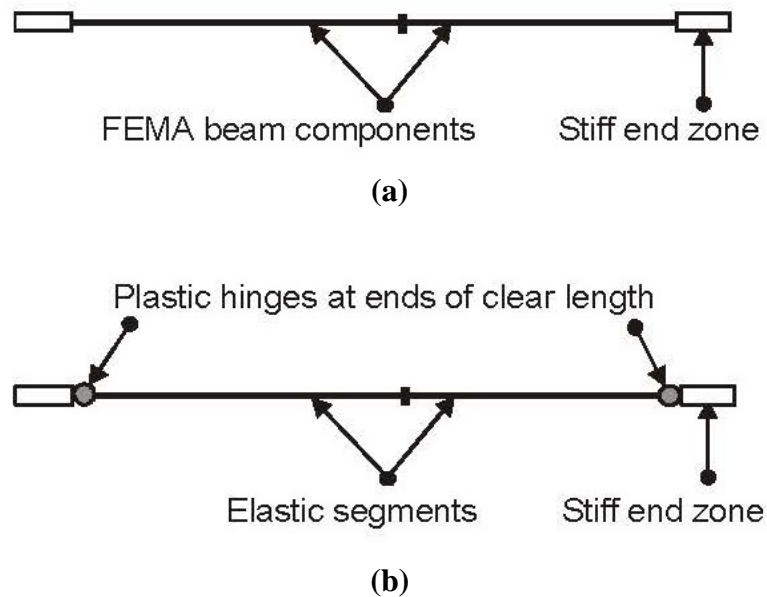


Figure 4-5: FEMA Frame Component (a) Basic Components for Chord Rotation Model (b) Implementation of Chord Rotation Model (CSI 2006)

4.5.2 BRB Elements Modeling

The BRBs in the braced frame are modeled as chevron braces and the gap elements are placed as shown in Figure 4-6. The BRB elements are modeled with post-yield hardening properties. The strength after full hardening (FUH) is taken as 1.4 of the yield strength (FU0) in the tension zone of the BRB backbone curve. In the compression zone, the FUHComp equals to 1.07 of FUHTen. Figure 4-7 shows the backbone curve of the BRB elements.

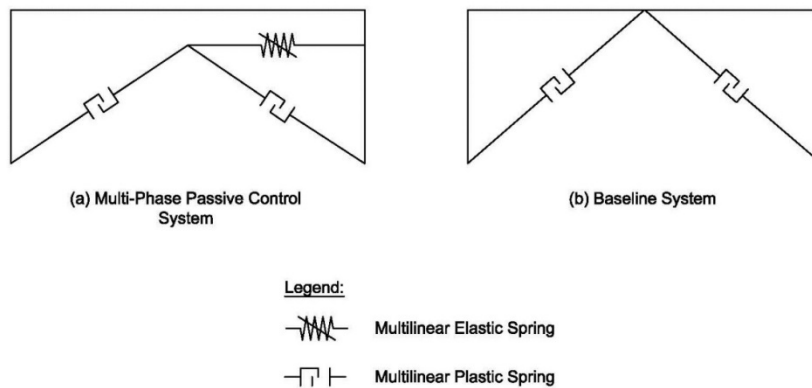


Figure 4-6: System Arrangement

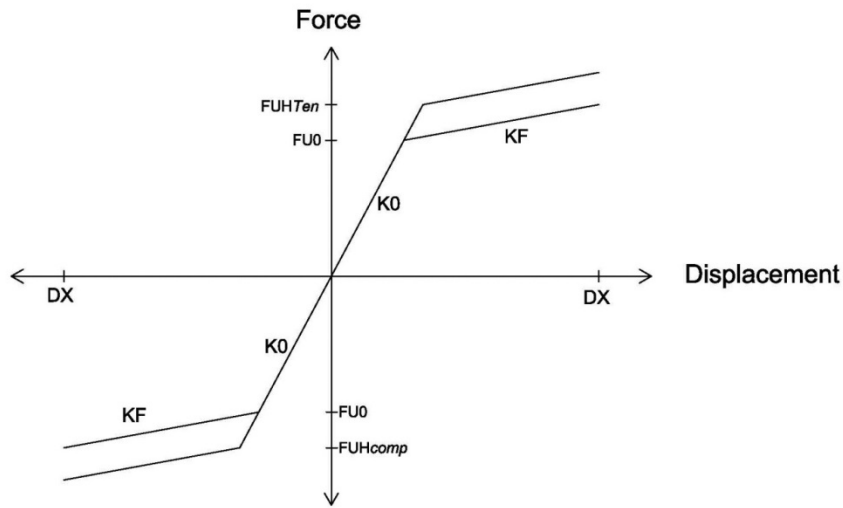


Figure 4-7: BRB Backbone Curve

4.5.3 Gap Element Modeling

The gap elements are modeled using nonlinear elastic gap-hook with multilinear elastic properties. The gap element was placed in series with the BRB element in the braced frame. The backbone curve of the gap was developed by assuming an initial stiffness of 0.5 kip/in. Figure 4-8 displays the gap backbone curve behavior where the maximum tension and compression forces are assumed to be 125% of the BRB tension and compression forces of the same story. The displacement of the moment frame is dependent on the gap size. When the moment frame reaches the desired displacement, the mechanism will lock out and the gap will become extremely stiff. Then, the seismic loads will be carried by both the BRB and moment frame elements based on their stiffness.

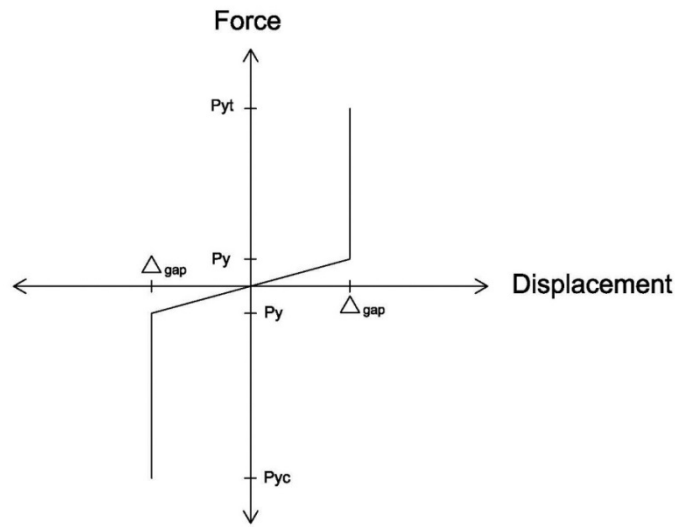


Figure 4-8: Gap Backbone Curve

4.5.4 Moment Frame Connections Modeling

The connection panel zones with multilinear plastic behavior are assigned to the moment frame beam-column joints. The beam-column panel zone in Perform 3D (CSI 2011) is based on the Krawinkler model. The model for the panel zone component is shown in Figure 4-9 consists of four rigid links connected with rotational springs at the corners. The beam-column connection transfers bending moment from beams to columns subjecting the panel zone to shear stresses and causing beam and column cross sections rotation as shown in Figure 4-10. The moments and shears of adjacent columns and beams are acting on the rigid links. The strength and stiffness of the connection is provided by the rotational springs (CSI 2006).

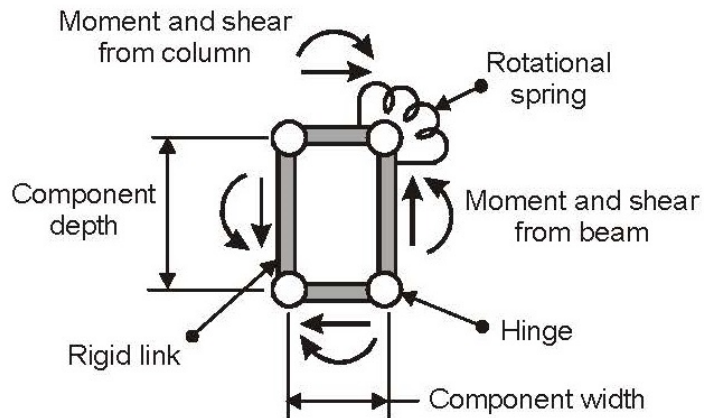


Figure 4-9: Model for Panel Zone Component (CSI 2006)

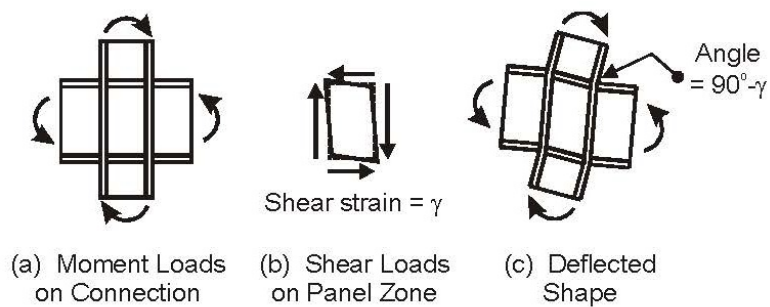


Figure 4-10: Distortion in Connection Panel Zone (CSI 2006)

Each component of the Krawinkler model has the force deformation behavior presented in Figure 4-11. The vertical axis is presenting the shear force and the horizontal axis presenting the strain due to the shear. It can be observed from the force deformation relationship that the panel will resist the shear immediately. After the panel yields, the flange will start providing resistance until it yields at 4.0 times the yield strain of the panel (Charney and Marshall 2006).

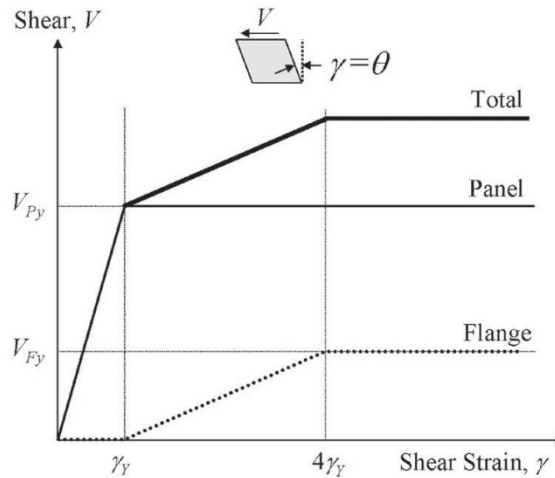


Figure 4-11: Force-Deformation Relationship for the Krawinkler Model (Charney and Marshall 2006)

4.5.5 Inherent Damping

Modal damping of 3% was used for the first and second modes periods. Additionally, damping equal to 0.025% was added to the system through Rayleigh proportional damping for the natural periods between 0.25 to 1.5 seconds. The model periods of each system are obtained directly from Perform models. The values of the model periods are varied with the change of the system ratio and building height as seen in Table 4-1. The addition of the gap element has no effect on the model periods.

Table 4-1: The First and Second Mode Periods of Different Prototypes

	Building Height	System Ratio	First Mode Period (s)	Second Mode Period (s)
Multi-Phase System & Baseline System	3-Story Building	40M60B	1.253	0.26
		50M50B	1.191	0.248
		60M40B	1.057	0.225
	6-Story Building	40M60B	2.242	0.702
		50M50B	2.108	0.671
		60M40B	1.957	0.641

4.6 Summary

In this chapter, the design procedure of the prototype buildings is discussed in detail. The design was completed using the AISC Seismic Provisions for Structural Steel Buildings (AISC 2005) and ASCE Standard 7-10 (ASCE 2010) along with the computer program SAP2000 (CSI 2012). The final prototype buildings were presented after the drift check is completed. Also, this chapter discussed the finite element modeling procedure for moment frame and braced frame components by using Perform 3D (CSI 2011). Next, the analysis will be established for the models to provide the results leading to the best system combination.

Chapter 5: Analysis of Results and Data Presentation

5.1 Introduction

In this chapter, a broad analytical parametric study was accomplished by involving all system combinations across all earthquake levels to identify the best system performance. Nonlinear dynamic response history analysis was completed using the Computers and Structures, Inc. (CSI) program Perform 3D (2009). An overall comparison between the multi-phase systems and baseline systems was completed to show the benefits of a multi-phase system. The effect of the building height, gap size, strength ratio, and earthquake level was taken into consideration when analyzing the results. A more specific analysis was made by calculating system indices in order to clearly identify the best system combination. A check was made to find the effect of the gap lockout mechanism on generating large accelerations by comparing the gap force and displacement responses with nodal accelerations.

5.2 Comparison to Baseline Systems

The analysis of the multi-phase systems is completed by comparing them to the baseline systems based on the story drift, nodal acceleration, moment frame plastic hinge rotation, and cumulative BRB ductility results. Figures 5-1 through 5-3 show the

comparisons between the 3-story buildings with the 40M60B system ratio for each gap size with the baseline system. Similarly, Figure 5-4 through Figure 5-6 illustrate the performance of the 6-story building with 40M60B system ratio for the three gap sizes and the baseline system. The rest of the results for the other system combinations are available in Appendix B.

The multi-phase system is represented in these figures by the box plot to display the distribution of the data based on five numbers: minimum value, first quartile, median, third quartile, and maximum value. The baseline system is represented by two solid lines demonstrating the maximum and the average values. The results in each figure involve all the load cases of the eleven ground motions for different scale factors.

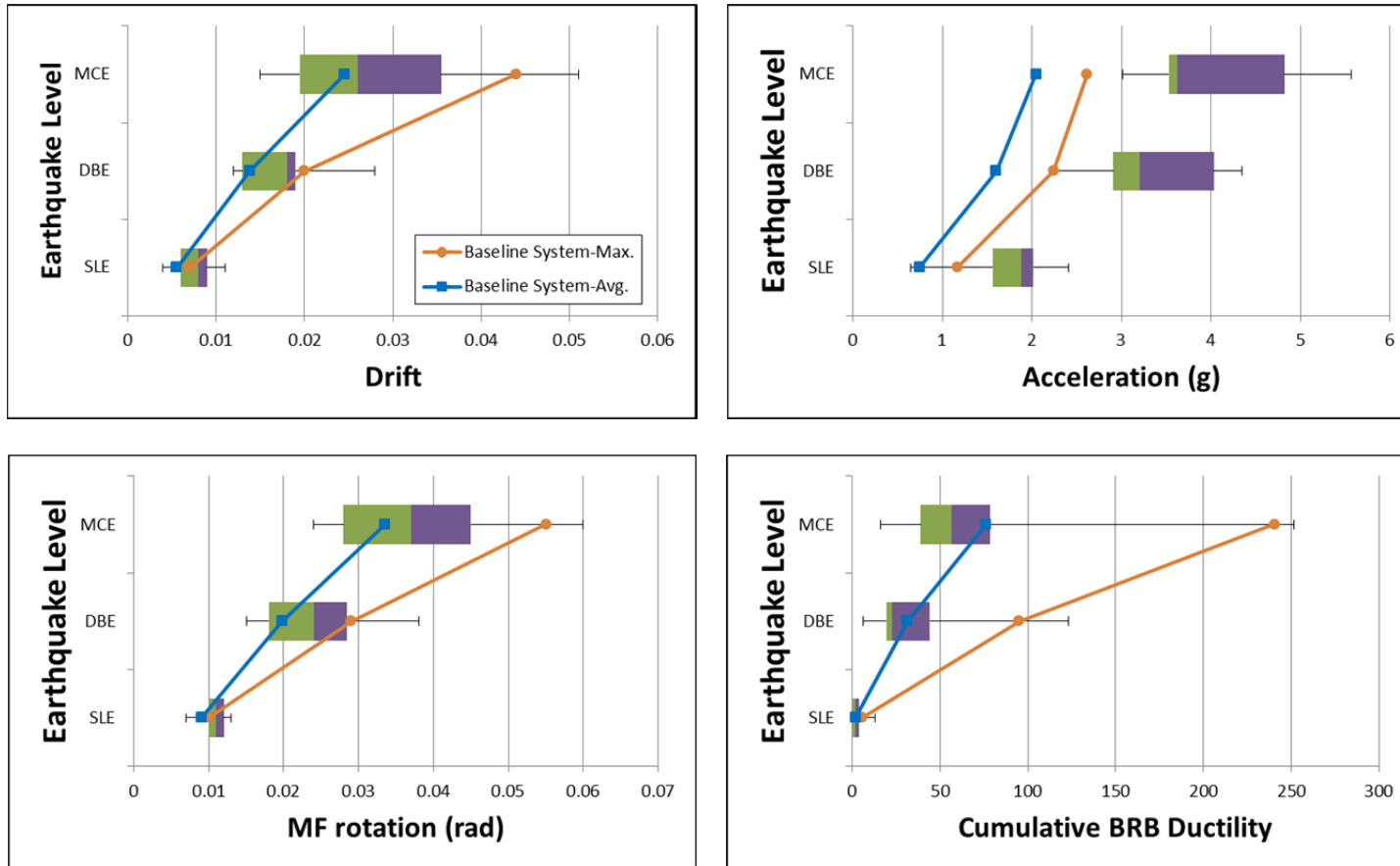


Figure 5-1: 3-Story_40M60B_Gap0.45% with Baseline System

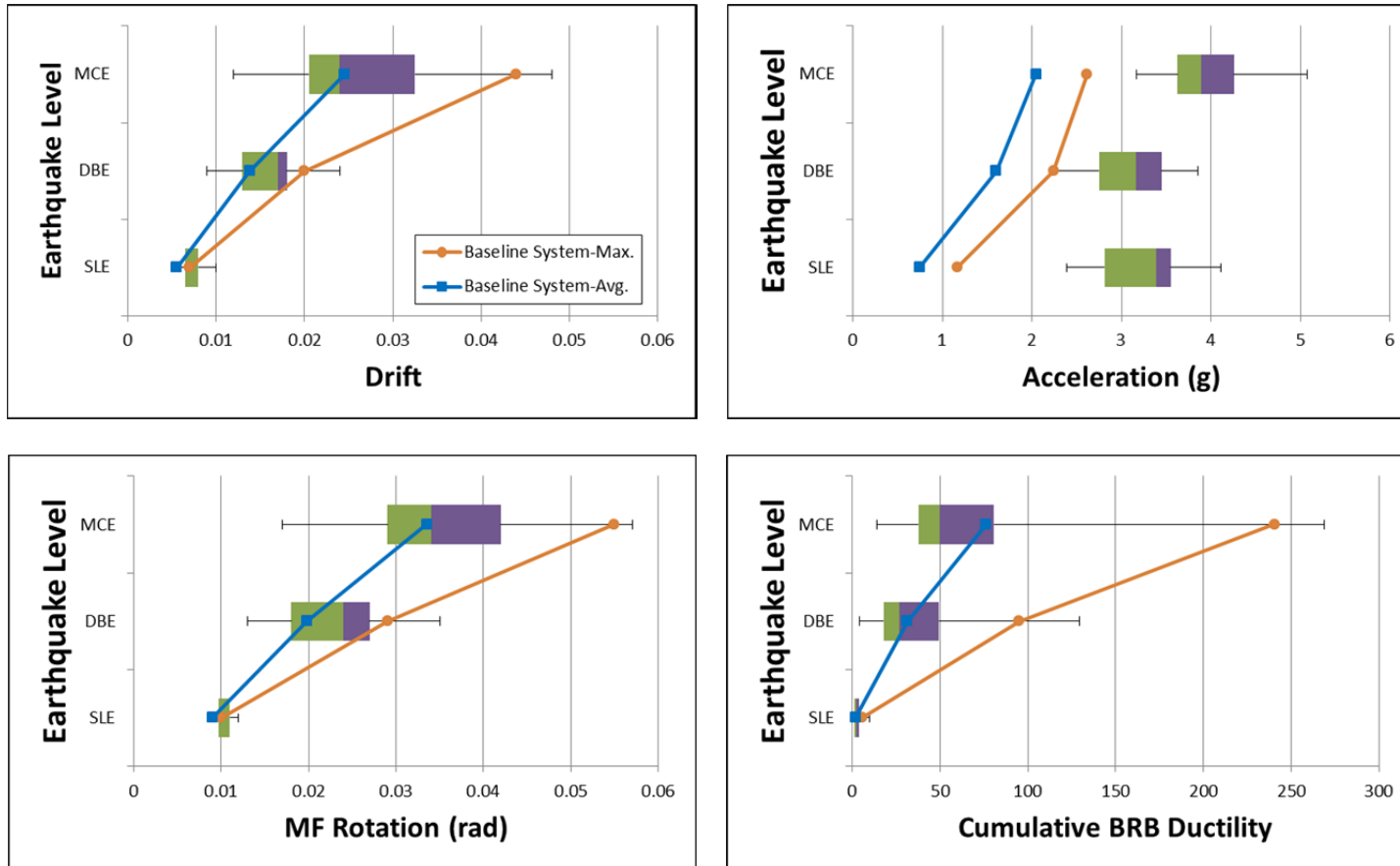


Figure 5-2: 3-Story_40M60B_Gap0.30% with Baseline System

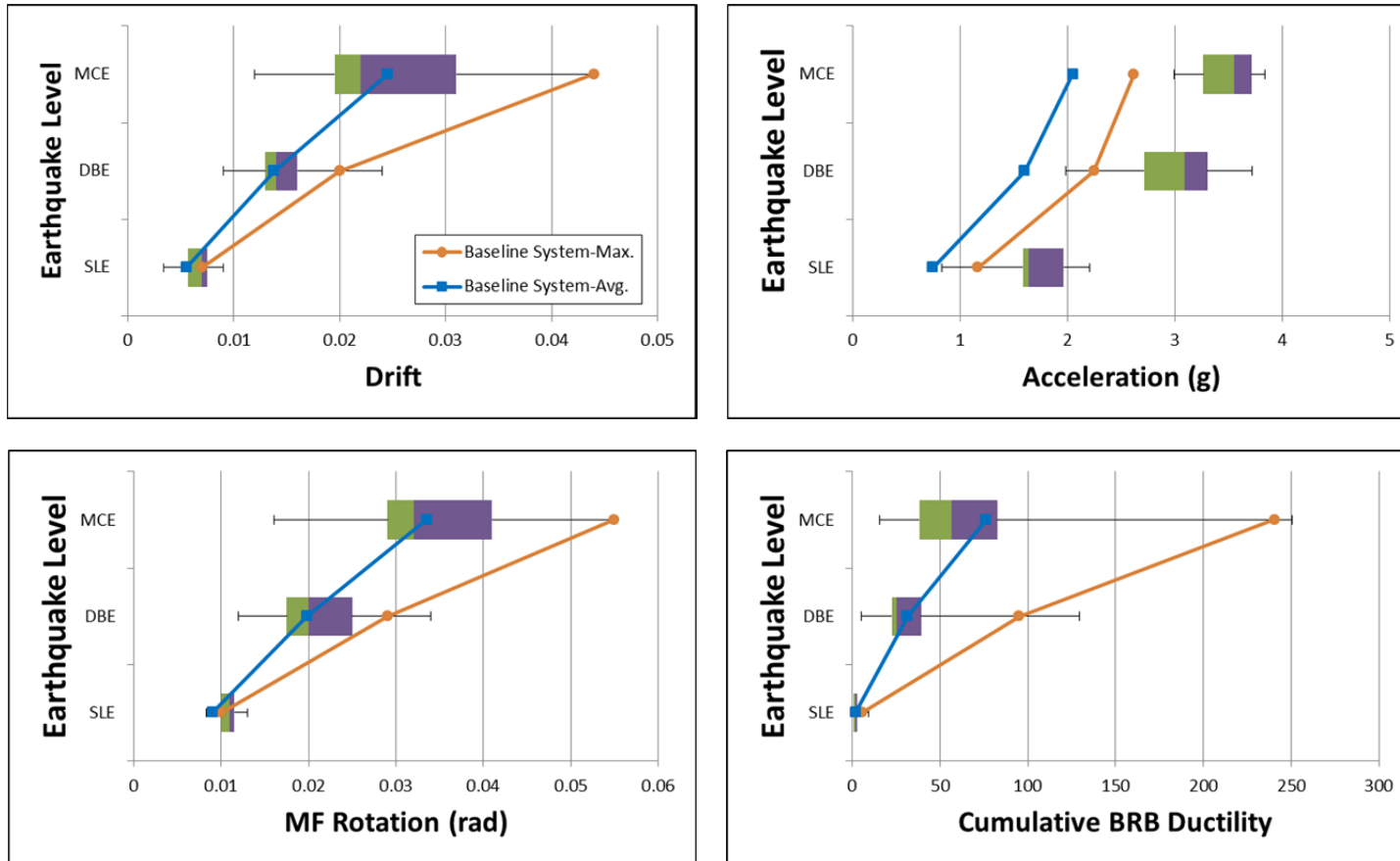


Figure 5-3: 3-Story_40M60B_Gap0.15% with Baseline System

By observing the 3-story building responses in Figures 5-1 through 5-3, it is noticed that the 0.15% gap size combined with the 40M60B system ratio results in a slightly better performance relative to the other gap sizes. Responses at the MCE level show better behavior in the 40M60B system across all response quantities for the three gap sizes except acceleration, where the performance is varied between the SLE and DBE levels. Overall, all the 40M60B system combinations have poor performance when compared to the baseline systems.

In the 50M50B system ratio, the best performance in each response quantity varies with the gap size variation. The 0.15% gap has better story drift response and MF ductility response relative to the 0.45% and 0.30% gap sizes in all levels as a result of decreasing the moment frame yielding limit in the 0.15% gap size. The acceleration response is slightly better in the 0.45% gap size than the other two sizes. The BRB ductility response shows better performance in the 0.45% gap size across all earthquake levels. The BRB ductility response has remarkably improved in the 50M50B system ratio compared to the 40M60B system ratio. However, the MF ductility response has decreased in the 50M50B due to increasing the strength ratio of the moment frame.

For the 60M40B system ratio, the BRB ductility response shows the best performance in the 0.45% gap relative to the 0.30% and 0.15% gap sizes through all earthquake levels. Story drifts and MF ductility show better responses in the 0.15% as in 50M50B system ratio. Acceleration response varies through all the gap sizes and earthquake levels.

When comparing different system ratios responses, it was observed that the story drifts have superior performance in the 40M60B system with small gap size at MCE level and the average value at the DBE level, this is normal for having less moment frame resistance and strength ratio. On the other hand, the maximum values at the DBE level for 50M50B and 60M40B systems with small gap sizes performed better than the 40M60B system. Very small values exist at the SLE level that makes the best performance hard to recognize. The MF ductility is showing better performance in the 40M60B system with small gap size comparing to the other two systems across all levels except for the maximum value at the DBE level. The BRB ductility has the best performance in systems with high moment frame strength ratio and large gap size where more resistance and participation is provided by the moment frame.

In general, the 3-story building shows poor performance when compared to the baseline system except in the BRB ductility response that improved significantly in the 50M50B and 60M40B system ratios especially at the MCE and DBE levels. Also, story drifts are better than the baseline system in the 40M60B system with 0.15% gap size at the MCE level that is due to the limited yielding of the moment frame as well as less moment frame strength ratio. The variation and the great increase in the acceleration responses might be caused by acceleration spikes generated from the gap lockout mechanism.

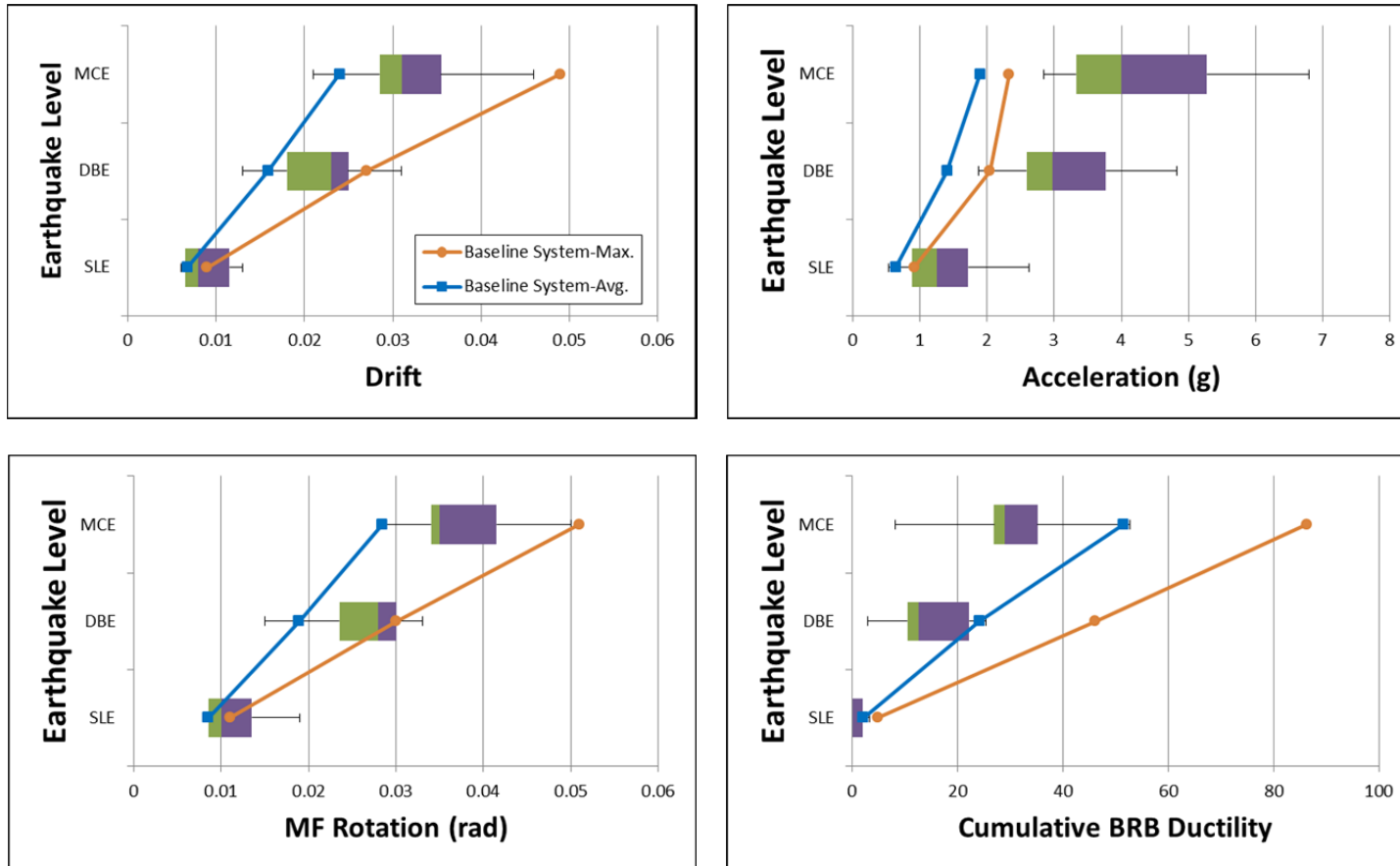


Figure 5-4: 6-Story_40M60B_Gap0.45% with Baseline System

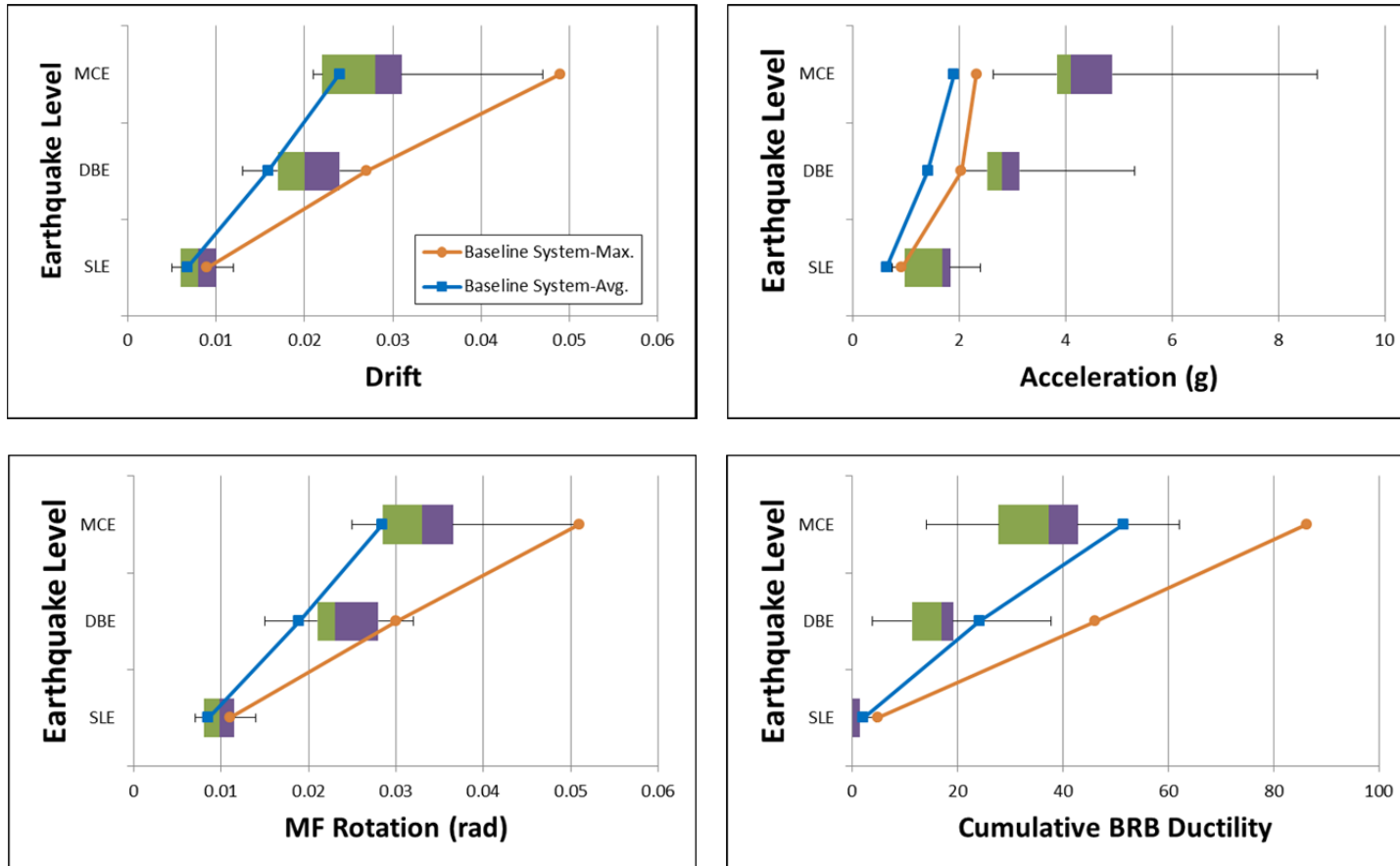


Figure 5-5: 6-Story_40M60B_Gap0.30% with Baseline System

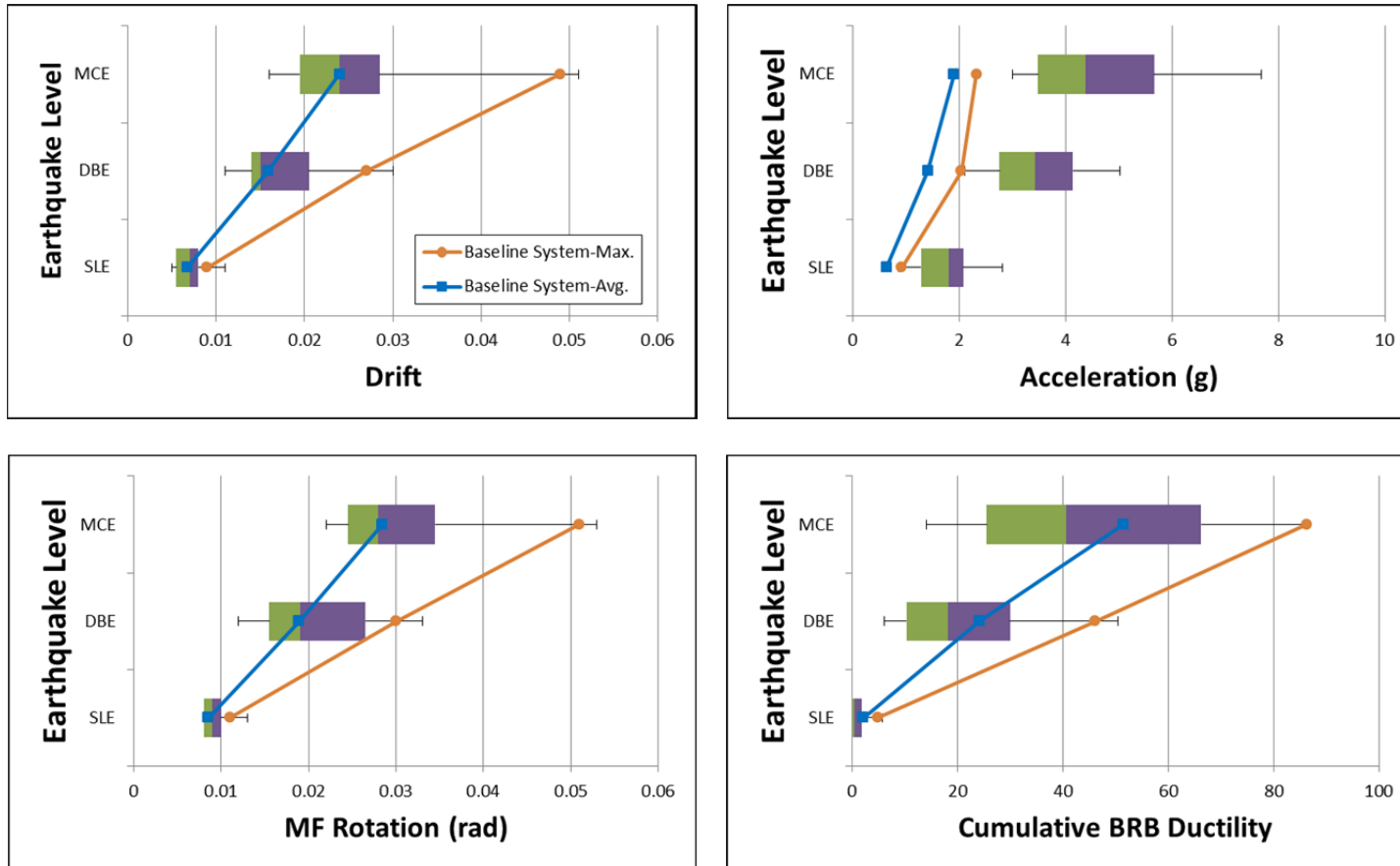


Figure 5-6: 6-Story_40M60B_Gap0.15% with Baseline System

By observing the 6-story building responses in Figures 5-4 through 5-6, it was noticed that the 0.15% gap size combined with different system ratios has an overall better performance in the story drifts and moment frame ductility responses comparing to the other gap sizes across all earthquake levels. The 0.45% gap size in different system ratios performed the best regarding the BRB ductility at all earthquake levels comparing to the 0.30% and 0.15% gap sizes. The acceleration responses are very close for the different gap sizes in each system ratio and earthquake level.

After taking a comprehensive look on the different system combinations, it was noticed that the 0.15% gap size story drift and MF ductility responses are performing better in the average values across all earthquake levels comparing to other gap sizes. However, the 0.30% gap size has better maximum story drift results in all system ratios especially at the MCE and DBE levels. And the MF ductility maximum values have improved in the 0.45% and 0.30% gap sizes at the MCE level of all system ratios comparing to the 0.15% gap size.

The BRB ductility maximum values are slightly better in the 60M40B system with small gap size at the MCE and DBE levels compared to other system ratios with the same gap size. For large gap sizes, the average values of the BRB ductility at the DBE level are somewhat improved with the increase of the braced frame strength ratio. The acceleration values present constant responses with the change of the system ratio except some small improvements at the SLE level when increasing the moment frame strength ratio and decreasing the braced frame strength ratio.

By looking at the story drift results in different system ratios, similar responses occur with the change of the system ratio in all earthquake levels except in the 60M40B system with different gap sizes at the DBE level, the drift responses are relatively poor. The MF ductility responses show a slightly better performance in the 50M50B system with 0.30% and 0.15% gap sizes compared to other system ratios.

Overall, the 6-story building performed much better than the 3-story building when compared to the baseline system. A great improvement was demonstrated in the 6-story multi-phase systems regarding the story drift, MF ductility, and BRB ductility responses in certain combinations. The high accelerations in the multi-phase systems compared to the baseline systems might be due to the sharp stiffness transition that the system is subjected to during the activation of the gap elements. This means that these accelerations might be partially due to numerical issues and the building will not suffer the same magnitudes in a real event. The effect of the high acceleration spikes caused by the lockout mechanism will be discussed later in this chapter.

In order to identify the best system combination in the two buildings, the indices in Table 5-1 through Table 5-2 were found for the four parameters (drift, acceleration, MF rotation, cumulative BRB ductility) per system. These indices will help to indicate the best performance by finding the ratio value of multi-phase system performance to the baseline system. Where, the average of the maximum values for all ground motions of a multi-phase system over the average of the maximum values for all ground motions of a corresponding baseline system gives a better evaluation on the multi-phase system

performance. Also, the ductility performance index (DPI) was found to determine the amount of overall ductility improvement in a system. The DPI value is obtained from equation 5-1.

$$DPI = \left(\frac{MF \text{ Rotation}}{\text{Baseline MF Rotation}} + \frac{BRB \text{ Ductility}}{\text{Baseline BRB Ductility}} \right) * \frac{1}{2} \quad \text{Equation 5-1}$$

To achieve the ductility demand goal, the DPI ratio must be less than or equal to 1.0. Values more than 1.0 verify that the multi-phase system performance was decreased compared to the baseline system.

Table 5-1: 3-Story Building Systems Indices

Response Quantity	40M60B w/ 0.45% Gap			50M50B w/ 0.45% Gap			60M40B w/ 0.45% Gap		
	MCE	DBE	SLE	MCE	DBE	SLE	MCE	DBE	SLE
Drift	1.19	1.27	1.41	1.20	1.44	1.61	1.22	1.43	1.64
Acceleration	2.03	2.11	2.36	1.75	1.92	1.74	1.64	1.76	1.48
MF Rotation	1.15	1.23	1.20	1.17	1.46	1.45	1.21	1.44	1.46
Cum. BRB Ductility	0.98	1.13	1.48	0.80	0.69	1.48	0.75	0.61	1.26
DPI	1.07	1.18	1.34	0.98	1.07	1.46	0.98	1.03	1.36

Response Quantity	40M60B w/ 0.30% Gap			50M50B w/ 0.30% Gap			60M40B w/ 0.30% Gap		
	MCE	DBE	SLE	MCE	DBE	SLE	MCE	DBE	SLE
Drift	1.13	1.17	1.36	1.18	1.36	1.40	1.18	1.32	1.50
Acceleration	1.92	1.94	4.31	1.75	1.96	1.69	1.77	1.58	1.56
MF Rotation	1.08	1.16	1.17	1.16	1.36	1.26	1.18	1.34	1.27
Cum. BRB Ductility	1.03	1.21	1.60	0.95	0.86	1.11	0.90	0.82	1.16
DPI	1.05	1.18	1.39	1.05	1.11	1.19	1.04	1.08	1.21

Response Quantity	40M60B w/ 0.15% Gap			50M50B w/ 0.15% Gap			60M40B w/ 0.15% Gap		
	MCE	DBE	SLE	MCE	DBE	SLE	MCE	DBE	SLE
Drift	1.05	1.09	1.18	1.10	1.13	1.26	1.10	1.14	1.30
Acceleration	1.70	1.85	2.26	1.75	2.08	2.52	1.66	1.73	1.97
MF Rotation	1.03	1.07	1.20	1.08	1.16	1.13	1.09	1.16	1.16
Cum. BRB Ductility	1.02	1.19	1.30	1.04	1.08	1.45	1.03	1.06	1.47
DPI	1.02	1.13	1.25	1.06	1.12	1.29	1.06	1.11	1.32

From the Table 5-1, it is observed that the 3-story building showed poor performance compared to the baseline system. However, the BRB ductility and the DPI have small values in the 50M50B and 60M40B systems with large gap size at MCE and DBE levels. Also, the 50M50B and 60M40B systems with medium gap size have less BRB ductility at the MCE and DBE levels. The reason behind that is the increase of the gap size will decrease the BRB ductility due to less energy dissipation required from the hysteretic braces. Moreover, high moment strength ratio increases the moment frame resistance.

Table 5-2: 6-Story Building Systems Indices

Response Quantity	40M60B w/ 0.45% Gap			50M50B w/ 0.45% Gap			60M40B w/ 0.45% Gap		
	MCE	DBE	SLE	MCE	DBE	SLE	MCE	DBE	SLE
Drift	1.36	1.37	1.34	1.29	1.36	1.34	1.20	2.24	1.29
Acceleration	2.35	2.29	2.13	2.08	2.20	1.95	1.86	2.08	1.65
MF Rotation	1.33	1.39	1.36	1.30	1.11	1.27	1.22	1.43	1.22
Cum. BRB Ductility	0.60	0.62	0.51	0.58	0.59	0.51	0.62	0.61	0.42
DPI	0.96	1.01	0.94	0.94	0.85	0.89	0.92	1.02	0.82

Response Quantity	40M60B w/ 0.30% Gap			50M50B w/ 0.30% Gap			60M40B w/ 0.30% Gap		
	MCE	DBE	SLE	MCE	DBE	SLE	MCE	DBE	SLE
Drift	1.23	1.26	1.22	1.20	1.25	1.21	1.14	2.07	1.16
Acceleration	2.47	2.21	2.34	2.19	2.39	2.02	1.95	2.22	1.76
MF Rotation	1.22	1.28	1.17	1.20	0.99	1.16	1.14	1.26	1.16
Cum. BRB Ductility	0.72	0.73	0.48	0.76	0.69	0.39	0.75	0.70	0.49
DPI	0.97	1.01	0.82	0.98	0.84	0.78	0.95	0.98	0.82

Response Quantity	40M60B w/ 0.15% Gap			50M50B w/ 0.15% Gap			60M40B w/ 0.15% Gap		
	MCE	DBE	SLE	MCE	DBE	SLE	MCE	DBE	SLE
Drift	1.09	1.09	1.07	1.08	1.11	1.12	1.05	1.80	1.11
Acceleration	2.46	2.48	2.74	2.19	2.30	2.22	1.82	2.28	2.13
MF Rotation	1.10	1.10	1.11	1.08	1.09	1.09	1.02	1.09	1.12
Cum. BRB Ductility	0.90	0.91	0.69	0.88	0.86	0.57	0.86	0.88	0.63
DPI	1.00	1.01	0.90	0.98	0.97	0.83	0.94	0.99	0.87

As seen in Table 5-2, the 6-story building has clearly improved compared to the 3-story building. In comparison to the baseline system, the BRB ductility values and the DPI values display significant improvement in all system combinations. Also, the MF ductility performance was improved in some combinations especially in systems with small gap sizes but the performance was far from ideal.

During the examination of the two buildings ductility values, it was noticed that the BRB ductility is less than the MF ductility in all cases of the 6-story building. In the 3-story building, the BRB ductility is smaller than the MF ductility in most cases. But, higher BRB ductility values especially in the high earthquake levels were required because of the extensive energy dissipation capabilities and the ability to replace the BRB element after an event. As previously discussed, the goal of this study is developing a multi-phase system that can protect the moment frame by limiting yielding to the replaceable element because the damage of moment frame is expensive and hard to repair. Further solutions for moment frame protection need to be investigated.

In conclusion, it was shown that employing a gap element has some benefits. The gap enhanced the overall ductility of the system by reducing the ductility demands between the moment frame and the braced frame. But this enhancement comes at the cost, though, of higher acceleration response and poor moment frame performance. If there is a way to improve the multi-phase system performance further is by adding some early phase energy dissipation to the system to decrease the accelerations and thus reduce the deformations in the system. There is a potential to show great benefits from the multi-

phase system by adding early phase damping to it. Yet, the high acceleration values of the multi-phase system could be resulting from large acceleration spikes generated during the phase transitions. More details about this subject will be described in the next section.

5.3 Effect of Acceleration Spikes

As seen before, the multi-phase systems suffered high acceleration values compared to the baseline systems, which could be related to the lockout mechanism of the gap where sharp stiffness transitions are created during the process. These transitions are caused by closing and opening the gap coinciding with the movement of the structure. In order to investigate the acceleration spikes effect, the Imperial Valley, CA record at the MCE level was selected to examine the response of the 6-story building with 40M-60B ratio and 0.30% gap size because of the high acceleration indices it demonstrated earlier.

Figure 5-7 shows the comparison between the nodal acceleration of the multi-phase system and the baseline system at the roof. Large acceleration magnitudes were attributed by the multi-phase system which may have been caused by the opening and closing of the gap elements. Figure 5-8 displays the force and displacement response of the first floor gap element. It is clear from the displacement response that the gap is closing. Also, the force and the displacement behaviors are very closely related. Meaning that, the two parameters are responding to the gap lockout mechanism.

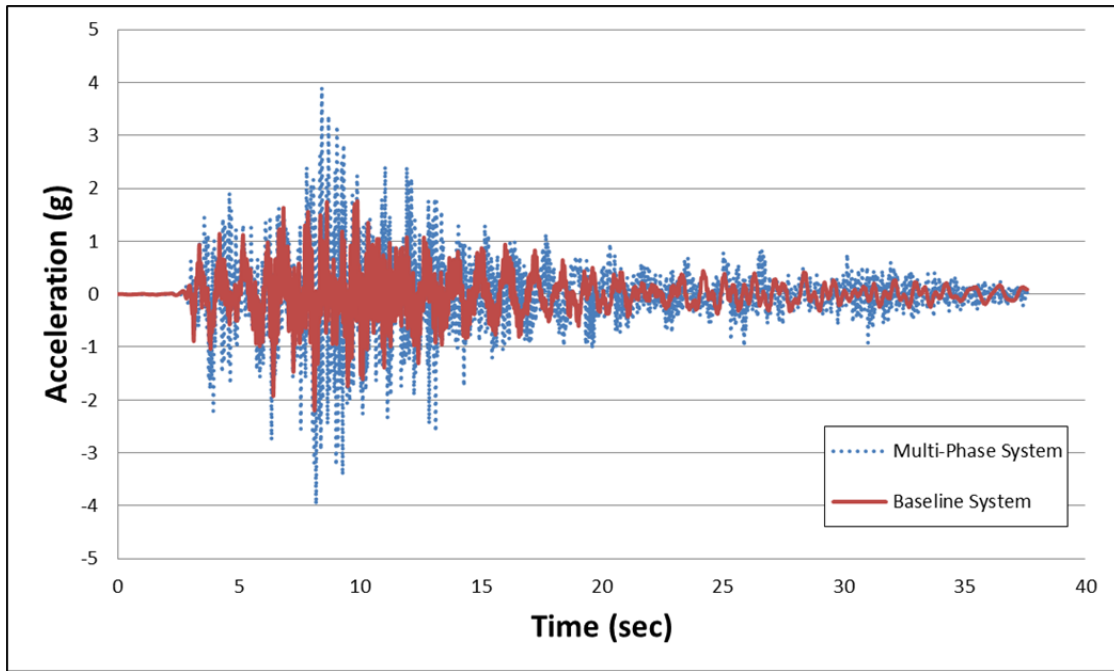


Figure 5-7: Roof Accelerations of Multi-Phase System and Baseline System

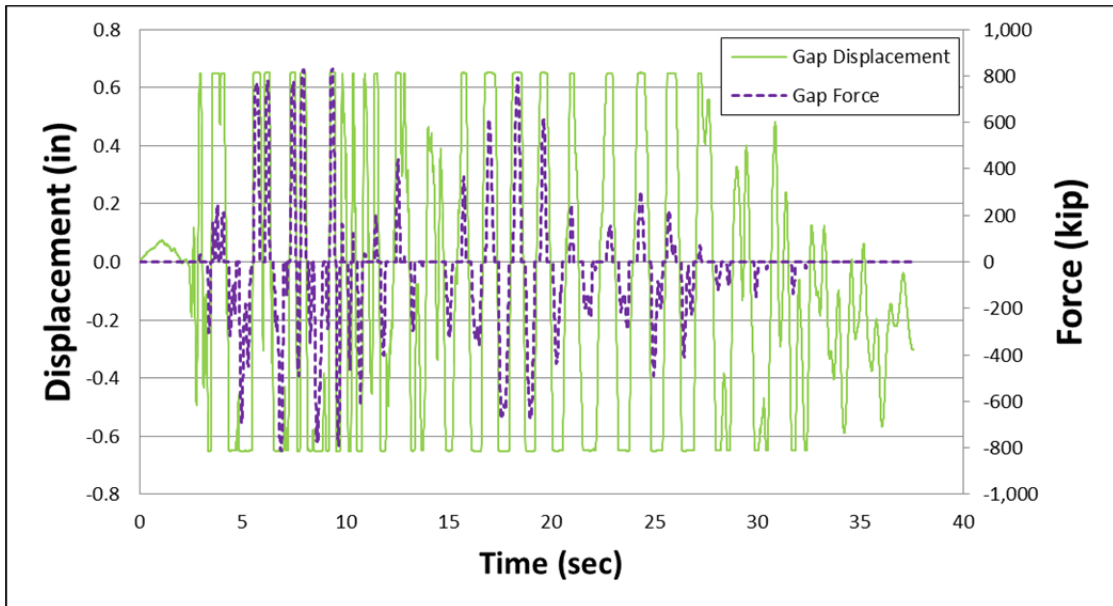


Figure 5-8: 1st Floor Gap Forces and Displacements

A close look at the acceleration response corresponding to the gap element behavior is taken through comparing the nodal acceleration response with the gap element force and displacement responses in the first floor as shown in Figures 5-9 and 5-10. From these figures it does not look like there is any huge spike generated by the gap element. Probably some of these accelerations are due to the fact that other gaps are closing and opening at the same time creating stiffness discontinuity in addition to the ground acceleration. Some spikes could be created due to the greater flexibility of the system. However, the results do not show clear effect by the acceleration spikes on acceleration response in the multi-phase system. Adding more damping to the system might help in reducing the high accelerations. Also, the gap transition modeling needs to be investigated by using a less sharp force-displacement behavior.

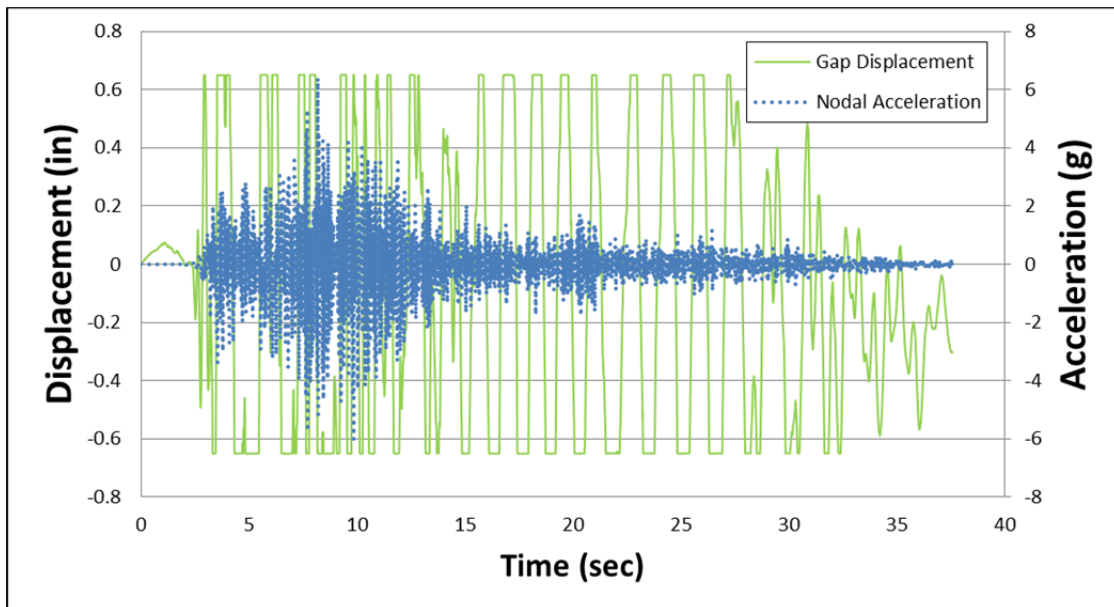


Figure 5-9: 1st Floor Gap Displacements versus Nodal Accelerations

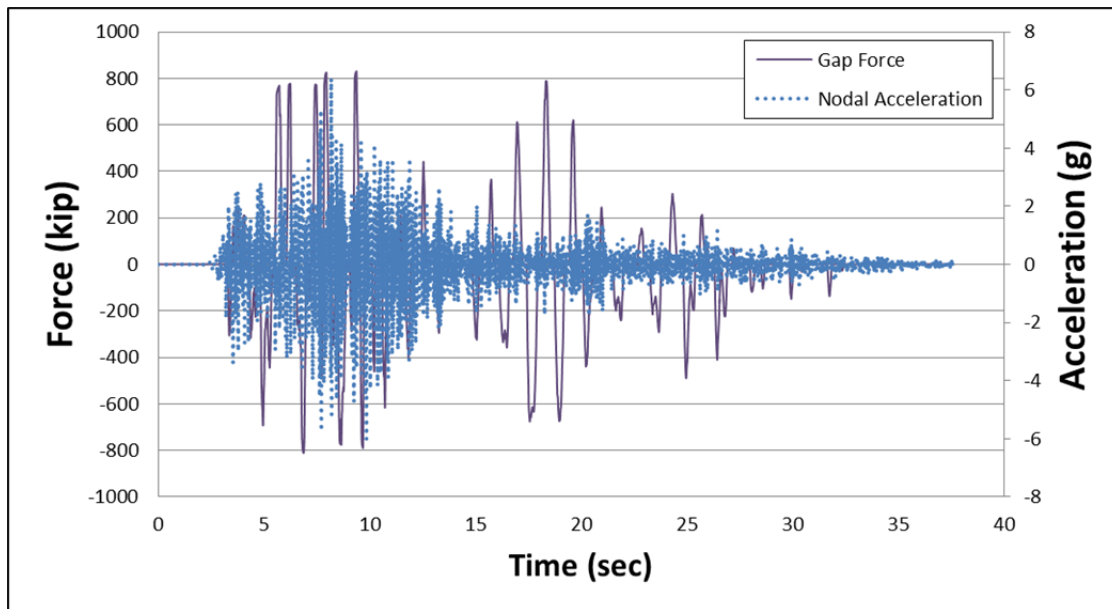


Figure 5-10: 1st Floor Gap Forces versus Nodal Accelerations

5.4 Summary

The efforts to identify the best system parameters were described in this chapter. The analysis of the multi-phase systems was completed by investigating the story drift, nodal acceleration, moment frame plastic hinge rotation, and cumulative BRB ductility responses relative to the baseline system. The analysis also included the comparison between different system ratios as well as different gap sizes at each earthquake level. The multi-phase systems of the 3-story building showed poor responses compared to the corresponding baseline systems.

The 6-story building exhibited superior responses especially when it comes to the BRB ductility. The MF ductility responses in the 6-story building are found to be higher than the BRB ductility. Adding damping devices to the system can help in improving the

MF ductility. System indices were found to indicate the best system performance in the four response quantities. Also, the overall ductility of all system combinations was calculated by the DPI index. A significant overall ductility improvement was demonstrated by the multi-phase systems when compared to the baseline systems especially in the 6-story building.

After presenting a broad analysis for different multi-phase systems, it was concluded that adding gap elements to the system is beneficial in improving the overall ductility performance for specific combinations. Selecting the best system combination is difficult. The best story drift and MF ductility response was dependent on the decrease of the gap size and moment frame strength ratio. In contrast, the superior BRB ductility response was demonstrated by systems with larger gap sizes and more moment frame strength ratio.

The accelerations were found to be large compared to the baseline system. For that, an analysis for the effect of acceleration spikes was completed to see whether the accelerations are produced by the gap lockout mechanism or not. The results did not clarify the effect of the gap on the accelerations. A further investigation need to be made in future studies to check the benefit of adding damping device on reducing these accelerations. Also, it is important to look at the transition modeling of the gap element such as using softer force-displacement behavior.

Chapter 6: Summary and Conclusions

6.1 Summary

In this work, the goal was to investigate the multi-phase systems in multi-degree of freedom (MDOF) structures. For that, a literature review was provided to discuss different types of structural control systems that fulfill the performance-based design concept as well as the general idea behind their mechanism and behavior under lateral loads. Combined structural systems that were developed by previous studies were also outlined. The advantages of the multi-phase systems in combined structural systems are also clarified. A brief discussion on the single degree of freedom (SDOF) work that built a solid groundwork for the MDOF study was provided. Variables and system combinations that showed the best influence on the response of the SDOF system were presented to provide a full understanding of the work undertaken in this study.

Subsequently, the parametric development and study plan were specified. A detailed description on the proposed prototype buildings was completed. The seismic design procedure of the buildings was briefly explained. The factors involved in the analysis were listed such as the moment frame and braced frame strength ratios, gap sizes, and seismic hazard levels. Moment frame and braced frame strength ratios of 40M60B, 50M50B, and 60M40B were selected because of their superior performance in the SDOF research. The gap sizes were decided to be equivalent to 0.45%, 0.30%, and 0.15% of the story height. These sizes were selected based on the BRB and moment

frame yield limit at around 0.5% and 1% of the story height respectively. The gap is designed to prevent the moment frame from yielding prior to the transition occurring and ensure that the BRBs yield first. Three seismic hazard levels were used in this study with scale factors of 1.0, 2/3, and 1/4 to account for earthquakes with various return periods. The building height was considered in the analysis to determine its effect on the multi-phase system behavior. The arrangements of the multi-phase and baseline systems were developed and illustrated and the system combinations were outlined.

The design procedure of the prototype buildings is discussed in details by using the AISC Seismic Provisions for Structural Steel Buildings (AISC 2005) and ASCE Standard 7-10 (ASCE 2010) along with the computer program SAP2000 (CSI 2012). The final designs of the prototype buildings were presented after the drift check is completed. Also, the finite element modeling procedure was discussed by using Perform 3D (CSI 2011). A detailed description was provided for the components that have been used during the modeling process for moment frame elements, BRBs, gap elements, and connection panel zones.

In the next stage, a more broad analysis was accomplished by involving all system combinations across all earthquake levels to identify the best system performance. The analysis of the multi-phase systems was completed by using Perform 3D and the results were investigated based on the story drift, nodal acceleration, moment frame plastic hinge rotation, and cumulative BRB ductility responses. The analysis included the comparison between the multi-phase system responses relative to the baseline systems and also the

comparison between different system combinations at each earthquake level. System indices were found to indicate the best system performance in each response quantity. The overall ductility of the moment frame and braced frame for the different system combinations was determined by calculating the ductility performance index (DPI).

6.2 Conclusions

After examining the results and different system responses it was found that the multi-phase systems of the 3-story building showed overall poor responses compared to the baseline systems. The 6-story building showed better responses compared to the baseline system especially when considering the BRB ductility. The MF ductility responses in the 6-story building are found to be higher than the BRB ductility. Adding a damping device during the initial phase of the system might help in improving the MF ductility as well as displacements. A significant overall ductility improvement was demonstrated by the six-story multi-phase systems as shown by the DPI indices. In general, it was concluded that adding gap elements to the system is beneficial to improve the overall ductility performance. Selecting the best system combination is difficult. The story drift and MF ductility responses improved with the decrease of the gap size and moment frame strength ratio. In contrast, the best BRB ductility response was demonstrated by systems with larger gap size and higher moment frame strength ratio. The accelerations in the multi-phase systems were found to be higher than the baseline systems. Additional analysis was completed to see the effect of acceleration spikes and if

they are produced by the closing and opening of the gap during the structure movement. The results did not clarify the influence of the gap lockout mechanism on the accelerations. More studies need to be done regarding this matter.

6.3 Recommendations

This research helped to identify the factors that affected the multi-phase system performance the most in the MDOF system. The results provided a significant insight towards the fundamental behavior of the multi-phase systems. It was noticed that the multi-phase systems helped successfully in improving the overall ductility of the structure. The distribution of the overall ductility between the moment frame and the braced frame need to be improved in future studies. More ductility needs to be provided by the replaceable elements than the moment frame. The poor nodal acceleration response that attributed by the multi-phase system could be enhanced by increasing the damping or having a different transition element.

For future work, early phase energy dissipation needs to be added to the system to decrease the accelerations and thus reduce the deformations in the system. This can be done by adding a friction damper or viscoelastic damper to the multi-phase system. By combining the damper's hysteretic behavior with the gap element's multilinear elastic behavior as seen in Figure 6-1, the moment frame will be allowed to deform until a certain limit before the gap locks out. The difference is that in the case of the gap element only the system will be elastic but no enough dissipation is provided. For that, the damper

will add more benefits to the system. The best placement of the damper can be investigated in future studies. Different system arrangements need to be considered. Also, different damper types might need to be tested to find the ideal combination.

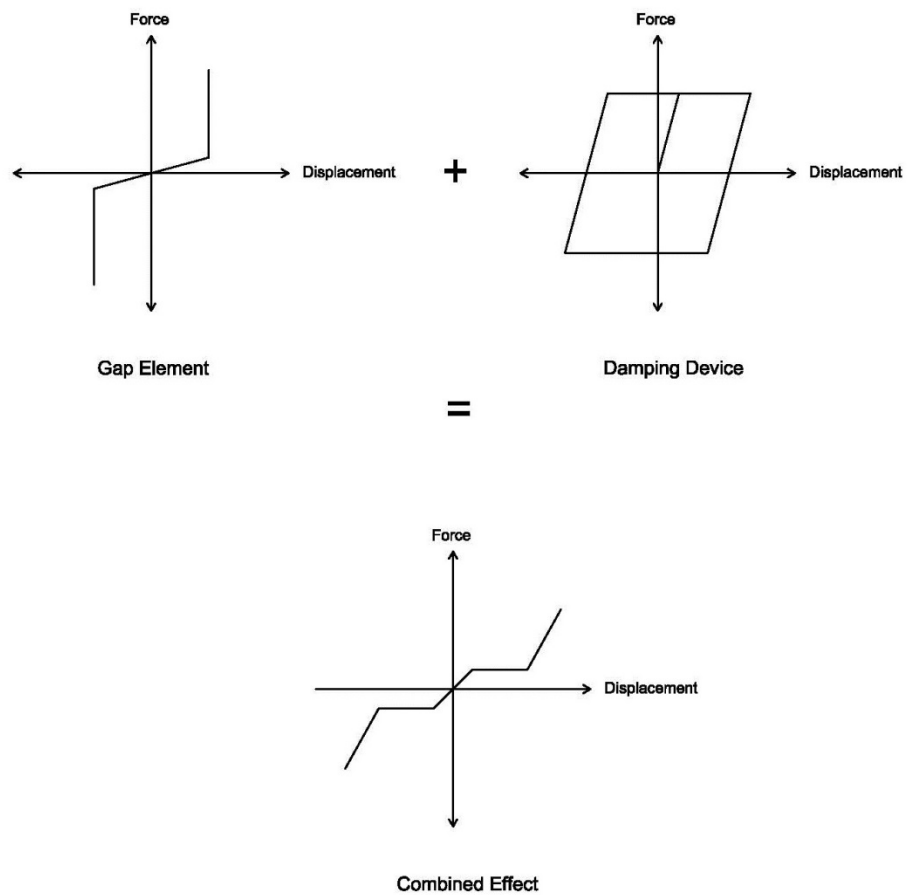


Figure 6-1: Combined Effect of Damping Device with Gap Element

The recommendations for future work can be summarized as outlined below:

- Early phase energy dissipation needs to be provided for the system to create a balance in the overall ductility performance of the structure and reduce acceleration response.
- Different types of dissipation devices need to be investigated such as friction damper or viscoelastic damper to find the best combination.
- Various system arrangements must be considered in future studies to reach the ideal placement of the damper relative to the gap element and other system components.
- A sharp transition behavior was used in this research for the gap elements. This might be the reason behind having large accelerations in multi-phase systems. A softer transition might need to be used for the force-displacement curve. Conducting experimental work to identify the soft transition behavior of the gap element is needed.
- The effect of the gap size was significant on the story drifts as well as the overall ductility of the system. It is necessary to involve different gap sizes in future work to study its effect on different system responses.
- Eleven ground motions representing various site conditions were used in this work. Using a wider range of ground motions is beneficial to test the system performance across numerous seismic hazards.

- Three seismic hazard levels were considered in this work, which are the MCE, DBE, and SLE levels. Various earthquake levels might need to be involved in future research to provide further understanding on the multi-phase system behavior by examining its responses under different seismic hazard levels.
- 3- and 6-story buildings have been investigated and the effect of the building height is found to be important. Considering a 9-story building in future study will evidence the impact of building height on system responses.

References

- AISC. *Seismic Provisions for Structural Steel Buildings*. Chicago, IL: American Institute of Steel Construction, 2005.
- Alehashem, Seyed Masoud Sajjadi, Ali Keyhani, and Hassan Pourmohammad. "Behavior and Performance of Structures Equipped With ADAS & TADAS Dampers (a Comparison with Conventional Structures)." *The 14th World Conference on Earthquake Engineering*. Beijing, China: Indian Institute of Technology Kanpur (IITK), 2008.
- ASCE. *Minimum Design Loads for Buildings and Other Structures*. Reston, VA: American Society of Civil Engineers, 2010.
- . *Minimum Design Loads for Buildings and Other Structures*. Reston, VA: American Society of Civil Engineers, 2013.
- Asgarian, B. , and H. R. Shokrgozar. "BRBF response modification factor." *Journal of Constructional Steel Research* 65, no. 2 (February 2009): 290–298.
- Calado, Luís , Jorge Miguel Proença, Andreia Panão, Emad Nsieri, Avigdor Rutenbr, and Robert Levy. *Buckling-Restrained Braces*. Technical Report, Technion, n.d.
- Charney, Finley A., and Justin Marshall. "A Comparison of the Krawinkler and Scissors Models for Including Beam-Column Joint Deformations in the Analysis of Moment-Resisting Steel Frames." *Engineering Journal*, 2006: 31-48.
- Choi, Eunsoo , Sung-Chul Cho, Jong Wan Hu, Taehyo Park, and Young-Soo Chung. "Recovery and residual stress of SMA wires and applications for concrete structures." *Smart Materials and Structures*, 2010: IOP Publishing.

- Chopra, A. K. *Dynamics of Structures: Theory and Application to Earthquake Engineering (3rd ed.)*. Upper Saddle River, New Jersey: Pearson/Prentice Hall, 2007.
- Colajanni, Piero, and Maurizio Papia. "Seismic response of braced frames with and without friction dampers." *Engineering Structures* 17, no. 2 (February 1995): 129–140.
- Connor, Jerome J. *Introduction to Structural Motion Control*. New Jersey 07458: Pearson Education, Inc., Upper Saddle River, 2002.
- Constantinou, M. C., A. S. Mokha, and A. M. Reinhorn. "Study of Sliding Bearing and Helical-Steel-Spring Isolation System." *Journal of Structural Engineering* 117 (April 1991): 1257-1275.
- Constantinou, Michael C., Tsu T. Soong, and Gary F. Dargush. *Passive Energy Dissipation Systems for Structural Design and Retrofit*. Monograph No. 1 Multidisciplinary Center for Earthquake Engineering Research, Buffalo (NY): MCEER, 1998.
- CSI *Analysis Reference Manual*. Berkeley, CA: Computers and Structures, Inc, 2009.
- CSI. *CSI Analysis Reference Manual*. Berkeley, CA: Computers and Structures, Inc, 2012.
- . *CSI Analysis Reference Manual*. Berkeley, CA: Computers and Structures, Inc, 2011.
- . *PERFORM Components and Elements*. Berkeley, CA: Computers and Structures, Inc, 2006.

- Erkal, Aykut, Semih S. Tezcan, and Debra F. Laefer. "Assessment and Code Considerations for the Combined Effect of Seismic Base Isolation and Viscoelastic Dampers." *International Scholarly Research Notices* , 2011.
- Esteves, Nuno Miguel Canhão. *Seismic Isolation with Friction Pendulum System*. Technical Report, Portugal: Instituto Superior Técnico, 2010.
- Fadi, Fabio , and Michael C. Constantinou. "Evaluation of Simplified Methods of Analysis for Structures with Triple Friction Pendulum Isolators." *Earthquake Engineering and Structural Dynamics* (Wiley InterScience), June 2009: 5-22.
- FEMA-356. *Prestandard and Commentary for the Seismic Rehabilitation of Buildings*. Washington, D.C.: Public.Resource.Org, 2000.
- Fenz, Daniel M. , and Michael C. Constantinou. "Behaviour of The Double Concave Friction Pendulum Bearing." *Earthquake Engineering and Structural Dynamics* (Wiley InterScience), June 2009: 5–22.
- Ghobarah, Ahmed. "Performance-based design in earthquake engineering: state of development." *Engineering Structure* (Auburn University), 2001.
- Hwang, Jenn-Shin. "Seismic Design of Structures with Viscous Dampers." *International Training Programs for Seismic Design of Building Structures*. Taipei, Taiwan: National Center for Research on Earthquake Engineering, 2002. 124-138.
- Kourakis, Ioannis. *Structural Systems and Tuned Mass Dampers of Super-Tall Buildings: Case Study of Taipei 101*. Boston, MA: DSpaceat@MIT, 2007.

- Krishnamoorthy, A. "Response of Sliding Structure with Restoring Force Device to Earthquake Support Motion." *Journal of Seismology and Earthquake Engineering* 10 (2008): 25-39.
- Leblouba, Moussa. "Combined Systems for Seismic Protection of Buildings." *International Symposium on Strong Vrancea Earthquakes and Risk Mitigation*. Bucharest, Romania: KIT Library, 2007. 363-373.
- Liu, Yanqing, Hiroshi Matsuhisa, Hideo Utsuno, and Jeong Gyu Park. "Vibration Isolation by a Variable Stiffness and Damping System." *The Japan Society of Mechanical Engineers (JSME)* 48 (2005): 305-310.
- Marshall, Justin D. *Development, Analysis and Testing of a Hybrid Passive Control Device for Seismic Protection of Framed Structures*. Blacksburg, VA: Ph.D. Dissertation, Virginia Polytechnic Institute and State University, 2008.
- Midorikawa, Mistumasa, Izuru Okawa, Masanori Iiba, and Masaomi Teshigawara. *Performance-Based Seismic Design Code for Buildings in Japan*. Task Committee to Draft Performance-based Building Provisions of the Building Research Institute, Japan: Chinese Taiwan Society for Earthquake Engineering, 2001.
- Moehle, Jack, and Gregory G. Deierlein. "A Framework Methodology for Performance-Based Earthquake Engineering." *13th World Conference on Earthquake Engineering*. Vancouver, B.C., Canada: Indian Institute of Technology Kanpur, 2004.

- Muthumani, K., and R. Sreekala. "Structural Application of Smart Materials." *Conference of Women Scientists and Technologists: Role in National Development*. Vigyan Bhawan, New Delhi: Department of Biotechnology (DBT), 2002.
- Palacios-Quinonero, Francisco, Josep M. Rossell, Jose Rodellar, and Raul Pons-Lopez. "Passive-active vibration control for connected multi-building structures." *8th International Conference on Structural Dynamics*. Leuven, Belgium: Eurodyn2011, 2011. 1931-1938.
- Pall, Avtar S., and Rashmi Pall. "Friction-Dampers for Seismic Control of Buildings "A Canadian Experience"." *Eleventh World Conference on Earthquake Engineering*. Montreal, Canada: Indian Institute of Technology Kanpur (IITK), 1998.
- Rai, Durgesh C., Praveen K. Annam, and Tripti Pradhan. "Seismic testing of steel braced frames with aluminum shear yielding dampers." *Engineering Structures* 46 (January 2013): 737–747.
- Rawlinson, Taylor A. *Characterization of Multi-Phase Performance-Based Passive Control Systems*. Auburn, Alabama: Civil Engineering Dept., Auburn University, 2011.
- Reinhorn, A. M., T. T. Soong, R. C. Lin, and M. A. Riley. *Active Bracing System: A Full Scale Implementation of Active Control*. Technical Report NCEER-92-0020, Buffalo, NY: University at Buffalo, The State University of New York, 1992.
- Robinson, W. H., and A. G. Tucker. "A lead-Rubber Shear Damper." (The NZSEE Inc.) 10 (September 1977): 151-153.

- Sabelli, R. *Research on Improving the Design and Analysis of Earthquake-Resistant Steel-Braced Frames*. Professional Fellowship Report No. PF2000-9, NEHRP, Washington, DC: The Earthquake Engineering Research Institute (EERI), 2001.
- Sabu. *Base Isolation*. May 13, 2006. <http://baseisolation.blogspot.com/> (accessed June 1, 2014).
- Sadek, Fahim, Bijan Mohraz, Andrew W. Taylor, and Riley M. Chung. *Passive Energy Dissipation Devices for Seismic Applications*. Technical report NISTIR 5923, Gaithersburg, MD: Building and Fire Research Laboratory, National Institute of Standards and Technology, 1996.
- Scheller, Jorn , and Uwe Starossek. "A versatile active mass damper for structural vibration control." *8th International Conference on Structural Dynamics*. Leuven, Belgium: Technischen Universität Hamburg (TUHH), 2011. 1777-1784.
- Soong, T. T., and B. F. Spencer, JR. "Active, Semi-Active and Hybrid Control of Structures." *12th World Conference on Earthquake Engineering*. Auckland, New Zealand: Indian Institute of Technology Kanpur (IITK), 2000. 1-16.
- Spencer Jr., B. F., and S. Nagarajaiah. "State of Art of Structural Control." *Journal of Structural Engineering*, 2003: 845–856.
- Sreekala , R, K Muthumani , and Iyer R. Nagesh . *Vibration Analysis and Control - New Trends and Developments*. CSIR, India: InTech, 2011.
- Staff. *TechBlog*. July 31, 2008. <http://www.techeblog.com/index.php/tech-gadget/tuned-mass-damper> (accessed June 12, 2014).

Stroscher. "Tuned Mass Dampers." *PowerPoint presentation*.

www14.informatik.tumuenchen.de/konferenzen/

Jass06/courses/4/Stroscher/Stroscher.ppt, n.d.

Symans, M. D., et al. "Energy Dissipation Systems for Seismic Applications: Current Practice and Recent Developments." *Journal of Structural Engineering* 134 (January 2008): 3-21.

Symans, Michael D. , and Michael C. Constantinou. "Semi-active control systems for seismic protection of structures: a state-of-the-art review." *Engineering Structures* 21, no. 6 (June 1999): 469–487.

Symans, Michael D. *Seismic protective systems: seismic isolation*. Rensselaer Polytechnic Institute, Instructional Material Complementing FEMA 451, Design examples, Civil Engineering Department, University of Memphis, 2009.

Tamura, Yukio, Kunio Fujii, Tamio Ohtsuki, Toshihiro Wakahara, and Ryuichi Kohsaka. "Effectiveness of Tuned Liquid Dampers Under Wind Excitation." *Engineering Structures* 17 (1995): 609-621.

Tan, Ping , Fulin Zhou , and Weiming Yan . "A Semi-Active Variable Stiffness and Damping System for Vibration Control of Civil Engineering Structures." *2004 ANCEER Annual Meeting*. Honolulu, Hawaii: MCEER, 2004.

Tongaokar, N. P., and R. S. Jangid. "Seismic Response of Bridges with Sliding isolation Devices." *ISET Journal of Earthquake Technology*, 1998: 9-27.

- Trelleborg. *RoadTraffic-Technology: Trelleborg - Elastomeric Bridge Bearings and Tunnel Seals*. 2010. <http://www.roadtraffic-technology.com/contractors/bridges/trelleborg-bearings/> (accessed June 5, 2014).
- UC. *5 Base Isolation and Damping Devices*. University of Canterbury Research Report No. 2011-02, Christchurch, New Zealand: The Canterbury Earthquakes Royal Commission, 2011.
- Woodford, Chris. *Earthquakes*. November 6, 2013. <http://www.explainthatstuff.com/earthquakes.html> (accessed June 12, 2014).
- Yamamoto, Masashi , and Takayuki Sone. "Behavior of active mass damper (AMD) installed in high-rise building during 2011 earthquake off Pacific coast of Tohoku and verification of regenerating system of AMD based on monitoring." *Structural Control and Health Monitoring*, 2013: 634–647.

Appendix A: Selected Design Calculations

Three-Story Building

-Design response spectrum for building

$$S_s := 2.423 \quad S_1 := 0.849$$

Site coefficients F_a & F_v calculated from Tables 11.4-1 & Table 11.4-2 respectively for site class D

$$F_a := 1$$

$$F_v := 1.5$$

Spectral response acceleration parameters calc. From eqs. 11.4-1 & 11.4-2

$$S_{MS} := F_a \cdot S_s = 2.423 \quad S_{M1} := F_v \cdot S_1 = 1.273$$

Design spectral acceleration parameters From eqs. 11.4-3 & 11.4-4

$$S_{DS} := \frac{2}{3} \cdot S_{MS} = 1.615 \quad S_{D1} := \frac{2}{3} \cdot S_{M1} = 0.849$$

Fundamental periods of the structure calc. as in section 11.4-5

$$T_0 := 0.2 \cdot \frac{S_{D1}}{S_{DS}} = 0.105 \text{ s}$$

$$T_s := \frac{S_{D1}}{S_{DS}} = 0.526 \text{ s}$$

Long-period transition period from fig. (22-12)

$$T_L := 8 \text{ s}$$

-Effective seismic weight broken down by floor

$$\text{Heights: } h_1 := 13\text{ft} \quad h_2 := 13\text{ft} \quad h_{ph} := 12\text{ft} \quad h_{par} := 3.5\text{ft}$$

Bldg Dimensions:

$$B_{ex} := (30\text{ft} \cdot 6) + 4\text{ft} = 184\text{ft} \quad L_{ex} := (30\text{ft} \cdot 4) + 4\text{ft} = 124\text{ft}$$

$$B_{int} := 30\text{ft} \cdot 6 = 180\text{ft} \quad L_{int} := 30\text{ft} \cdot 4 = 120\text{ft}$$

Weight/floor:

$$W_{roof} := 7\text{psf} \quad W_m := 7\text{psf} \quad W_{m_ph} := 47\text{psf}$$

$$W_{c_f} := 3\text{psf} \quad W_p := 10\text{psf} \quad W_{ex_wall} := 25\text{psf}$$

$$W_{steel} := 13\text{psf} \quad W_{f_r} := 42\text{psf}$$

$$W_{ext_1} := W_{ex_wall} \cdot \frac{h_1 + h_2}{2} \cdot B_{ex} \cdot 2 + W_{ex_wall} \cdot \frac{h_1 + h_2}{2} \cdot L_{ex} \cdot 2 = 200.2 \text{ kip}$$

$$W_{ext_2} := W_{ex_wall} \cdot h_2 \cdot B_{ex} \cdot 2 + W_{ex_wall} \cdot h_2 \cdot L_{ex} \cdot 2 = 200.2 \text{ kip}$$

$$W_{\text{ext}_3} := W_{\text{ex_wall}} \cdot \left(\frac{h_2}{2} + h_{\text{par}} \right) \cdot B_{\text{ex}} \cdot 2 + W_{\text{ex_wall}} \cdot \left(\frac{h_2}{2} + h_{\text{par}} \right) \cdot L_{\text{ex}} \cdot 2 = 154 \text{ kip}$$

$$W_{\text{ext_ph}} := W_{\text{ex_wall}} \cdot h_{\text{ph}} \cdot 64\text{ft} \cdot 2 + W_{\text{ex_wall}} \cdot h_{\text{ph}} \cdot 34\text{ft} \cdot 2 = 58.8 \text{ kip}$$

Seismic Weights:

$$W_1 := (W_{\text{steel}} + W_{\text{f}_r} + W_{\text{c}_f} + W_m + W_p) \cdot B_{\text{int}} \cdot L_{\text{int}} + W_{\text{ext}_1} = 1.82 \times 10^3 \text{ kip}$$

$$W_2 := (W_{\text{steel}} + W_{\text{f}_r} + W_{\text{c}_f} + W_m + W_p) \cdot B_{\text{int}} \cdot L_{\text{int}} + W_{\text{ext}_2} = 1.82 \times 10^3 \text{ kip}$$

$$W_3 := (W_{\text{steel}} + W_{\text{f}_r} + W_{\text{c}_f} + W_m + W_p + W_{\text{roof}}) \cdot B_{\text{int}} \cdot L_{\text{int}} + W_{\text{ext}_3} = 1.925 \times 10^3 \text{ kip}$$

$$W_4 := (W_{\text{steel}} + W_{\text{f}_r} + W_{\text{c}_f} + W_{\text{m_ph}} + W_p) \cdot 30\text{ft} \cdot 60\text{ft} + W_{\text{ext_ph}} = 265.8 \text{ kip}$$

$$W = \begin{pmatrix} 1.82 \times 10^3 \\ 1.82 \times 10^3 \\ 1.925 \times 10^3 \\ 265.8 \end{pmatrix} \text{ kip} \quad h := \begin{pmatrix} 13 \\ 26 \\ 39 \\ 51 \end{pmatrix} \text{ ft} \quad h_n := 39$$

$$\text{Mass} := \frac{W}{32.2 \frac{\text{ft}}{\text{s}^2}} = \begin{pmatrix} 4.711 \\ 4.711 \\ 4.982 \\ 0.688 \end{pmatrix} \cdot \frac{\text{kip} \cdot \text{s}^2}{\text{in}}$$

-Approximate natural period in both directions

$$C_u := 1.4 \quad \text{from table 12.8-1}$$

For N-S & E-W directions where steel buckling-restrained braced frames are used

$$C_t := 0.03 \quad x := 0.75 \quad \text{table 12.8-2}$$

$$T_a := C_t \cdot h_n^x = 0.468 \quad \text{eq. 12.8-7}$$

$$T_{a_max} := C_u \cdot T_a = 0.655$$

-Seismic base shear

$$I_e := 1.0 \quad \text{table 1.5-2 for Risk Category II}$$

$$R_v := 8$$

$$C_{s_1} := \frac{S_{Ds}}{R \cdot I_e} = 0.202 \quad \text{eq. 12.8-2}$$

$$C_{s_2} := \frac{S_{D1}}{R \cdot T_a} = 0.227 \quad \text{eq. 12.8-2}$$

$$C_s := \min(C_{s_2}, C_{s_1}) = 0.202$$

$$W_t := W_1 + W_2 + W_3 + W_4 = 5.831 \times 10^3 \text{ kip}$$

$$V_v := C_s \cdot W_t = 1.177 \times 10^3 \text{ kip}$$

$$k := 1$$

$$\text{sumWixhi} := W_1 \cdot \left(\frac{h_1}{\text{ft}}\right)^k + W_2 \cdot \left(\frac{h_2}{\text{ft}}\right)^k + W_3 \cdot \left(\frac{h_3}{\text{ft}}\right)^k + W_4 \cdot \left(\frac{h_4}{\text{ft}}\right)^k = 1.596 \times 10^5 \text{ kip}$$

$$C_{v_1} := \frac{W_1 \cdot \left(\frac{h_1}{\text{ft}}\right)^k}{\text{sumWixhi}} = 0.148$$

$$C_{v_3} := \frac{W_3 \cdot \left(\frac{h_3}{\text{ft}}\right)^k}{\text{sumWixhi}} = 0.47$$

$$C_{v_2} := \frac{W_2 \cdot \left(\frac{h_2}{\text{ft}}\right)^k}{\text{sumWixhi}} = 0.296$$

$$C_{v_4} := \frac{W_4 \cdot \left(\frac{h_4}{\text{ft}}\right)^k}{\text{sumWixhi}} = 0.085$$

$$C_v = \begin{pmatrix} 0.148 \\ 0.296 \\ 0.47 \\ 0.085 \end{pmatrix} \quad \text{eq. 12.8-12}$$

$$F_v := V \cdot C_v = \begin{pmatrix} 174.543 \\ 349.086 \\ 553.835 \\ 99.992 \end{pmatrix} \text{ kip} \quad \text{eq. 12.8-11}$$

$$C_{v_1} + C_{v_2} + C_{v_3} + C_{v_4} = 1$$

$$F_1 := \frac{F}{2} = \begin{pmatrix} 87.272 \\ 174.543 \\ 276.918 \\ 49.996 \end{pmatrix} \cdot \text{kip} \quad \text{Forces applied at one side of the building}$$

Accidental Torsion

E_W direction

$$M_T := 0.05 \cdot B_{\text{int}} \cdot F = \begin{pmatrix} 1.571 \times 10^3 \\ 3.142 \times 10^3 \\ 4.985 \times 10^3 \\ 899.928 \end{pmatrix} \text{ ft-kip}$$

N_S direction

$$M_T := 0.05 \cdot L_{\text{int}} \cdot F = \begin{pmatrix} 1.047 \times 10^3 \\ 2.095 \times 10^3 \\ 3.323 \times 10^3 \\ 599.952 \end{pmatrix} \text{ ft-kip}$$

Forces Divided According to Frame Ratios

40 MOMENT FRAME : 60 BRACED FRAME

$$F_{m_1} := 0.4 \cdot F1 = \begin{pmatrix} 34.909 \\ 69.817 \\ 110.767 \\ 19.998 \end{pmatrix} \text{ kip} \quad F_{b_1} := 0.6 \cdot F1 = \begin{pmatrix} 52.363 \\ 104.726 \\ 166.151 \\ 29.998 \end{pmatrix} \text{ kip}$$

50 MOMENT FRAME : 50 BRACED FRAME

$$F_{m_2} := 0.5 \cdot F1 = \begin{pmatrix} 43.636 \\ 87.272 \\ 138.459 \\ 24.998 \end{pmatrix} \text{ kip} \quad F_{b_2} := 0.5 \cdot F1 = \begin{pmatrix} 43.636 \\ 87.272 \\ 138.459 \\ 24.998 \end{pmatrix} \text{ kip}$$

60 MOMENT FRAME : 40 BRACED FRAME

$$F_{m_3} := 0.6 \cdot F1 = \begin{pmatrix} 52.363 \\ 104.726 \\ 166.151 \\ 29.998 \end{pmatrix} \text{ kip} \quad F_{b_3} := 0.4 \cdot F1 = \begin{pmatrix} 34.909 \\ 69.817 \\ 110.767 \\ 19.998 \end{pmatrix} \text{ kip}$$

Joint Mass Calculation:

In below calculations we will consider our building as a square structure with 4 bays at each side.

$W_{steel} := 15 \text{ psf}$ To account for high-rise buildings in this study

$$W_{f_r} = 42 \cdot \text{psf} \quad W_{c_f} = 3 \cdot \text{psf} \quad W_m = 7 \cdot \text{psf} \quad W_p = 10 \cdot \text{psf} \quad W_{ex_wall} = 25 \cdot \text{psf}$$

$$W_{ext_ph} := W_{ex_wall} \cdot h_{ph} \cdot 60\text{ft} = 18 \text{ kip}$$

$$W_1 := (W_{steel} + W_{f_r} + W_{c_f} + W_m + W_p) \cdot 60\text{ft} \cdot 120\text{ft} + W_{ex_wall} \cdot \frac{h_1 + h_2}{2} \cdot 120\text{ft} = 593.4 \text{ kip}$$

$$W_2 := (W_{steel} + W_{f_r} + W_{c_f} + W_m + W_p) \cdot 60\text{ft} \cdot 120\text{ft} + W_{ex_wall} \cdot h_2 \cdot 120\text{ft} = 593.4 \text{ kip}$$

$$W_3 := (W_{steel} + W_{f_r} + W_{c_f} + W_m + W_p + W_{roof}) \cdot 60\text{ft} \cdot 120\text{ft} + W_{ex_wall} \cdot \left(\frac{h_2}{2} + h_{par} \right) \cdot 120\text{ft} = 634.8 \text{ kip}$$

$$W_4 := (W_{steel} + W_{f_r} + W_{c_f} + W_{m_ph} + W_p) \cdot 30\text{ft} \cdot 60\text{ft} + W_{ext_ph} = 228.6 \text{ kip}$$

$$W = \begin{pmatrix} 593.4 \\ 593.4 \\ 634.8 \\ 228.6 \end{pmatrix} \cdot \text{kip} \quad W_{\text{floor}} := W + \begin{pmatrix} 0 \\ 0 \\ W_4 \\ -W_4 \end{pmatrix} = \begin{pmatrix} 593.4 \\ 593.4 \\ 863.4 \\ 0 \end{pmatrix} \cdot \text{kip} \quad \text{Adding the penthouse weight to the third floor.}$$

Corner joints will carry 1/8 of the floor weight, while edge joints will carry 1/4 of the floor weight because we have 4 bays in our model which will make a total of 8 segments.

$$M := \frac{W_{\text{floor}}}{386.4 \frac{\text{in}}{\text{sec}^2}} = \begin{pmatrix} 1.536 \\ 1.536 \\ 2.234 \\ 0 \end{pmatrix} \cdot \frac{\text{kip} \cdot \text{sec}^2}{\text{in}}$$

P-Delta Loads Applied on Ghost Column:

Dead load and live load applied on beams are:

$$DL := 1.5 \frac{\text{kip}}{\text{ft}} \quad LL := 0.75 \frac{\text{kip}}{\text{ft}}$$

$$\text{dead} := \frac{DL}{(15\text{ft})} = 100 \cdot \text{psf} \quad \text{live} := \frac{LL}{(15\text{ft})} = 50 \cdot \text{psf} \quad \text{-Too high need a reduction factor by 0.75}$$

$$P_{DL} := (30\text{ft} \cdot 4) \cdot (30\text{ft} \cdot 2.5) \cdot (0.75 \cdot \text{dead}) = 675 \cdot \text{kip}$$

$$P_{LL} := (30\text{ft} \cdot 4) \cdot (30\text{ft} \cdot 2.5) \cdot (0.75 \cdot \text{live}) = 337.5 \cdot \text{kip} \quad \text{-These loads are for 1st \& 2nd stories only}$$

$$P_{DL_{\text{roof}}} := (30\text{ft} \cdot 4) \cdot (30\text{ft} \cdot 2.5) \cdot (0.6 \cdot \text{dead}) = 540 \cdot \text{kip}$$

$$P_{LL_{\text{roof}}} := (30\text{ft} \cdot 4) \cdot (30\text{ft} \cdot 2.5) \cdot (0.5 \cdot \text{live}) = 225 \cdot \text{kip} \quad \text{-These loads are applied on roof only}$$

Six-Story Building

-Design response spectrum for building

$$S_s := 2.423 \quad S_1 := 0.849$$

Site coefficients F_a & F_v calculated from Tables 11.4-1 & Table 11.4-2 respectively for site class D

$$F_a := 1$$

$$F_v := 1.5$$

Spectral response acceleration parameters calc. From eqs. 11.4-1 & 11.4-2

$$S_{MS} := F_a \cdot S_s = 2.423 \quad S_{M1} := F_v \cdot S_1 = 1.273$$

Design spectral acceleration parameters From eqs. 11.4-3 & 11.4-4

$$S_{DS} := \frac{2}{3} \cdot S_{MS} = 1.615 \quad S_{D1} := \frac{2}{3} \cdot S_{M1} = 0.849$$

Fundamental periods of the structure calc. as in section 11.4-5

$$T_0 := 0.2 \cdot \frac{S_{D1}}{S_{DS}} = 0.105 \text{ s}$$

$$T_s := \frac{S_{D1}}{S_{DS}} = 0.526 \text{ s}$$

Long-period transition period from fig. (22-12)

$$T_L := 8 \text{ s}$$

-Effective seismic weight broken down by floor

$$\text{Heights: } h_1 := 18\text{ft} \quad h_2 := 13\text{ft} \quad h_{ph} := 12\text{ft} \quad h_{par} := 3.5\text{ft}$$

Bldg Dimensions:

$$B_{ex} := (30\text{ft} \cdot 5) + 4\text{ft} = 154\text{ft} \quad L_{ex} := (30\text{ft} \cdot 5) + 4\text{ft} = 154\text{ft}$$

$$B_{int} := 30\text{ft} \cdot 5 = 150\text{ft} \quad L_{int} := 30\text{ft} \cdot 5 = 150\text{ft}$$

Weight/floor:

$$W_{roof} := 7\text{psf} \quad W_m := 7\text{psf} \quad W_{m_ph} := 47\text{psf}$$

$$W_{c_f} := 3\text{psf} \quad W_p := 10\text{psf} \quad W_{ex_wall} := 25\text{psf}$$

$$W_{steel} := 13\text{psf} \quad W_{f_r} := 42\text{psf}$$

$$W_{ext_1} := W_{ex_wall} \cdot \frac{h_1 + h_2}{2} \cdot B_{ex} \cdot 2 + W_{ex_wall} \cdot \frac{h_1 + h_2}{2} \cdot L_{ex} \cdot 2 = 238.7 \text{ kip}$$

$$W_{ext_2} := W_{ex_wall} \cdot h_2 \cdot B_{ex} \cdot 2 + W_{ex_wall} \cdot h_2 \cdot L_{ex} \cdot 2 = 200.2 \text{ kip}$$

$$W_{\text{ext}_3} := W_{\text{ex_wall}} \cdot \left(\frac{h_2}{2} + h_{\text{par}} \right) \cdot B_{\text{ex}} \cdot 2 + W_{\text{ex_wall}} \cdot \left(\frac{h_2}{2} + h_{\text{par}} \right) \cdot L_{\text{ex}} \cdot 2 = 154 \text{ kip}$$

$$W_{\text{ext_ph}} := W_{\text{ex_wall}} \cdot h_{\text{ph}} \cdot 64\text{ft} \cdot 2 + W_{\text{ex_wall}} \cdot h_{\text{ph}} \cdot 34\text{ft} \cdot 2 = 58.8 \text{ kip}$$

Seismic Weights:

$$W_1 := (W_{\text{steel}} + W_{\text{f}_r} + W_{\text{c}_f} + W_m + W_p) \cdot B_{\text{int}} \cdot L_{\text{int}} + W_{\text{ext}_1} = 1.926 \times 10^3 \text{ kip}$$

$$W_2 := (W_{\text{steel}} + W_{\text{f}_r} + W_{\text{c}_f} + W_m + W_p) \cdot B_{\text{int}} \cdot L_{\text{int}} + W_{\text{ext}_2} = 1.888 \times 10^3 \text{ kip}$$

$$W_3 := (W_{\text{steel}} + W_{\text{f}_r} + W_{\text{c}_f} + W_m + W_p) \cdot B_{\text{int}} \cdot L_{\text{int}} + W_{\text{ext}_2} = 1.888 \times 10^3 \text{ kip}$$

$$W_4 := (W_{\text{steel}} + W_{\text{f}_r} + W_{\text{c}_f} + W_m + W_p) \cdot B_{\text{int}} \cdot L_{\text{int}} + W_{\text{ext}_2} = 1.888 \times 10^3 \text{ kip}$$

$$W_5 := (W_{\text{steel}} + W_{\text{f}_r} + W_{\text{c}_f} + W_m + W_p) \cdot B_{\text{int}} \cdot L_{\text{int}} + W_{\text{ext}_2} = 1.888 \times 10^3 \text{ kip}$$

$$W_6 := (W_{\text{steel}} + W_{\text{f}_r} + W_{\text{c}_f} + W_m + W_p + W_{\text{root}}) \cdot B_{\text{int}} \cdot L_{\text{int}} + W_{\text{ext}_3} = 1.999 \times 10^3 \text{ kip}$$

$$W_7 := (W_{\text{steel}} + W_{\text{f}_r} + W_{\text{c}_f} + W_{\text{m_ph}} + W_p) \cdot 30\text{ft} \cdot 60\text{ft} + W_{\text{ext_ph}} = 265.8 \text{ kip}$$

$$W = \begin{pmatrix} 1.926 \times 10^3 \\ 1.888 \times 10^3 \\ 1.888 \times 10^3 \\ 1.888 \times 10^3 \\ 1.888 \times 10^3 \\ 1.888 \times 10^3 \\ 1.999 \times 10^3 \\ 265.8 \end{pmatrix} \text{ kip} \quad h = \begin{pmatrix} 18 \\ 31 \\ 44 \\ 57 \\ 70 \\ 83 \\ 95 \end{pmatrix} \text{ ft} \quad h_n := 83 \quad \text{Mass} := \frac{W}{g} = \begin{pmatrix} 4.989 \\ 4.889 \\ 4.889 \\ 4.889 \\ 4.889 \\ 5.178 \\ 0.688 \end{pmatrix} \cdot \frac{\text{kip} \cdot \text{s}^2}{\text{in}}$$

-Approximate natural period in both directions

$$C_u := 1.4 \quad \text{from table 12.8-1}$$

For N-S&E-W directions where steel buckling-restrained braced frames are used

$$C_t := 0.03 \quad x := 0.75 \quad \text{table 12.8-2}$$

$$T_a := C_t \cdot h_n^x = 0.825 \quad \text{eq. 12.8-7}$$

$$T_{a_max} := C_u \cdot T_a = 1.155$$

-Seismic base shear

$I_e := 1.0$ table 1.5-2 for Risk Category II

$R := 8$

$$C_{s_1} := \frac{S_{DS}}{\frac{R}{I_e}} = 0.202 \quad \text{eq. 12.8-2} \quad C_{s_2} := \frac{S_{D1}}{\frac{R}{I_e} \cdot T_a} = 0.129 \quad \text{eq. 12.8-2}$$

$$C_s := \min(C_{s_2}, C_{s_1}) = 0.129$$

$$Wt := W_1 + W_2 + W_3 + W_4 + W_5 + W_6 + W_7 = 1.174 \times 10^4 \text{ kip}$$

$$V := C_s \cdot Wt = 1.511 \times 10^3 \text{ kip}$$

$$k := 2 + \frac{T_a - 2.5}{0.5 - 2.5} \cdot (1 - 2) = 1.162$$

$$\text{sumWixhi} := W_1 \cdot \left(\frac{h_1}{\text{ft}}\right)^k + W_2 \cdot \left(\frac{h_2}{\text{ft}}\right)^k + W_3 \cdot \left(\frac{h_3}{\text{ft}}\right)^k + W_4 \cdot \left(\frac{h_4}{\text{ft}}\right)^k + W_5 \cdot \left(\frac{h_5}{\text{ft}}\right)^k + W_6 \cdot \left(\frac{h_6}{\text{ft}}\right)^k + W_7 \cdot \left(\frac{h_7}{\text{ft}}\right)^k = 1.175 \times 10^6 \text{ kip}$$

$$C_{v_1} := \frac{W_1 \cdot \left(\frac{h_1}{\text{ft}}\right)^k}{\text{sumWixhi}} = 0.047$$

$$C_{v_5} := \frac{W_5 \cdot \left(\frac{h_5}{\text{ft}}\right)^k}{\text{sumWixhi}} = 0.224$$

$$C_{v_2} := \frac{W_2 \cdot \left(\frac{h_2}{\text{ft}}\right)^k}{\text{sumWixhi}} = 0.087$$

$$C_{v_6} := \frac{W_6 \cdot \left(\frac{h_6}{\text{ft}}\right)^k}{\text{sumWixhi}} = 0.289$$

$$C_{v_3} := \frac{W_3 \cdot \left(\frac{h_3}{\text{ft}}\right)^k}{\text{sumWixhi}} = 0.131$$

$$C_{v_7} := \frac{W_7 \cdot \left(\frac{h_7}{\text{ft}}\right)^k}{\text{sumWixhi}} = 0.045$$

$$C_{v_4} := \frac{W_4 \cdot \left(\frac{h_4}{\text{ft}}\right)^k}{\text{sumWixhi}} = 0.177$$

$$C_v = \begin{pmatrix} 0.047 \\ 0.087 \\ 0.131 \\ 0.177 \\ 0.224 \\ 0.289 \\ 0.045 \end{pmatrix} \quad \text{eq. 12.8-12}$$

$$F := V \cdot C_v = \begin{pmatrix} 71.26 \\ 131.379 \\ 197.392 \\ 266.696 \\ 338.639 \\ 437.136 \\ 68.004 \end{pmatrix} \text{ kip} \quad \text{eq. 12.8-11}$$

$$F1 := \frac{F}{2} = \begin{pmatrix} 35.63 \\ 65.69 \\ 98.696 \\ 133.348 \\ 169.319 \\ 218.568 \\ 34.002 \end{pmatrix} \cdot \text{kip} \quad \text{Forces applied at one side of the building.}$$

$$C_{v_1} + C_{v_2} + C_{v_3} + C_{v_4} + C_{v_5} + C_{v_6} + C_{v_7} = 1$$

Accidental Torsion

E_W direction

$$M_{T_EW} := 0.05 \cdot B_{int} \cdot F = \begin{pmatrix} 534.451 \\ 985.344 \\ 1.48 \times 10^3 \\ 2 \times 10^3 \\ 2.54 \times 10^3 \\ 3.279 \times 10^3 \\ 510.028 \end{pmatrix} \text{ ft} \cdot \text{kip}$$

N_S direction

$$M_{T_NS} := 0.05 \cdot L_{int} \cdot F = \begin{pmatrix} 534.451 \\ 985.344 \\ 1.48 \times 10^3 \\ 2 \times 10^3 \\ 2.54 \times 10^3 \\ 3.279 \times 10^3 \\ 510.028 \end{pmatrix} \text{ ft} \cdot \text{kip}$$

Forces Divided According to Frame Ratios

40 MOMENT FRAME : 60 BRACED FRAME

$$F_{m_1} := 0.4 \cdot F1 = \begin{pmatrix} 14.252 \\ 26.276 \\ 39.478 \\ 53.339 \\ 67.728 \\ 87.427 \\ 13.601 \end{pmatrix} \text{ kip}$$

$$F_{b_1} := 0.6 \cdot F1 = \begin{pmatrix} 21.378 \\ 39.414 \\ 59.218 \\ 80.009 \\ 101.592 \\ 131.141 \\ 20.401 \end{pmatrix} \text{ kip}$$

50 MOMENT FRAME : 50 BRACED FRAME

$$F_{m_2} := 0.5 \cdot F1 = \begin{pmatrix} 17.815 \\ 32.845 \\ 49.348 \\ 66.674 \\ 84.66 \\ 109.284 \\ 17.001 \end{pmatrix} \text{ kip}$$

$$F_{b_2} := 0.5 \cdot F1 = \begin{pmatrix} 17.815 \\ 32.845 \\ 49.348 \\ 66.674 \\ 84.66 \\ 109.284 \\ 17.001 \end{pmatrix} \text{ kip}$$

60 MOMENT FRAME : 40 BRACED FRAME

$$F_{m_3} := 0.6 \cdot F1 = \begin{pmatrix} 21.378 \\ 39.414 \\ 59.218 \\ 80.009 \\ 101.592 \\ 131.141 \\ 20.401 \end{pmatrix} \text{ kip} \quad F_{b_3} := 0.4 \cdot F1 = \begin{pmatrix} 14.252 \\ 26.276 \\ 39.478 \\ 53.339 \\ 67.728 \\ 87.427 \\ 13.601 \end{pmatrix} \text{ kip}$$

Joint Mass Calculation:

In below calculations we will consider our building as a square structure with 4 bays at each side.

~~W_{steel}~~ := 15psf To account for high-rise buildings in this study

W_{f_r} = 42 · psf W_{c_f} = 3 · psf W_m = 7 · psf W_p = 10 · psf W_{ex_wall} = 25 · psf

~~W_{ext_ph}~~ := W_{ex_wall} · h_{ph} · 60ft = 18kip

$$W_1 := (W_{\text{steel}} + W_{f_r} + W_{c_f} + W_m + W_p) \cdot 60\text{ft} \cdot 120\text{ft} + W_{\text{ex_wall}} \cdot \frac{h_1 + h_2}{2} \cdot 120\text{ft} = 600.9 \text{ kip}$$

$$W_2 := (W_{\text{steel}} + W_{f_r} + W_{c_f} + W_m + W_p) \cdot 60\text{ft} \cdot 120\text{ft} + W_{\text{ex_wall}} \cdot h_2 \cdot 120\text{ft} = 593.4 \text{ kip}$$

$$W_3 := (W_{\text{steel}} + W_{f_r} + W_{c_f} + W_m + W_p) \cdot 60\text{ft} \cdot 120\text{ft} + W_{\text{ex_wall}} \cdot h_2 \cdot 120\text{ft} = 593.4 \text{ kip}$$

$$W_4 := (W_{\text{steel}} + W_{f_r} + W_{c_f} + W_m + W_p) \cdot 60\text{ft} \cdot 120\text{ft} + W_{\text{ex_wall}} \cdot h_2 \cdot 120\text{ft} = 593.4 \text{ kip}$$

$$W_5 := (W_{\text{steel}} + W_{f_r} + W_{c_f} + W_m + W_p) \cdot 60\text{ft} \cdot 120\text{ft} + W_{\text{ex_wall}} \cdot h_2 \cdot 120\text{ft} = 593.4 \text{ kip}$$

$$W_6 := (W_{\text{steel}} + W_{f_r} + W_{c_f} + W_m + W_p + W_{\text{roof}}) \cdot 60\text{ft} \cdot 120\text{ft} + W_{\text{ex_wall}} \cdot \left(\frac{h_2}{2} + h_{\text{par}}\right) \cdot 120\text{ft} = 634.8 \text{ kip}$$

$$W_7 := (W_{\text{steel}} + W_{f_r} + W_{c_f} + W_{m_{\text{ph}}} + W_p) \cdot 30\text{ft} \cdot 60\text{ft} + W_{\text{ext_ph}} = 228.6 \text{ kip}$$

$$W = \begin{pmatrix} 600.9 \\ 593.4 \\ 593.4 \\ 593.4 \\ 593.4 \\ 634.8 \\ 228.6 \end{pmatrix} \cdot \text{kip} \quad W_{\text{floor}} := W + \begin{pmatrix} 0 \\ 0 \\ 0 \\ 0 \\ 0 \\ W_7 \\ -W_7 \end{pmatrix} = \begin{pmatrix} 600.9 \\ 593.4 \\ 593.4 \\ 593.4 \\ 593.4 \\ 863.4 \\ 0 \end{pmatrix} \cdot \text{kip} \quad \text{Adding the penthouse weight to the sixth floor.}$$

Corner joints will carry 1/8 of the floor weight, while edge joints will carry 1/4 of the floor weight

because we have 4 bays in our model which will make a total of 8 segments.

$$M := \frac{W_{\text{floor}}}{386.4 \frac{\text{in}}{\text{sec}^2}} = \begin{pmatrix} 1.555 \\ 1.536 \\ 1.536 \\ 1.536 \\ 1.536 \\ 2.234 \\ 0 \end{pmatrix} \cdot \frac{\text{kip} \cdot \text{sec}^2}{\text{in}}$$

P-Delta Loads Applied on Ghost Column:

Dead load and live load applied on beams are:

$$DL := 1.5 \frac{\text{kip}}{\text{ft}} \quad LL := 0.75 \frac{\text{kip}}{\text{ft}}$$

$$\text{dead} := \frac{DL}{(15\text{ft})} = 100 \cdot \text{psf} \quad \text{live} := \frac{LL}{(15\text{ft})} = 50 \cdot \text{psf} \quad \text{-Too high need a reduction factor by 0.75}$$

$$P_{DL} := (30\text{ft} \cdot 4) \cdot (30\text{ft} \cdot 2.5) \cdot (0.75 \cdot \text{dead}) = 675 \cdot \text{kip}$$

$$P_{LL} := (30\text{ft} \cdot 4) \cdot (30\text{ft} \cdot 2.5) \cdot (0.75 \cdot \text{live}) = 337.5 \cdot \text{kip} \quad \text{-These loads are for all stories except the roof}$$

$$P_{DL_{\text{roof}}} := (30\text{ft} \cdot 4) \cdot (30\text{ft} \cdot 2.5) \cdot (0.6 \cdot \text{dead}) = 540 \cdot \text{kip}$$

$$P_{LL_{\text{roof}}} := (30\text{ft} \cdot 4) \cdot (30\text{ft} \cdot 2.5) \cdot (0.5 \cdot \text{live}) = 225 \cdot \text{kip} \quad \text{-These loads are applied on roof only}$$

Frame Design:

40 MOMENT FRAME: 60 BRACED FRAME

$f_{y_{col}} := 50\text{ksi}$ $f_{y_{brb}} := 40\text{ksi}$ $L1 := 392.35\text{in}$ assumed length of diagonal bracing
 $E := 29000\text{ksi}$ $L_w := 0.5 \cdot L1 = 196.175\text{-in}$

Moment Frame:

Columns with W18x158: $A_{col_m_1st} := 46.3\text{in}^2$ $Z_{x_{col_m_1st}} := 356\text{in}^3$
 $\theta := 90$

From SAP file:

$P_{r_{col_m_1st}} :=$	$\begin{pmatrix} 72 \\ 235 \\ 230 \\ 230 \\ 151 \\ 49 \\ 157 \\ 154 \\ 154 \\ 100 \\ 26 \\ 79 \\ 77 \\ 77 \\ 47 \end{pmatrix}$	$\cdot \text{kip}$	$M_{r_{col_m_1st}} :=$	$\begin{pmatrix} 6111 \\ 6829 \\ 6718 \\ 6662 \\ 6614 \\ 1313 \\ 3862 \\ 3741 \\ 3716 \\ 3614 \\ 577 \\ 3823 \\ 3468 \\ 3334 \\ 3857 \end{pmatrix}$	$\cdot \text{kip}\cdot\text{in}$
--------------------------	--	--------------------	--------------------------	---	----------------------------------

$P_{c_{col_m_1st}} := 0.9 \cdot f_{y_{col}} \cdot A_{col_m_1st} = 2083.5 \cdot \text{kip}$

$M_{c_{col_m_1st}} := 0.9 \cdot f_{y_{col}} \cdot Z_{x_{col_m_1st}} = 16020 \cdot \text{kip}\cdot\text{in}$

$i := 1 .. 15$

$$Check_{col_m_1st_i} := \begin{cases} \frac{P_{r_{col_m_1st_i}}}{P_{c_{col_m_1st}}} + \frac{8}{9} \cdot \left(\frac{M_{r_{col_m_1st_i}}}{M_{c_{col_m_1st}}} \right) & \text{if } \frac{P_{r_{col_m_1st_i}}}{P_{c_{col_m_1st}}} \geq 0.2 \\ \frac{P_{r_{col_m_1st_i}}}{2P_{c_{col_m_1st}}} + \left(\frac{M_{r_{col_m_1st_i}}}{M_{c_{col_m_1st}}} \right) & \text{otherwise} \end{cases}$$

0.399
0.483
0.475

0.471
0.449
0.094
0.279
0.27
0.269
0.25
0.042
0.258
0.235
0.227
0.252

< 1.0 Then it's okay

For 1st & 2nd Floor Beams with W18x65: $A_{beam_m} := 19.1in^2$ $Z_{x_beam_m} := 133in^3$

From SAP file:

$$Pr_{beam_m} := \begin{pmatrix} 17 \\ 12 \\ 8 \\ 5 \\ 51 \\ 41 \\ 27 \\ 11 \end{pmatrix} \cdot \text{kip} \quad Mr_{beam_m} := \begin{pmatrix} 4924 \\ 4752 \\ 4730 \\ 4732 \\ 5039 \\ 4877 \\ 4810 \\ 4832 \end{pmatrix} \cdot \text{kip} \cdot \text{in}$$

$$Pc_{beam_m} := 0.9 \cdot fy_{col} \cdot A_{beam_m} = 859.5 \cdot \text{kip}$$

$$Mc_{beam_m} := 0.9 \cdot fy_{col} \cdot Z_{x_beam_m} = 5985 \cdot \text{kip} \cdot \text{in}$$

i := 1 .. 8

$$Check_{beam_m_i} := \begin{cases} \frac{Pr_{beam_m_i}}{Pc_{beam_m}} + \frac{8}{9} \cdot \left(\frac{Mr_{beam_m_i}}{Mc_{beam_m}} \right) & \text{if } \frac{Pr_{beam_m_i}}{Pc_{beam_m}} \geq 0.2 \\ \frac{Pr_{beam_m_i}}{2Pc_{beam_m}} + \left(\frac{Mr_{beam_m_i}}{Mc_{beam_m}} \right) & \text{otherwise} \end{cases}$$

Check_{beam_m_i} =

0.833
0.801
0.795
0.794
0.872
0.839
0.819

0.814

For 3rd Floor Beams with W18x65: $A_{\text{beam_m_3rd}} := 19.1 \text{ in}^2$ $Z_x_{\text{beam_m_3rd}} := 133 \text{ in}^3$

From SAP file:

$$Pr_{\text{beam_m_3rd}} := \begin{pmatrix} 134 \\ 98 \\ 65 \\ 34 \end{pmatrix} \cdot \text{kip} \quad Mr_{\text{beam_m_3rd}} := \begin{pmatrix} 4353 \\ 4046 \\ 3993 \\ 3857 \end{pmatrix} \cdot \text{kip} \cdot \text{in}$$

$$Pc_{\text{beam_m_3rd}} := 0.9 \cdot fy_{\text{col}} \cdot A_{\text{beam_m_3rd}} = 859.5 \cdot \text{kip}$$

$$Mc_{\text{beam_m_3rd}} := 0.9 \cdot fy_{\text{col}} \cdot Z_x_{\text{beam_m_3rd}} = 5985 \cdot \text{kip} \cdot \text{in}$$

$i := 1 .. 4$

$$Check_{\text{beam_m_3rd}_i} := \begin{cases} \frac{Pr_{\text{beam_m_3rd}_i}}{Pc_{\text{beam_m_3rd}}} + \frac{8}{9} \cdot \left(\frac{Mr_{\text{beam_m_3rd}_i}}{Mc_{\text{beam_m_3rd}}} \right) & \text{if } \frac{Pr_{\text{beam_m_3rd}_i}}{Pc_{\text{beam_m_3rd}}} \geq 0.2 \\ \frac{Pr_{\text{beam_m_3rd}_i}}{2Pc_{\text{beam_m_3rd}}} + \left(\frac{Mr_{\text{beam_m_3rd}_i}}{Mc_{\text{beam_m_3rd}}} \right) & \text{otherwise} \end{cases}$$

$Check_{\text{beam_m_3rd}_i} =$

0.805
0.733
0.705
0.664

Braced Frame:

For Columns with W18x158:

$$A_{col_b} := 46.3 \text{ in}^2$$

$$Z_{x_{col_b}} := 356 \text{ in}^3$$

$$\theta_{col_b} := 90$$

From SAP file:

$$P_{col_b} := \begin{pmatrix} 101 \\ 331 \\ 9 \\ 162 \\ 38 \\ 39 \end{pmatrix} \cdot \text{kip} \quad M_{col_b} := \begin{pmatrix} 0 \\ 0 \\ 0 \\ 0 \\ 0 \\ 0 \end{pmatrix} \cdot \text{kip} \cdot \text{in}$$

$$A_{col_brace} := \frac{P_{col_b}}{f_{y_{col}}} = \begin{pmatrix} 2.02 \\ 6.62 \\ 0.18 \\ 3.24 \\ 0.76 \\ 0.78 \end{pmatrix} \cdot \text{in}^2 \quad K_{col_brace} := \frac{A_{col_brace} \cdot E}{L} \cdot \cos(\theta_{col_b})^2 = \begin{pmatrix} 59.952 \\ 196.477 \\ 5.342 \\ 96.161 \\ 22.556 \\ 23.15 \end{pmatrix} \cdot \frac{\text{kip}}{\text{in}}$$

For 1st & 2nd Floors Beams with W18x65:

$$A_{beam_b} := 19.1 \text{ in}^2$$

$$Z_{x_{beam_b}} := 133 \text{ in}^3$$

$$\theta_{beam_b} := 0$$

From SAP file:

$$P_{r_{beam_b}} := \begin{pmatrix} 203 \\ 203 \end{pmatrix} \cdot \text{kip} \quad M_{r_{beam_b}} := \begin{pmatrix} 3427 \\ 3427 \end{pmatrix} \cdot \text{kip} \cdot \text{in}$$

$$P_{c_{beam_b}} := 0.9 \cdot f_{y_{col}} \cdot A_{beam_b} = 859.5 \cdot \text{kip}$$

$$M_{c_{beam_b}} := 0.9 \cdot f_{y_{col}} \cdot Z_{x_{beam_b}} = 5985 \cdot \text{kip} \cdot \text{in}$$

i := 1 .. 2

$$\text{Check}_{beam_b_i} := \begin{cases} \frac{P_{r_{beam_b_i}}}{P_{c_{beam_b}}} + \frac{8}{9} \cdot \left(\frac{M_{r_{beam_b_i}}}{M_{c_{beam_b}}} \right) & \text{if } \frac{P_{r_{beam_b_i}}}{P_{c_{beam_b}}} \geq 0.2 \\ \frac{P_{r_{beam_b_i}}}{2P_{c_{beam_b}}} + \left(\frac{M_{r_{beam_b_i}}}{M_{c_{beam_b}}} \right) & \text{otherwise} \end{cases}$$

$$\text{Check}_{beam_b_i} =$$

0.745
0.745

For 3rd Floor Beam with W18x65: $A_{\text{beam_b_3rd}} := 19.1 \text{ in}^2$ $Z_{x\text{beam_b_3rd}} := 133 \text{ in}^3$

From SAP file:

$$P_{r\text{beam_b_3rd}} := 196 \cdot \text{kip} \quad M_{r\text{beam_b_3rd}} := 3427 \cdot \text{kip} \cdot \text{in}$$

$$P_{c\text{beam_b_3rd}} := 0.9 \cdot f_{y\text{col}} \cdot A_{\text{beam_b_3rd}} = 859.5 \cdot \text{kip}$$

$$M_{c\text{beam_b_3rd}} := 0.9 \cdot f_{y\text{col}} \cdot Z_{x\text{beam_b_3rd}} = 5985 \cdot \text{kip} \cdot \text{in}$$

$$\text{Check}_{\text{beam_b_3rd}} := \begin{cases} \frac{P_{r\text{beam_b_3rd}}}{P_{c\text{beam_b_3rd}}} + \frac{8}{9} \cdot \left(\frac{M_{r\text{beam_b_3rd}}}{M_{c\text{beam_b_3rd}}} \right) & \text{if } \frac{P_{r\text{beam_b_3rd}}}{P_{c\text{beam_b_3rd}}} \geq 0.2 \\ \frac{P_{r\text{beam_b_3rd}}}{2P_{c\text{beam_b_3rd}}} + \left(\frac{M_{r\text{beam_b_3rd}}}{M_{c\text{beam_b_3rd}}} \right) & \text{otherwise} \end{cases}$$

$$\text{Check}_{\text{beam_b_3rd}} = 0.737 < 1.0 \text{ Then it's okay}$$

For Braces:

$$\text{For 1st floor Braces with W12x53: } A_{T_r_b} := 15.6 \text{ in}^2$$

$$\text{For 2nd floor Brsces with W12x50: } A_{T_r_b} := 14.6 \text{ in}^2$$

$$\text{For 3rd floor Brsces with W12x40: } A_{T_r_b} := 11.7 \text{ in}^2$$

$$\theta_{T_r_b} := 41 \quad \Omega_o := 1.5$$

From SAP file:

$$P_{T_r_b} := \begin{pmatrix} 234 \\ 233 \\ 199 \\ 199 \\ 130 \\ 129 \end{pmatrix} \cdot \text{kip} \quad M_{T_r_b} := \begin{pmatrix} 0 \\ 0 \\ 0 \\ 0 \\ 0 \\ 0 \end{pmatrix} \cdot \text{kip} \cdot \text{in}$$

$$A_{Tr_brace} := \frac{P_{Tr} \cdot b \cdot \Omega_o}{f_{y_{brb}}} = \begin{pmatrix} 8.775 \\ 8.738 \\ 7.462 \\ 7.462 \\ 4.875 \\ 4.837 \end{pmatrix} \cdot \text{in}^2$$

Design of BRBs:

$$\theta_{brb} := 0 \quad \theta_{BRB} := 23.43 \text{ assumed as diagonal brace}$$

From SAP file:

$$P_{BRB} := \begin{pmatrix} 353.4 \\ 301 \\ 196 \end{pmatrix} \cdot \text{kip} \quad M_{BRB} := \begin{pmatrix} 0 \\ 0 \\ 0 \end{pmatrix} \cdot \text{kip} \cdot \text{in}$$

$$F_{BRB} := \frac{P_{BRB}}{\cos\left(\theta_{BRB} \cdot \frac{\pi}{180}\right)} = \begin{pmatrix} 385.16 \\ 328.05 \\ 213.61 \end{pmatrix} \cdot \text{kip}$$

$$A_{BRB} := \frac{F_{BRB}}{f_{y_{brb}}} = \begin{pmatrix} 9.629 \\ 8.201 \\ 5.34 \end{pmatrix} \cdot \text{in}^2 \quad A_{BRB} := \begin{pmatrix} 10 \\ 8.5 \\ 5.5 \end{pmatrix} \cdot \text{in}^2$$

$$K_{BRB} := \frac{A_{BRB} \cdot E}{L} \cdot \cos\left(\theta_{BRB} \cdot \frac{\pi}{180}\right)^2 = \begin{pmatrix} 1244.545 \\ 1057.863 \\ 684.5 \end{pmatrix} \frac{\text{kip}}{\text{in}} \quad \text{-multiplied by } \cos \theta_{BRB} \text{ to account for diagonal bracing}$$

$$i := 1 \dots \text{rows}(F_{BRB})$$

$$\delta_{y_i} := \frac{L \cdot F_{BRB_i}}{A_{BRB_i} \cdot E} + \frac{L \cdot F_{BRB_i}}{5 \cdot A_{BRB_i} \cdot E} \quad \delta_y = \begin{pmatrix} 0.3127 \\ 0.3133 \\ 0.3153 \end{pmatrix} \cdot \text{in} \quad P_y := f_{y_{brb}} \cdot A_{BRB} = \begin{pmatrix} 400 \\ 340 \\ 220 \end{pmatrix} \cdot \text{kip}$$

$$15 \cdot \delta_{y_i} = \boxed{4.69} \cdot \text{in} \quad P_{y_i} := P_y + 0.03 \cdot K_{BRB_i} \cdot (15 \cdot \delta_{y_i} - \delta_{y_i}) \quad P_{yt} = \begin{pmatrix} 563.428 \\ 479.195 \\ 310.639 \end{pmatrix} \cdot \text{kip}$$

4.699
4.729

$$\beta := 0.07 \quad P_{yc} := (1 + \beta) \cdot P_{yt} = \begin{pmatrix} 602.867 \\ 512.739 \\ 332.384 \end{pmatrix} \cdot \text{kip}$$

CHECK COLUMN-BEAM MOMENT RATIO FOR MOMENT FRAME

Columns W18x158

$$A_{g_col} := 46.3 \text{ in}^2 \quad d_{col} := 19.7 \text{ in} \quad t_{f_col} := 1.44 \text{ in} \quad t_{w_col} := 0.81 \text{ in} \quad Z_{x_col} := 356 \text{ in}^3$$

$$b_{f_col} := 11.3 \text{ in}$$

Beams W18x65

$$A_{g_beam} := 19.1 \text{ in}^2 \quad d_{beam} := 18.4 \text{ in} \quad t_{f_beam} := 0.75 \text{ in} \quad Z_{x_beam} := 133 \text{ in}^3$$

Material Properties for all beams and columns: $f_y := 50 \text{ ksi}$ $F_u := 65 \text{ ksi}$

Gravity loads on all beams: $w_D := 1.5 \frac{\text{kip}}{\text{ft}}$ $w_L := 0.75 \frac{\text{kip}}{\text{ft}}$

For Grade 50 steel $R_y := 1.1$

Bay length: $L_w := 360 \text{ in}$

Calculate the sum of the moments in the column above and below the joint at the intersection of the beam and column centerlines:

$$P_D := w_D \cdot L = 45 \cdot \text{kip} \quad P_L := w_L \cdot L = 22.5 \cdot \text{kip} \quad P_S := 0 \quad B_2 := 1.2 \text{ assumed}$$

In order to calculate P_{QE} we remove joint constraints between the moment frame & braced frame and find the max. load on columns due to earthquake loads.

Seismic Loads From SAP:

Joint 1	Joint 2	Joint 3	Joint 4	
$P_{QE1} := 41 \text{ kip}$	$P_{QE2} := 3.2 \text{ kip}$	$P_{QE3} := 11 \text{ kip}$	$P_{QE4} := 1.3 \text{ kip}$	From EQ loads only
$P_{QE11} := 26.3 \text{ kip}$	$P_{QE22} := 2.2 \text{ kip}$			

Determine the factored loads on the columns:

From ASCE7-10, seismic design category is D

$$S_{DS} := 1.615 \quad \rho := 1.0 \quad \text{it should be 1.3 but in this case we will assume it's 1.0}$$

Nontranslation forces due to dead and live loads:

$$P_{nt} := (1.2 + 0.2S_{DS}) \cdot P_D + 0.5P_L + 0.2 \cdot P_S = 79.785 \cdot \text{kip}$$

Lateral-Translation forces due to seismic load:

$$\text{Joint 1} \quad P_{lt1} := \rho \cdot P_{QE1} + 0.2 \cdot P_S = 41 \cdot \text{kip} \quad \text{Joint 2} \quad P_{lt2} := \rho \cdot P_{QE2} + 0.2 \cdot P_S = 3.2 \cdot \text{kip}$$

$$P_{lt11} := \rho \cdot P_{QE11} + 0.2 \cdot P_S = 26.3 \cdot \text{kip} \quad P_{lt22} := \rho \cdot P_{QE22} + 0.2 \cdot P_S = 2.2 \cdot \text{kip}$$

$$\text{Joint 3} \quad P_{lt3} := \rho \cdot P_{QE3} + 0.2 \cdot P_S = 11 \cdot \text{kip} \quad \text{Joint 4} \quad P_{lt4} := \rho \cdot P_{QE4} + 0.2 \cdot P_S = 1.3 \cdot \text{kip}$$

The factored loads on the columns:

$$\text{Joint 1} \quad P_{u1} := P_{nt} + B_2 \cdot P_{lt1} = 128.985 \cdot \text{kip} \quad \text{Joint 2} \quad P_{u2} := P_{nt} + B_2 \cdot P_{lt2} = 83.625 \cdot \text{kip}$$

$$P_{u11} := P_{nt} + B_2 \cdot P_{lt11} = 111.345 \cdot \text{kip} \quad P_{u22} := P_{nt} + B_2 \cdot P_{lt22} = 82.425 \cdot \text{kip}$$

$$\text{Joint 3} \quad P_{u3} := P_{nt} + B_2 \cdot P_{lt3} = 92.985 \cdot \text{kip} \quad \text{Joint 4} \quad P_{u4} := P_{nt} + B_2 \cdot P_{lt4} = 81.345 \cdot \text{kip}$$

The flexural strength of the columns at the beams centerlines:

$$M_{pc1} := (Z_{x_col}) \cdot \left(f_y - \frac{P_{u1}}{A_{g_col}} \right) + (Z_{x_col}) \cdot \left(f_y - \frac{P_{u11}}{A_{g_col}} \right) = 33752 \cdot \text{kip} \cdot \text{in}$$

For the joints with two columns & one beam connected
(Joint 1)

$$M_{pc2} := Z_{x_col} \cdot \left(f_y - \frac{P_{u2}}{A_{g_col}} \right) + (Z_{x_col}) \cdot \left(f_y - \frac{P_{u22}}{A_{g_col}} \right) = 34323 \cdot \text{kip} \cdot \text{in}$$

For the joints with two columns & two beams connected
(Joint 2)

$$M_{pc3} := Z_{x_col} \cdot \left(f_y - \frac{P_{u3}}{A_{g_col}} \right) = 17085 \cdot \text{kip} \cdot \text{in}$$

For the joints with one column & one beam connected
(Joint 3)

$$M_{pc4} := Z_{x_col} \left(f_y - \frac{P_{u4}}{A_{g_col}} \right) = 17175 \cdot \text{kip} \cdot \text{in}$$

For the joints with one column & two beams connected (**Joint 4**)

Determine the probable moment at the plastic hinge for joints with W18x65 beam:

$$C_{pr} := \frac{f_y + F_u}{2 \cdot f_y} = 1.15 \quad C_{pr} < 1.2 \text{ then it's ok}$$

Minimum plastic section modulus at the reduced beam section:

$$Z_e := Z_{x_beam} = 133 \cdot \text{in}^3$$

So the moment at the plastic hinge is:

$$M_{pr} := C_{pr} \cdot R_y \cdot f_y \cdot Z_e = 8412.25 \cdot \text{kip} \cdot \text{in}$$

Calculate the expected shear at the plastic hinge:

First calculate the factored uniform gravity load:

$$w_u := 1.2w_D + 0.5w_L = 2.175 \cdot \frac{\text{kip}}{\text{ft}}$$

The distance between plastic hinges:

$$L' := L - 2 \cdot \frac{d_{col}}{2} - 2 \cdot \frac{d_{beam}}{2} = 321.9 \cdot \text{in}$$

The required shear strength at the plastic hinge due to gravity loads:

$$V_{gH} := 0.5 \cdot w_u \cdot L' = 29.172 \cdot \text{kip}$$

So the expected shears at the plastic hinge is:

$$V_H := \frac{2 \cdot M_{pr}}{L'} + V_{gH} = 81.438 \cdot \text{kip} \quad V'_H := \frac{2 \cdot M_{pr}}{L'} - V_{gH} = 23.094 \cdot \text{kip}$$

$$V_{H_max} := \max(V_H, V'_H) = 81.438 \cdot \text{kip} \quad V_{H_min} := \min(V_H, V'_H) = 23.094 \cdot \text{kip}$$

Calculate the sum of the moments produced at the column centerline by the shear at the plastic hinges for W18x65:

$$M_{v_max} := (V_{H_max}) \cdot \left(\frac{d_{beam}}{2} + \frac{d_{col}}{2} \right) = 1551 \cdot \text{kip} \cdot \text{in}$$

$$M_{v_min} := (V_{H_min}) \cdot \left(\frac{d_{beam}}{2} + \frac{d_{col}}{2} \right) = 440 \cdot \text{kip} \cdot \text{in}$$

So the expected flexural demands of the W18x65 beam at the column centerline are:

$$M_{pb_max} := M_{pr} + M_{v_max} = 9963.652\text{-kip}\cdot\text{in}$$

$$M_{pb_min} := M_{pr} + M_{v_min} = 8852.192\text{-kip}\cdot\text{in}$$

Finally find the Column-Beam Moment Ratio:

At Joint 1:

$$\frac{M_{pc1}}{M_{pb_max}} = 3.388 > 1.2 \text{ okay}$$

At Joint 2:

$$\frac{M_{pc2}}{M_{pb_max} + M_{pb_min}} = 1.824 > 1.2 \text{ okay}$$

At Joint 3:

$$\frac{M_{pc3}}{M_{pb_max}} = 1.715 > 1.2 \text{ okay}$$

At Joint 4:

$$\frac{M_{pc4}}{M_{pb_max} + M_{pb_min}} = 0.913 < 1.2 \text{ okay according to AISC for roof members.}$$

PANEL ZONE DESIGN-DOUBLER PLATE FOR SMF

Minimum thickness of doubler plate is: $\phi := 0.9$

$$t_{min} := \frac{(d_{col} - 2 \cdot t_{f_col}) + (d_{beam} - 2 \cdot t_{f_beam})}{90} = 0.375\text{-in}$$

The expected flexural demands of the W18x65 beam at the column face are:

$$M_{f_max} := M_{pr} + V_{H_max} \left(\frac{d_{beam}}{2} \right) = 9161.483\text{-kip}\cdot\text{in}$$

$$M_{f_min} := M_{pr} + V_{H_min} \left(\frac{d_{beam}}{2} \right) = 8624.715\text{-kip}\cdot\text{in}$$

The shear forces at the column faces:

$$F_{f1} := \frac{M_{f_max}}{(d_{beam} - t_{f_beam})} = 519.064\text{-kip} \quad F_{f2} := \frac{M_{f_min}}{(d_{beam} - t_{f_beam})} = 488.652\text{-kip}$$

$$F_f := \max(F_{f1}, F_{f2}) = 519.064\text{-kip}$$

The available shear strength of the panel zone in joints with **one beam** is:

Column height: $h := 13\text{ft}$

$$V_{c1} := \frac{M_{f_max}}{h} = 58.727\text{-kip} \quad V_{u1} := F_f - V_{c1} = 460.337\text{-kip}$$

Capacity determined of the web panel zone:

$$R_{n1} := \phi \cdot 0.6 \cdot f_y \cdot d_{col} \cdot t_{w_col} = 430.839\text{-kip} \quad \text{Since } R_n < V_u, \text{ a doubler plate is required}$$

The required column panel zone thickness is found as follows

$$t_{p1} := \frac{V_{u1}}{\phi \cdot 0.6 \cdot f_y \cdot d_{col}} = 0.865\text{-in} > t_{w_col} = 0.81\text{-in}$$

The extra thickness or the required thickness of the doubler plate is:

$$t_{dp1} := t_{p1} - t_{w_col} = 0.055\text{-in}$$

or use $t_{dp1} := \max(t_{dp1}, 0.25\text{in}) = 0.25\text{-in}$

The available shear strength of the panel zone in joints with **two beams** is:

$$V_{c2} := \frac{M_{f_max} + M_{f_min}}{h} = 114.014\text{-kip} \quad V_{u2} := F_{f1} + F_{f2} - V_{c2} = 893.703\text{-kip}$$

Capacity determined of the web panel zone:

$$R_{n2} := \phi \cdot 0.6 \cdot f_y \cdot d_{col} \cdot t_{w_col} = 430.839\text{-kip} \quad \text{Since } R_n < V_u, \text{ a doubler plate is required}$$

The required column panel zone thickness is found as follows

$$t_{p2} := \frac{V_{u2}}{\phi \cdot 0.6 \cdot f_y \cdot d_{col}} = 1.68\text{-in} > t_{w_col} = 0.81\text{-in}$$

The extra thickness or the required thickness of the doubler plate is:

$$t_{dp2} := t_{p2} - t_{w_col} = 0.87\text{-in}$$

or use $t_{dp2} := \max(t_{dp2}, 0.25\text{in}) = 0.87\text{-in}$

Panel-Zone Support Link Calculations by Using the Scissors Model:

Shear Modulus of steel: $G := 11500000 \text{ psi} = 11500 \text{ ksi}$

Calculate the ratios of the effective depth of the column to the span length and the effective depth of the beam to the column height, respectively:

$$\alpha := \frac{d_{\text{col}} - t_{\text{f_col}}}{L} = 0.051 \quad \beta := \frac{d_{\text{beam}} - t_{\text{f_beam}}}{h} = 0.113$$

For joints with one beam:

The volume of the panel zone is:

$$t_{\text{plw}} := t_{\text{w_col}} + t_{\text{dp1}} = 1.06 \text{ in}$$

$$V_{\text{P1}} := \alpha \cdot L \cdot \beta \cdot h \cdot t_{\text{pl}} = 341.626 \text{ in}^3$$

The properties for the Scissors Model:

PANEL

$$K_{\text{PS1}} := \frac{G \cdot V_{\text{P1}}}{(1 - \alpha - \beta)^2} = 5.619 \times 10^6 \text{ kip-in}$$

$$M_{\text{PS1}} := \frac{0.6 \cdot f_y \cdot V_{\text{P1}}}{(1 - \alpha - \beta)} = 12257.313 \text{ kip-in}$$

$$\Theta_{\text{PS1}} := \frac{M_{\text{PS1}}}{K_{\text{PS1}}} = 0.00218$$

FLANGES

$$K_{\text{FS1}} := \frac{0.78 \cdot G \cdot b_{\text{f_col}} \cdot t_{\text{f_col}}^2}{(1 - \alpha - \beta)^2} = 3.006 \times 10^5 \text{ kip-in}$$

$$M_{\text{FS1}} := \frac{1.87 \cdot f_y \cdot b_{\text{f_col}} \cdot t_{\text{f_col}}^2}{(1 - \alpha - \beta)} = 2620.22 \text{ kip-in}$$

$$\Theta_{\text{FS1}} := \frac{M_{\text{FS1}}}{K_{\text{FS1}}} = 0.00872$$

TOTAL

$$M_{\text{add1}} := \Theta_{\text{PS1}} \cdot \frac{M_{\text{FS1}}}{\Theta_{\text{FS1}}} = 655.756 \text{ kip-in} \quad K_{\text{tot1}} := K_{\text{PS1}} + K_{\text{FS1}} = 5920095.896 \text{ kip-in}$$

$$M_{\text{P_tot1}} := M_{\text{PS1}} + M_{\text{add1}} = 12913.069 \text{ kip-in with } \Theta_{\text{PS1}} = 0.00218$$

$$M_{\text{F_tot1}} := M_{\text{FS1}} + M_{\text{PS1}} = 14877.533 \text{ kip-in with } \Theta_{\text{FS1}} = 0.00872 \text{ extend to } 10 \cdot \Theta_{\text{PS1}} = 0.022$$

For joints with two beams:

The volume of the panel zone is:

$$t_{p2} := t_{w_col} + t_{dp2} = 1.68 \cdot \text{in}$$

$$V_{p2} := \alpha \cdot L \cdot \beta \cdot h \cdot t_{p2} = 541.513 \cdot \text{in}^3$$

The properties for the Scissors Model:

PANEL:

$$K_{PS2} := \frac{G \cdot V_{p2}}{(1 - \alpha - \beta)^2} = 8.907 \times 10^6 \cdot \text{kip} \cdot \text{in}$$

$$M_{PS2} := \frac{0.6 \cdot f_y \cdot V_{p2}}{(1 - \alpha - \beta)} = 19429.089 \cdot \text{kip} \cdot \text{in}$$

$$\Theta_{PS2} := \frac{M_{PS2}}{K_{PS2}} = 0.00218$$

FLANGES:

$$K_{FS2} := \frac{0.78 \cdot G \cdot b_f \cdot t_{f_col}^2}{(1 - \alpha - \beta)^2} = 3.006 \times 10^5 \cdot \text{kip} \cdot \text{in}$$

$$M_{FS2} := \frac{1.87 \cdot f_y \cdot b_f \cdot t_{f_col}^2}{(1 - \alpha - \beta)} = 2620.22 \cdot \text{kip} \cdot \text{in}$$

$$\Theta_{FS2} := \frac{M_{FS2}}{K_{FS2}} = 0.00872$$

TOTAL

$$M_{add2} := \Theta_{PS2} \cdot \frac{M_{FS2}}{\Theta_{FS2}} = 655.756 \cdot \text{kip} \cdot \text{in}$$

$$K_{tot2} := K_{PS2} + K_{FS2} = 9208051.472 \cdot \text{kip} \cdot \text{in}$$

$$M_{P_tot2} := M_{PS2} + M_{add2} = 20084.844 \cdot \text{kip} \cdot \text{in} \quad \text{with} \quad \Theta_{PS2} = 0.00218$$

$$M_{F_tot2} := M_{FS2} + M_{PS2} = 22049.308 \cdot \text{kip} \cdot \text{in} \quad \text{with} \quad \Theta_{FS2} = 0.00872 \quad \text{extend to} \quad 10 \cdot \Theta_{PS2} = 0.022$$

BEAM HINGES:

Add hinges for each beam at the locations below:

$$\text{RelativeDistance}_1 := \frac{d_{\text{beam}} + d_{\text{col}}}{L} = 0.106$$

$$\text{RelativeDistance}_2 := 1 - \text{RelativeDistance}_1 = 0.894$$

Gap Elements' Backbone Curve Calculations:

$$k_{\text{intial}} := 0.5 \frac{\text{kip}}{\text{in}}$$

$$\text{Gap} := 0.0045 \cdot h = 0.7 \cdot \text{in} \quad \text{-Less than brace frame yielding limit} = 0.005 \cdot h$$

$$\delta_g := \text{Gap} = 0.7 \cdot \text{in} \quad P_{\text{gt}} := \begin{pmatrix} -k_{\text{intial}} \cdot \text{Gap} \\ -1.25 \cdot P_{\text{yt}1} \end{pmatrix} = \begin{pmatrix} -0.351 \\ -704.284 \end{pmatrix} \cdot \text{kip} \quad P_{\text{gc}} := \begin{pmatrix} k_{\text{intial}} \cdot \text{Gap} \\ 1.25 \cdot P_{\text{yc}1} \end{pmatrix} = \begin{pmatrix} 0.351 \\ 753.584 \end{pmatrix} \cdot \text{kip}$$

$$\text{Gap2} := 0.003 \cdot h = 0.47 \cdot \text{in}$$

$$\delta_{g2} := \text{Gap2} = 0.47 \cdot \text{in}$$

$$P_{\text{gt}2} := \begin{pmatrix} -k_{\text{intial}} \cdot \text{Gap2} \\ -1.25 \cdot P_{\text{yt}1} \end{pmatrix} = \begin{pmatrix} -0.234 \\ -704.284 \end{pmatrix} \cdot \text{kip} \quad P_{\text{gc}2} := \begin{pmatrix} k_{\text{intial}} \cdot \text{Gap2} \\ 1.25 \cdot P_{\text{yc}1} \end{pmatrix} = \begin{pmatrix} 0.234 \\ 753.584 \end{pmatrix} \cdot \text{kip}$$

$$\text{Gap3} := 0.0015 \cdot h = 0.23 \cdot \text{in}$$

$$\delta_{g3} := \text{Gap3} = 0.23 \cdot \text{in}$$

$$P_{\text{gt}3} := \begin{pmatrix} -k_{\text{intial}} \cdot \text{Gap3} \\ -1.25 \cdot P_{\text{yt}1} \end{pmatrix} = \begin{pmatrix} -0.117 \\ -704.284 \end{pmatrix} \cdot \text{kip} \quad P_{\text{gc}3} := \begin{pmatrix} k_{\text{intial}} \cdot \text{Gap3} \\ 1.25 \cdot P_{\text{yc}1} \end{pmatrix} = \begin{pmatrix} 0.117 \\ 753.584 \end{pmatrix} \cdot \text{kip}$$

Frame Design:

40 MOMENT FRAME: 60 BRACED FRAME

$f_{y_{col}} := 50\text{ksi}$ $f_{y_{brb}} := 40\text{ksi}$ $E := 29000\text{ksi}$

Moment Frame:

For 1st & 2nd floors Columns with W18x283: $A_{col_m_1st} := 83.3\text{in}^2$ $Z_{x_{col_m_1st}} := 676\text{in}^3$

$\theta := 90$

From SAP file:

$P_{r_{col_m_1st}} :=$	·kip)	(104	·kip-in)	(10085
				466				11313
				460				11355
				457				11361
				350				10975
				92				2435
				388				6320
				384				6082
				381				6090
				286				4813

$P_{c_{col_m_1st}} := 0.9 \cdot f_{y_{col}} \cdot A_{col_m_1st} = 3748.5\text{-kip}$

$M_{c_{col_m_1st}} := 0.9 \cdot f_{y_{col}} \cdot Z_{x_{col_m_1st}} = 30420\text{-kip-in}$

$i := 1..10$

$$Check_{col_m_1st_i} := \begin{cases} \frac{P_{r_{col_m_1st_i}}}{P_{c_{col_m_1st}}} + \frac{8}{9} \cdot \left(\frac{M_{r_{col_m_1st_i}}}{M_{c_{col_m_1st}}} \right) & \text{if } \frac{P_{r_{col_m_1st_i}}}{P_{c_{col_m_1st}}} \geq 0.2 \\ \frac{P_{r_{col_m_1st_i}}}{2P_{c_{col_m_1st}}} + \left(\frac{M_{r_{col_m_1st_i}}}{M_{c_{col_m_1st}}} \right) & \text{otherwise} \end{cases}$$

$Check_{col_m_1st_i} =$

0.345
0.434
0.435
0.434
0.407
0.092
0.26
0.251
0.251
0.196

For 3rd & 4th floors Columns with W18x192: $A_{col_m_2nd} := 56.4in^2$ $Z_{x_col_m_2nd} := 442in^3$

From SAP file:

$$Pr_{col_m_2nd} := \begin{pmatrix} 82 \\ 310 \\ 307 \\ 305 \\ 220 \\ 69 \\ 233 \\ 230 \\ 229 \\ 157 \end{pmatrix} \cdot \text{kip}$$

$$Mr_{col_m_2nd} := \begin{pmatrix} 1910 \\ 4907 \\ 4905 \\ 4944 \\ 3903 \\ 1724 \\ 4804 \\ 4760 \\ 4814 \\ 3998 \end{pmatrix} \cdot \text{kip}\cdot\text{in}$$

$$Pc_{col_m_2nd} := 0.9 \cdot fy_{col} \cdot A_{col_m_2nd} = 2538 \cdot \text{kip}$$

$$Mc_{col_m_2nd} := 0.9 \cdot fy_{col} \cdot Z_{x_col_m_2nd} = 19890 \cdot \text{kip}\cdot\text{in}$$

$i := 1 .. 10$

$$Check_{col_m_2nd_i} := \begin{cases} \frac{Pr_{col_m_2nd_i}}{Pc_{col_m_2nd}} + \frac{8}{9} \cdot \left(\frac{Mr_{col_m_2nd_i}}{Mc_{col_m_2nd}} \right) & \text{if } \frac{Pr_{col_m_2nd_i}}{Pc_{col_m_2nd}} \geq 0.2 \\ \frac{Pr_{col_m_2nd_i}}{2Pc_{col_m_2nd}} + \left(\frac{Mr_{col_m_2nd_i}}{Mc_{col_m_2nd}} \right) & \text{otherwise} \end{cases}$$

$Check_{col_m_2nd_i} =$

0.112
0.308
0.307
0.309
0.24
0.1
0.287
0.285
0.287
0.232

< 1.0 Then it's okay

For 5th & 6th floors Columns with W18x192: $A_{col_m_3rd} := 56.4in^2$ $Z_{x_col_m_3rd} := 442in^3$

From SAP file:

$$Pr_{col_m_3rd} := \begin{pmatrix} 53 \\ 155 \\ 154 \\ 153 \\ 97 \\ 28 \\ 78 \\ 77 \\ 77 \\ 46 \end{pmatrix} \cdot kip$$

$$Mr_{col_m_3rd} := \begin{pmatrix} 1282 \\ 3596 \\ 3721 \\ 3823 \\ 3651 \\ 1061 \\ 3329 \\ 3094 \\ 2972 \\ 3681 \end{pmatrix} \cdot kip \cdot in$$

$$Pc_{col_m_3rd} := 0.9 \cdot fy_{col} \cdot A_{col_m_3rd} = 2538 \cdot kip$$

$$Mc_{col_m_3rd} := 0.9 \cdot fy_{col} \cdot Z_{x_col_m_3rd} = 19890 \cdot kip \cdot in$$

$i := 1 .. 10$

$$Check_{col_m_3rd_i} := \begin{cases} \frac{Pr_{col_m_3rd_i}}{Pc_{col_m_3rd}} + \frac{8}{9} \left(\frac{Mr_{col_m_3rd_i}}{Mc_{col_m_3rd}} \right) & \text{if } \frac{Pr_{col_m_3rd_i}}{Pc_{col_m_3rd}} \geq 0.2 \\ \frac{Pr_{col_m_3rd_i}}{2Pc_{col_m_3rd}} + \left(\frac{Mr_{col_m_3rd_i}}{Mc_{col_m_3rd}} \right) & \text{otherwise} \end{cases}$$

$$Check_{col_m_3rd_i} =$$

0.075
0.211
0.217
0.222
0.203
0.059
0.183
0.171
0.165
0.194

< 1.0 Then it's okay

For 1st & 2nd floors Beams with W21x83: $A_{beam_m} := 24.3in^2$ $Z_{x_beam_m} := 196in^3$

From SAP file:

$$Pr_{beam_m} := \begin{pmatrix} 10 \\ 2.5 \\ 3 \\ 7.5 \\ 27 \\ 18 \\ 10 \\ 3 \end{pmatrix} \cdot \text{kip} \quad Mr_{beam_m} := \begin{pmatrix} 6876 \\ 6717 \\ 6700 \\ 6845 \\ 7320 \\ 7182 \\ 7152 \\ 7348 \end{pmatrix} \cdot \text{kip} \cdot \text{in}$$

$$Pc_{beam_m} := 0.9 \cdot fy_{col} \cdot A_{beam_m} = 1093.5 \cdot \text{kip}$$

$$Mc_{beam_m} := 0.9 \cdot fy_{col} \cdot Zx_{beam_m} = 8820 \cdot \text{kip} \cdot \text{in}$$

i := 1 .. 8

$$Check_{beam_m_i} := \begin{cases} \frac{Pr_{beam_m_i}}{Pc_{beam_m}} + \frac{8}{9} \cdot \left(\frac{Mr_{beam_m_i}}{Mc_{beam_m}} \right) & \text{if } \frac{Pr_{beam_m_i}}{Pc_{beam_m}} \geq 0.2 \\ \frac{Pr_{beam_m_i}}{2Pc_{beam_m}} + \left(\frac{Mr_{beam_m_i}}{Mc_{beam_m}} \right) & \text{otherwise} \end{cases}$$

Check_{beam_m_i} =

0.784
0.763
0.761
0.78
0.842
0.823
0.815
0.834

For 3rd & 4th floors Beams with W21x73: $A_{beam_m_2nd} := 21.5 \text{in}^2$ $Zx_{beam_m_2nd} := 172 \text{in}^3$

From SAP file:

$$Pr_{beam_m_2nd} := \begin{pmatrix} 31 \\ 23 \\ 15 \\ 6.5 \\ 47 \\ 33 \\ 20 \\ 7 \end{pmatrix} \cdot \text{kip} \quad Mr_{beam_m_2nd} := \begin{pmatrix} 6670 \\ 6578 \\ 6560 \\ 6737 \\ 6082 \\ 6027 \\ 6002 \\ 6165 \end{pmatrix} \cdot \text{kip} \cdot \text{in}$$

$$Pc_{beam_m_2nd} := 0.9 \cdot fy_{col} \cdot A_{beam_m_2nd} = 967.5 \cdot \text{kip}$$

$$M_{c_{beam_m_2nd}} := 0.9 \cdot f_{y_{col}} \cdot Z_{x_{beam_m_2nd}} = 7740 \cdot \text{kip} \cdot \text{in}$$

$$i := 1..8$$

$$Check_{beam_m_2nd_i} := \begin{cases} \frac{Pr_{beam_m_2nd_i}}{P_{c_{beam_m_2nd}}} + \frac{8}{9} \cdot \left(\frac{Mr_{beam_m_2nd_i}}{M_{c_{beam_m_2nd}}} \right) & \text{if } \frac{Pr_{beam_m_2nd_i}}{P_{c_{beam_m_2nd}}} \geq 0.2 \\ \frac{Pr_{beam_m_2nd_i}}{2P_{c_{beam_m_2nd}}} + \left(\frac{Mr_{beam_m_2nd_i}}{M_{c_{beam_m_2nd}}} \right) & \text{otherwise} \end{cases} \quad Check_{beam_m_2nd_i}$$

0.878
0.862
0.855
0.874
0.81
0.796
0.786
0.8

For 5th & 6th Floor Beams with W21x57: $A_{beam_m_3rd} := 16.7 \text{in}^2$ $Z_{x_{beam_m_3rd}} := 129 \text{in}^3$

From SAP file:

$Pr_{beam_m_3rd} := \begin{pmatrix} 51 \\ 40 \\ 25 \\ 7 \\ 110 \\ 81 \\ 55 \\ 30 \end{pmatrix} \cdot \text{kip}$	$Mr_{beam_m_3rd} := \begin{pmatrix} 4686 \\ 4669 \\ 4610 \\ 4633 \\ 4033 \\ 3864 \\ 3800 \\ 3681 \end{pmatrix} \cdot \text{kip} \cdot \text{in}$
--	--

$$P_{c_{beam_m_3rd}} := 0.9 \cdot f_{y_{col}} \cdot A_{beam_m_3rd} = 751.5 \cdot \text{kip}$$

$$M_{c_{beam_m_3rd}} := 0.9 \cdot f_{y_{col}} \cdot Z_{x_{beam_m_3rd}} = 5805 \cdot \text{kip} \cdot \text{in}$$

$$i := 1..8$$

$$Check_{beam_m_3rd_i} := \begin{cases} \frac{Pr_{beam_m_3rd_i}}{P_{c_{beam_m_3rd}}} + \frac{8}{9} \cdot \left(\frac{Mr_{beam_m_3rd_i}}{M_{c_{beam_m_3rd}}} \right) & \text{if } \frac{Pr_{beam_m_3rd_i}}{P_{c_{beam_m_3rd}}} \geq 0.2 \\ \frac{Pr_{beam_m_3rd_i}}{2P_{c_{beam_m_3rd}}} + \left(\frac{Mr_{beam_m_3rd_i}}{M_{c_{beam_m_3rd}}} \right) & \text{otherwise} \end{cases}$$

Check_{beam_m_3rd_1} =

0.841
0.831
0.811
0.803
0.768
0.72
0.691
0.654

Braced Frame:

For 1st & 2nd floors Columns with W18x283:

$$A_{col_b} := 83.3in^2$$

For 3rd & 4th floors Columns with W18x192:

$$A_{col_b} := 56.4in^2$$

For 5th & 6th floors Columns with W18x192:

$$A_{col_b} := 56.4in^2$$

$$\theta_{col_b} := 90$$

From SAP file:

$P_{col_b} :=$	448	·kip	$M_{col_b} :=$	0	·kip-in
	908			0	
	299			0	
	682			0	
	167			0	
	474			0	
	61			0	
	291			0	
	11			0	
	143			0	
	38			0	
	38.5			0	

1

$$A_{\text{col_brace}} := \frac{P_{\text{col_b}}}{f_{y_{\text{col}}}} = \begin{array}{|c|c|} \hline 1 & 8.96 \\ \hline 2 & 18.16 \\ \hline 3 & 5.98 \\ \hline 4 & 13.64 \\ \hline 5 & 3.34 \\ \hline 6 & 9.48 \\ \hline 7 & 1.22 \\ \hline 8 & 5.82 \\ \hline 9 & 0.22 \\ \hline 10 & 2.86 \\ \hline 11 & 0.76 \\ \hline 12 & 0.77 \\ \hline \end{array} \cdot \text{in}^2$$

$$K_{\text{col_brace}} := \frac{A_{\text{col_brace}} \cdot E}{L} \cdot \cos(\theta_{\text{col_b}})^2 = \begin{array}{|c|c|} \hline & 1 \\ \hline 1 & 1.325 \cdot 10^6 \\ \hline 2 & 2.686 \cdot 10^6 \\ \hline 3 & 8.844 \cdot 10^5 \\ \hline 4 & 2.017 \cdot 10^6 \\ \hline 5 & 4.939 \cdot 10^5 \\ \hline 6 & 1.402 \cdot 10^6 \\ \hline 7 & 1.804 \cdot 10^5 \\ \hline 8 & 8.607 \cdot 10^5 \\ \hline 9 & 3.254 \cdot 10^4 \\ \hline 10 & 4.23 \cdot 10^5 \\ \hline 11 & 1.124 \cdot 10^5 \\ \hline 12 & 1.139 \cdot 10^5 \\ \hline \end{array} \frac{1}{\text{m}^2} \cdot \frac{\text{kip}}{\text{in}}$$

For 1st & 2nd Floors Beams with W21x83: $A_{\text{beam_b}} := 24.3 \text{in}^2$ $Z_{x_{\text{beam_b}}} := 196 \text{in}^3$
 $\theta_{\text{beam_b}} := 0$

From SAP file:

$$P_{r_{\text{beam_b}}} := \begin{pmatrix} 238 \\ 236 \end{pmatrix} \cdot \text{kip} \quad M_{r_{\text{beam_b}}} := \begin{pmatrix} 3427 \\ 3427 \end{pmatrix} \cdot \text{kip} \cdot \text{in}$$

$$P_{e_{\text{beam_b}}} := 0.9 \cdot f_{y_{\text{col}}} \cdot A_{\text{beam_b}} = 1093.5 \cdot \text{kip}$$

$$M_{e_{\text{beam_b}}} := 0.9 \cdot f_{y_{\text{col}}} \cdot Z_{x_{\text{beam_b}}} = 8820 \cdot \text{kip} \cdot \text{in}$$

$$i := 1 \dots 2$$

$$\text{Check}_{\text{beam}_b_i} := \begin{cases} \frac{Pr_{\text{beam}_b_i}}{Pc_{\text{beam}_b}} + \frac{8}{9} \left(\frac{Mr_{\text{beam}_b_i}}{Mc_{\text{beam}_b}} \right) & \text{if } \frac{Pr_{\text{beam}_b_i}}{Pc_{\text{beam}_b}} \geq 0.2 \\ \frac{Pr_{\text{beam}_b_i}}{2Pc_{\text{beam}_b}} + \left(\frac{Mr_{\text{beam}_b_i}}{Mc_{\text{beam}_b}} \right) & \text{otherwise} \end{cases} \quad \text{Check}_{\text{beam}_b_i} = \begin{matrix} 0.563 \\ 0.561 \end{matrix}$$

For 3rd & 4th Floors Beams with W21x73: $A_{\text{beam}_b_{2nd}} := 21.5 \text{in}^2$ $Z_{x_{\text{beam}_b_{2nd}}} := 172 \text{in}^3$

$$\theta_{\text{beam}_b_{2nd}} := 0$$

From SAP file:

$$Pr_{\text{beam}_b_{2nd}} := \left(\frac{227}{207} \right) \cdot \text{kip} \quad Mr_{\text{beam}_b_{2nd}} := \left(\frac{3427}{3427} \right) \cdot \text{kip-in}$$

$$Pc_{\text{beam}_b_{2nd}} := 0.9 \cdot fy_{\text{col}} \cdot A_{\text{beam}_b_{2nd}} = 967.5 \cdot \text{kip}$$

$$Mc_{\text{beam}_b_{2nd}} := 0.9 \cdot fy_{\text{col}} \cdot Z_{x_{\text{beam}_b_{2nd}}} = 7740 \cdot \text{kip-in}$$

$i := 1..2$

$$\text{Check}_{\text{beam}_b_{2nd}_i} := \begin{cases} \frac{Pr_{\text{beam}_b_{2nd}_i}}{Pc_{\text{beam}_b_{2nd}}} + \frac{8}{9} \left(\frac{Mr_{\text{beam}_b_{2nd}_i}}{Mc_{\text{beam}_b_{2nd}}} \right) & \text{if } \frac{Pr_{\text{beam}_b_{2nd}_i}}{Pc_{\text{beam}_b_{2nd}}} \geq 0.2 \\ \frac{Pr_{\text{beam}_b_{2nd}_i}}{2Pc_{\text{beam}_b_{2nd}}} + \left(\frac{Mr_{\text{beam}_b_{2nd}_i}}{Mc_{\text{beam}_b_{2nd}}} \right) & \text{otherwise} \end{cases} \quad \text{Check}_{\text{beam}_b_{2nd}_i} = \begin{matrix} 0.628 \\ 0.608 \end{matrix}$$

For 5th & 6th Floors Beams with W21x57: $A_{\text{beam}_b_{3rd}} := 16.7 \text{in}^2$ $Z_{x_{\text{beam}_b_{3rd}}} := 129 \text{in}^3$

$$\theta_{\text{beam}_b_{3rd}} := 0$$

From SAP file:

$$Pr_{\text{beam}_b_{3rd}} := \left(\frac{178}{152} \right) \cdot \text{kip} \quad Mr_{\text{beam}_b_{3rd}} := \left(\frac{3427}{3427} \right) \cdot \text{kip-in}$$

$$Pc_{\text{beam}_b_{3rd}} := 0.9 \cdot fy_{\text{col}} \cdot A_{\text{beam}_b_{3rd}} = 751.5 \cdot \text{kip}$$

$$Mc_{\text{beam}_b_{3rd}} := 0.9 \cdot fy_{\text{col}} \cdot Z_{x_{\text{beam}_b_{3rd}}} = 5805 \cdot \text{kip-in}$$

$i := 1..2$

$$\text{Check}_{\text{beam_b_3rd}_i} := \begin{cases} \frac{Pr_{\text{beam_b_3rd}_i}}{Pc_{\text{beam_b_3rd}}} + \frac{8}{9} \cdot \left(\frac{Mr_{\text{beam_b_3rd}_i}}{Mc_{\text{beam_b_3rd}}} \right) & \text{if } \frac{Pr_{\text{beam_b_3rd}_i}}{Pc_{\text{beam_b_3rd}}} \geq 0.2 \\ \frac{Pr_{\text{beam_b_3rd}_i}}{2Pc_{\text{beam_b_3rd}}} + \left(\frac{Mr_{\text{beam_b_3rd}_i}}{Mc_{\text{beam_b_3rd}}} \right) & \text{otherwise} \end{cases} \quad \text{Check}_{\text{beam_b_3rd}_i}$$

0.762
0.727

For Braces:

- For 1st floor Braces with W12x65: $A_{Tr_b} := 19.1 \text{ in}^2$
- For 2nd floor Braces with W12x53: $A_{Tr_b} := 15.6 \text{ in}^2$
- For 3rd floor Braces with W12x53: $A_{Tr_b} := 15.6 \text{ in}^2$
- For 4th floor Braces with W12x50: $A_{Tr_b} := 14.6 \text{ in}^2$
- For 5th floor Braces with W12x40: $A_{Tr_b} := 11.7 \text{ in}^2$
- For 6th floor Braces with W12x40: $A_{Tr_b} := 11.7 \text{ in}^2$

$\theta_{Tr_b} := 41$ $\Omega_o := 1.5$

From SAP file:

$P_{Tr_b} :=$.kip	355
		354
		286
		286
		260
		259
		221
		220
		168
		167
		100
		100
		0

$M_{Tr_b} :=$.kip-in	0
		0
		0
		0
		0
		0
		0
		0
		0
		0
		0
		0
		0
0		

$A_{Tr_brace} :=$	$\frac{P_{Tr_b} \cdot \Omega_o}{f_{y_{brb}}} =$.in ²	1
			13.313
			13.275
			10.725
			10.725
			9.75
			9.712
			8.287
			8.25
			6.3
			6.262
			3.75
			3.75

Design of BRBs:

$\theta_{BRB} := 30.96$ assumed as a diagonal brace for 1st story

$\theta_{BRB1} := 23.43$ assumed as a diagonal brace for all other stories

From SAP file:

$$P_{BRB} := \begin{pmatrix} 454 \\ 433 \\ 393 \\ 334 \\ 254 \\ 152 \end{pmatrix} \cdot \text{kip} \quad M_{BRB} := \begin{pmatrix} 0 \\ 0 \\ 0 \\ 0 \\ 0 \\ 0 \end{pmatrix} \cdot \text{kip} \cdot \text{in}$$

$$F_{BRB} := \frac{P_{BRB1}}{\cos\left(\theta_{BRB} \cdot \frac{\pi}{180}\right)} = 529.43 \cdot \text{kip} \quad F_{BRB1} := \frac{P_{BRB}}{\cos\left(\theta_{BRB1} \cdot \frac{\pi}{180}\right)} = \begin{pmatrix} 494.798 \\ 471.911 \\ 428.316 \\ 364.014 \\ 276.825 \\ 165.659 \end{pmatrix} \cdot \text{kip}$$

$$L1 := \sqrt{(18\text{ft})^2 + (30\text{ft})^2} = 419.829 \cdot \text{in} \quad L_1 := 0.5 \cdot L1 = 209.914 \cdot \text{in} \quad \text{diagonal brace for the 1st story}$$

$$L2 := \sqrt{(13\text{ft})^2 + (30\text{ft})^2} = 392.347 \cdot \text{in} \quad L_2 := 0.5 \cdot L2 = 196.173 \cdot \text{in} \quad \text{diagonal brace for all other stories}$$

$$A_{BRB} := \frac{F_{BRB}}{f_{ybrb}} = 13.236 \cdot \text{in}^2 \quad A_{BRB1} := \frac{F_{BRB1}}{f_{ybrb}} = \begin{pmatrix} 12.37 \\ 11.798 \\ 10.708 \\ 9.1 \\ 6.921 \\ 4.141 \end{pmatrix} \cdot \text{in}^2 \quad A_{BRB1} := \begin{pmatrix} 13.5 \\ 12 \\ 11 \\ 9.5 \\ 7 \\ 4.5 \end{pmatrix} \cdot \text{in}^2$$

$$K_{BRB} := \frac{A_{BRB1} \cdot E}{L_1} \cdot \cos^2\left(\theta_{BRB} \cdot \frac{\pi}{180}\right) = 1371.466 \cdot \frac{\text{kip}}{\text{in}} \quad \begin{array}{l} \text{-Multiplied by } \cos \theta_{BRB} \text{ to account} \\ \text{for diagonal bracing.} \\ \text{-This is for the 1st story only.} \end{array}$$

$$K_{BRB1} := \frac{A_{BRB1} \cdot E}{L_2} \cdot \cos^2\left(\theta_{BRB1} \cdot \frac{\pi}{180}\right) = \begin{pmatrix} 1680.149 \\ 1493.466 \\ 1369.011 \\ 1182.327 \\ 871.189 \\ 560.05 \end{pmatrix} \cdot \frac{\text{kip}}{\text{in}} \quad \begin{array}{l} \text{-Use the stiffness for all stories} \\ \text{except the 1st story.} \end{array}$$

$$i := 1 \dots \text{rows}(F_{BRB1})$$

$$\delta_y := \frac{L_1 \cdot F_{BRB}}{A_{BRB1} \cdot E} + \frac{L_1 \cdot F_{BRB}}{5 \cdot A_{BRB1} \cdot E} \quad \delta_y = 0.3406 \cdot \text{in} \quad 15 \cdot \delta_y = 5.11 \cdot \text{in}$$

$$\delta_{y1_i} := \frac{L_2 \cdot F_{BRB1_i}}{A_{BRB1} \cdot E} + \frac{L_2 \cdot F_{BRB1_i}}{5 \cdot A_{BRB1} \cdot E} \quad \delta_{y1} = \begin{pmatrix} 0.2975 \\ 0.3192 \\ 0.3161 \\ 0.311 \\ 0.321 \\ 0.2988 \end{pmatrix} \cdot \text{in} \quad 15 \cdot \delta_{y1_i} = \begin{matrix} \boxed{4.463} \\ \boxed{4.788} \\ \boxed{4.741} \\ \boxed{4.666} \\ \boxed{4.815} \\ \boxed{4.482} \end{matrix} \cdot \text{in}$$

$$P_y := f_{ybrb} \cdot A_{BRB} = \begin{pmatrix} 540 \\ 480 \\ 440 \\ 380 \\ 280 \\ 180 \end{pmatrix} \cdot \text{kip} \quad \beta := 0.07$$

$$P_{yt} := P_{y1} + 0.03 \cdot K_{BRB} \cdot (15 \cdot \delta_y - \delta_y) \quad P_{yt} = 736.216 \cdot \text{kip} \quad P_{yc} := (1 + \beta) \cdot P_{yt} = 787.751 \cdot \text{kip}$$

$$P_{yt1_i} := P_{y_i} + 0.03 \cdot K_{BRB1_i} \cdot (15 \cdot \delta_{y1_i} - \delta_{y1_i})$$

$$P_{yt1} = \begin{pmatrix} 749.949 \\ 680.238 \\ 621.74 \\ 534.456 \\ 397.461 \\ 250.291 \end{pmatrix} \cdot \text{kip} \quad P_{yc1} := (1 + \beta) \cdot P_{yt1} = \begin{pmatrix} 802.446 \\ 727.855 \\ 665.262 \\ 571.868 \\ 425.283 \\ 267.812 \end{pmatrix} \cdot \text{kip}$$

CHECK COLUMN-BEAM MOMENT RATIO FOR MOMENT FRAME

Columns W18x283 for Joints 1 & 2

$$A_{g_col} := 83.3\text{in}^2 \quad d_{col} := 21.9\text{in} \quad t_{f_col} := 2.5\text{in} \quad t_{w_col} := 1.4\text{in} \quad Z_{x_col} := 676\text{in}^3 \\ b_{f_col} := 11.9\text{in}$$

Columns W18x192 for Joints 3 & 4

$$A_{g_col2} := 56.4\text{in}^2 \quad d_{col2} := 20.4\text{in} \quad t_{f_col2} := 1.75\text{in} \quad t_{w_col2} := 0.96\text{in} \quad Z_{x_col2} := 442\text{in}^3 \\ b_{f_col2} := 11.5\text{in}$$

Columns W18x192 for Joints 5, 6, 7 & 8

$$A_{g_col3} := 56.4\text{in}^2 \quad d_{col3} := 20.4\text{in} \quad t_{f_col3} := 1.75\text{in} \quad t_{w_col3} := 0.96\text{in} \quad Z_{x_col3} := 442\text{in}^3 \\ b_{f_col3} := 11.5\text{in}$$

Beams W21x83 for Joints 1 & 2

$$A_{g_beam} := 24.3\text{in}^2 \quad d_{beam} := 21.4\text{in} \quad t_{f_beam} := 0.835\text{in} \quad Z_{x_beam} := 196\text{in}^3$$

Beams W21x73 for Joints 3 & 4

$$A_{g_beam2} := 21.5\text{in}^2 \quad d_{beam2} := 21.2\text{in} \quad t_{f_beam2} := 0.74\text{in} \quad Z_{x_beam2} := 172\text{in}^3$$

Beams W21x57 for Joints 5, 6, 7 & 8

$$A_{g_beam3} := 16.7\text{in}^2 \quad d_{beam3} := 21.1\text{in} \quad t_{f_beam3} := 0.65\text{in} \quad Z_{x_beam3} := 129\text{in}^3$$

Material Properties for all beams and columns: $f_y := 50\text{ksi}$ $F_u := 65\text{ksi}$

Gravity loads on all beams: $w_D := 1.5 \frac{\text{kip}}{\text{ft}}$ $w_L := 0.75 \frac{\text{kip}}{\text{ft}}$

For Grade 50 steel $R_y := 1.1$ Bay length: $L_w := 360\text{in}$

Calculate the sum of the moments in the column above and below the joint at the intersection of the beam and column centerlines:

$$P_D := w_D \cdot L = 45 \cdot \text{kip} \quad P_L := w_L \cdot L = 22.5 \cdot \text{kip} \quad P_S := 0 \quad B_2 := 1.2 \text{ assumed}$$

In order to calculate P_{QE} we remove joint constrains between the moment frame & braced frame and find the max. load on columns due to earthquake loads.

Seismic Loads From SAP:

Joint 1	Joint 2	Joint 3	Joint 4
$P_{QE1} := 124\text{kip}$	$P_{QE2} := 6\text{kip}$	$P_{QE3} := 70\text{kip}$	$P_{QE4} := 3.32\text{kip}$
$P_{QE11} := 98.1\text{kip}$	$P_{QE22} := 5\text{kip}$	$P_{QE33} := 45\text{kip}$	$P_{QE44} := 2.23\text{kip}$
Joint 5	Joint 6	Joint 7	Joint 8
$P_{QE5} := 23.1\text{kip}$	$P_{QE6} := 1.23\text{kip}$	$P_{QE7} := 10\text{kip}$	$P_{QE8} := 1\text{kip}$
$P_{QE55} := 10\text{kip}$	$P_{QE66} := 1\text{kip}$		

Determine the factored loads on the columns:

From ASCE7-10, seismic design category is D

$S_{DS} := 1.615$ $\rho := 1.0$ it should be 1.3 but in this case we will assume it's 1.0

Nontranslation forces:

$$P_{nt} := (1.2 + 0.2S_{DS}) \cdot P_D + 0.5P_L + 0.2 \cdot P_S = 79.785 \cdot \text{kip}$$

Lateral-Translation forces due to seismic load:

Joint 1 $P_{lt1} := \rho \cdot P_{QE1} + 0.2 \cdot P_S = 124 \cdot \text{kip}$ **Joint 2** $P_{lt2} := \rho \cdot P_{QE2} + 0.2 \cdot P_S = 6 \cdot \text{kip}$

$P_{lt11} := \rho \cdot P_{QE11} + 0.2 \cdot P_S = 98.1 \cdot \text{kip}$ $P_{lt22} := \rho \cdot P_{QE22} + 0.2 \cdot P_S = 5 \cdot \text{kip}$

Joint 3 $P_{lt3} := \rho \cdot P_{QE3} + 0.2 \cdot P_S = 70 \cdot \text{kip}$ **Joint 4** $P_{lt4} := \rho \cdot P_{QE4} + 0.2 \cdot P_S = 3.32 \cdot \text{kip}$

$P_{lt33} := \rho \cdot P_{QE33} + 0.2 \cdot P_S = 45 \cdot \text{kip}$ $P_{lt44} := \rho \cdot P_{QE44} + 0.2 \cdot P_S = 2.23 \cdot \text{kip}$

Joint 5 $P_{lt5} := \rho \cdot P_{QE5} + 0.2 \cdot P_S = 23.1 \cdot \text{kip}$ **Joint 6** $P_{lt6} := \rho \cdot P_{QE6} + 0.2 \cdot P_S = 1.23 \cdot \text{kip}$

$P_{lt55} := \rho \cdot P_{QE55} + 0.2 \cdot P_S = 10 \cdot \text{kip}$ $P_{lt66} := \rho \cdot P_{QE66} + 0.2 \cdot P_S = 1 \cdot \text{kip}$

Joint 7 $P_{lt7} := \rho \cdot P_{QE7} + 0.2 \cdot P_S = 10 \cdot \text{kip}$ **Joint 8** $P_{lt8} := \rho \cdot P_{QE8} + 0.2 \cdot P_S = 1 \cdot \text{kip}$

The factored loads on the columns:

$$\text{Joint 1 } P_{u1} := P_{nt} + B_2 \cdot P_{lt1} = 228.585 \cdot \text{kip}$$

$$\text{Joint 2 } P_{u2} := P_{nt} + B_2 \cdot P_{lt2} = 86.985 \cdot \text{kip}$$

$$P_{u11} := P_{nt} + B_2 \cdot P_{lt11} = 197.505 \cdot \text{kip}$$

$$P_{u22} := P_{nt} + B_2 \cdot P_{lt22} = 85.785 \cdot \text{kip}$$

$$\text{Joint 3 } P_{u3} := P_{nt} + B_2 \cdot P_{lt3} = 163.785 \cdot \text{kip}$$

$$\text{Joint 4 } P_{u4} := P_{nt} + B_2 \cdot P_{lt4} = 83.769 \cdot \text{kip}$$

$$P_{u33} := P_{nt} + B_2 \cdot P_{lt33} = 133.785 \cdot \text{kip}$$

$$P_{u44} := P_{nt} + B_2 \cdot P_{lt44} = 82.461 \cdot \text{kip}$$

$$\text{Joint 5 } P_{u5} := P_{nt} + B_2 \cdot P_{lt5} = 107.505 \cdot \text{kip}$$

$$\text{Joint 6 } P_{u6} := P_{nt} + B_2 \cdot P_{lt6} = 81.261 \cdot \text{kip}$$

$$P_{u55} := P_{nt} + B_2 \cdot P_{lt55} = 91.785 \cdot \text{kip}$$

$$P_{u66} := P_{nt} + B_2 \cdot P_{lt66} = 80.985 \cdot \text{kip}$$

$$\text{Joint 7 } P_{u7} := P_{nt} + B_2 \cdot P_{lt7} = 91.785 \cdot \text{kip}$$

$$\text{Joint 8 } P_{u8} := P_{nt} + B_2 \cdot P_{lt8} = 80.985 \cdot \text{kip}$$

The flexural strength of the columns at the beams centerlines:

$$M_{pc1} := (Z_{x_col}) \cdot \left(f_y - \frac{P_{u1}}{A_{g_col}} \right) + (Z_{x_col}) \cdot \left(f_y - \frac{P_{u11}}{A_{g_col}} \right) = 64142 \cdot \text{kip} \cdot \text{in}$$

For the joints with two columns & one beam connected
(Joint 1)

$$M_{pc2} := Z_{x_col} \cdot \left(f_y - \frac{P_{u2}}{A_{g_col}} \right) + (Z_{x_col}) \cdot \left(f_y - \frac{P_{u22}}{A_{g_col}} \right) = 66198 \cdot \text{kip} \cdot \text{in}$$

For the joints with two columns & two beams connected
(Joint 2)

$$M_{pc3} := (Z_{x_col2}) \cdot \left(f_y - \frac{P_{u3}}{A_{g_col2}} \right) + (Z_{x_col2}) \cdot \left(f_y - \frac{P_{u33}}{A_{g_col2}} \right) = 41868 \cdot \text{kip} \cdot \text{in} \quad \text{Joint 3}$$

$$M_{pc4} := Z_{x_col2} \cdot \left(f_y - \frac{P_{u4}}{A_{g_col2}} \right) + (Z_{x_col2}) \cdot \left(f_y - \frac{P_{u44}}{A_{g_col2}} \right) = 42897 \cdot \text{kip} \cdot \text{in} \quad \text{Joint 4}$$

$$M_{pc5} := (Z_{x_col3}) \cdot \left(f_y - \frac{P_{u5}}{A_{g_col3}} \right) + (Z_{x_col3}) \cdot \left(f_y - \frac{P_{u55}}{A_{g_col3}} \right) = 42638 \cdot \text{kip} \cdot \text{in} \quad \text{Joint 5}$$

$$M_{pc6} := Z_{x_col3} \cdot \left(f_y - \frac{P_{u6}}{A_{g_col3}} \right) + \left(Z_{x_col3} \right) \cdot \left(f_y - \frac{P_{u66}}{A_{g_col3}} \right) = 42928 \cdot \text{kip} \cdot \text{in} \quad (\text{Joint 6})$$

$$M_{pc7} := Z_{x_col3} \cdot \left(f_y - \frac{P_{u7}}{A_{g_col3}} \right) = 21381 \cdot \text{kip} \cdot \text{in} \quad \text{For the joints with one column \& one beam connected (Joint 7)}$$

$$M_{pc8} := Z_{x_col3} \cdot \left(f_y - \frac{P_{u8}}{A_{g_col3}} \right) = 21465 \cdot \text{kip} \cdot \text{in} \quad \text{For the joints with one column \& two beams connected (Joint 8)}$$

Determine the probable moment at the plastic hinge for Joints 1 & 2 with W21x83 beam:

$$C_{pr} := \frac{f_y + F_u}{2 \cdot f_y} = 1.15 \quad C_{pr} < 1.2 \text{ then it's ok}$$

Minimum plastic section modulus at the reduced beam section:

$$Z_e := Z_{x_beam} = 196 \cdot \text{in}^3$$

So the moment at the plastic hinge is:

$$M_{pr} := C_{pr} \cdot R_y \cdot f_y \cdot Z_e = 12397 \cdot \text{kip} \cdot \text{in}$$

Calculate the expected shear at the plastic hinge:

First calculate the factored uniform gravity load:

$$w_u := 1.2w_D + 0.5w_L = 2.175 \cdot \frac{\text{kip}}{\text{ft}}$$

The distance between plastic hinges:

$$L' := L - 2 \cdot \frac{d_{col}}{2} - 2 \cdot \frac{d_{beam}}{2} = 316.7 \cdot \text{in}$$

The required shear strength at the plastic hinge due to gravity loads:

$$V_{gH} := 0.5 \cdot w_u \cdot L' = 28.701 \cdot \text{kip}$$

So the expected shear at the plastic hinge is:

$$V_H := \frac{2 \cdot M_{pr}}{L'} + V_{gH} = 106.99 \cdot \text{kip} \quad V'_H := \frac{2 \cdot M_{pr}}{L'} - V_{gH} = 49.588 \cdot \text{kip}$$

$$V_{H_max} := \max(V_H, V'_H) = 106.99 \cdot \text{kip} \quad V_{H_min} := \min(V_H, V'_H) = 49.588 \cdot \text{kip}$$

Calculate the sum of the moments produced at the column centerline by the shear at the plastic hinges for W21x83:

$$M_{v_max} := (V_{H_max}) \cdot \left(\frac{d_{beam}}{2} + \frac{d_{col}}{2} \right) = 2316 \cdot \text{kip} \cdot \text{in}$$

$$M_{v_min} := (V_{H_min}) \cdot \left(\frac{d_{beam}}{2} + \frac{d_{col}}{2} \right) = 1074 \cdot \text{kip} \cdot \text{in}$$

So the expected flexural demand of the W21x83 beam at the column centerline is:

$$M_{pb_max} := M_{pr} + M_{v_max} = 14713.324 \cdot \text{kip} \cdot \text{in}$$

$$M_{pb_min} := M_{pr} + M_{v_min} = 13470.573 \cdot \text{kip} \cdot \text{in}$$

Determine the probable moment at the plastic hinge for Joints 3 & 4 with W21x73 beam:

Minimum plastic section modulus at the reduced beam section:

$$Z_{e_2} := Z_{x_beam2} = 172 \cdot \text{in}^3$$

So the moment at the plastic hinge is:

$$M_{pr_2} := C_{pr} \cdot R_y \cdot f_y \cdot Z_{e_2} = 10879 \cdot \text{kip} \cdot \text{in}$$

Calculate the expected shear at the plastic hinge:

The distance between plastic hinges:

$$L'_2 := L - 2 \cdot \frac{d_{col2}}{2} - 2 \cdot \frac{d_{beam2}}{2} = 318.4 \cdot \text{in}$$

The required shear strength at the plastic hinge due to gravity loads:

$$V_{gH_2} := 0.5 \cdot w_u \cdot L'_2 = 28.855 \cdot \text{kip}$$

So the expected shear at the plastic hinge is:

$$V_{H_2} := \frac{2 \cdot M_{pr_2}}{L'_2} + V_{gH_2} = 97.19 \cdot \text{kip} \quad V'_{H_2} := \frac{2 \cdot M_{pr_2}}{L'_2} - V_{gH_2} = 39.48 \cdot \text{kip}$$

$$V_{H_max2} := \max(V_{H_2}, V'_{H_2}) = 97.19 \cdot \text{kip} \quad V_{H_min2} := \min(V_{H_2}, V'_{H_2}) = 39.48 \cdot \text{kip}$$

Calculate the sum of the moments produced at the column centerline by the shear at the plastic hinges for W21x73:

$$M_{v_max2} := (V_{H_max2}) \cdot \left(\frac{d_{beam2}}{2} + \frac{d_{col2}}{2} \right) = 2022 \cdot \text{kip} \cdot \text{in}$$

$$M_{v_min2} := (V_{H_min2}) \cdot \left(\frac{d_{beam2}}{2} + \frac{d_{col2}}{2} \right) = 821 \cdot \text{kip} \cdot \text{in}$$

So the expected flexural demand of the W21x73 beam at the column centerline is:

$$M_{pb_max2} := M_{pr_2} + M_{v_max2} = 12900.561 \cdot \text{kip} \cdot \text{in}$$

$$M_{pb_min2} := M_{pr_2} + M_{v_min2} = 11700.193 \cdot \text{kip} \cdot \text{in}$$

Determine the probable moment at the plastic hinge for Joints 5, 6, 7 & 8 with W21x57 beam:

Minimum plastic section modulus at the reduced beam section:

$$Z_{e_3} := Z_{x_beam3} = 129 \cdot \text{in}^3$$

So the moment at the plastic hinge is:

$$M_{pr_3} := C_{pr} \cdot R_y \cdot f_y \cdot Z_{e_3} = 8159.25 \cdot \text{kip} \cdot \text{in}$$

Calculate the expected shear at the plastic hinge:

The distance between plastic hinges:

$$L'_3 := L - 2 \cdot \frac{d_{col3}}{2} - 2 \cdot \frac{d_{beam3}}{2} = 318.5 \cdot \text{in}$$

The required shear strength at the plastic hinge due to gravity loads:

$$V_{gH_3} := 0.5 \cdot w_u \cdot L'_3 = 28.864 \cdot \text{kip}$$

So the expected shear at the plastic hinge is:

$$V_{H_3} := \frac{2 \cdot M_{pr_3}}{L'_3} + V_{gH_3} = 80.1 \cdot \text{kip} \quad V'_{H_3} := \frac{2 \cdot M_{pr_3}}{L'_3} - V_{gH_3} = 22.371 \cdot \text{kip}$$

$$V_{H_max3} := \max(V_{H_3}, V'_{H_3}) = 80.1 \cdot \text{kip} \quad V_{H_min3} := \min(V_{H_3}, V'_{H_3}) = 22.371 \cdot \text{kip}$$

Calculate the sum of the moments produced at the column centerline by the shear at the plastic hinges for W21x57:

$$M_{v_max3} := (V_{H_max3}) \cdot \left(\frac{d_{beam3}}{2} + \frac{d_{col3}}{2} \right) = 1662 \cdot \text{kip} \cdot \text{in}$$

$$M_{v_min3} := (V_{H_min3}) \cdot \left(\frac{d_{beam3}}{2} + \frac{d_{col3}}{2} \right) = 464 \cdot \text{kip} \cdot \text{in}$$

So the expected flexural demand of the W21x57 beam at the column centerline is:

$$M_{pb_max3} := M_{pr_3} + M_{v_max3} = 9821.315 \cdot \text{kip} \cdot \text{in}$$

$$M_{pb_min3} := M_{pr_3} + M_{v_min3} = 8623.457 \cdot \text{kip} \cdot \text{in}$$

Finally find the Column-Beam Moment Ratio:

At **Joint 1:**

$$\frac{M_{pc1}}{M_{pb_max}} = 4.359 > 1.2 \text{ okay}$$

At **Joint 2:**

$$\frac{M_{pc2}}{M_{pb_max} + M_{pb_min}} = 2.349 > 1.2 \text{ okay}$$

At **Joint 3:**

$$\frac{M_{pc3}}{M_{pb_max2}} = 3.245 > 1.2 \text{ okay}$$

At **Joint 4:**

$$\frac{M_{pc4}}{M_{pb_max2} + M_{pb_min2}} = 1.744 > 1.2 \text{ okay}$$

At **Joint 5:**

$$\frac{M_{pc5}}{M_{pb_max3}} = 4.341 > 1.2 \text{ okay}$$

At **Joint 6:**

$$\frac{M_{pc6}}{M_{pb_max3} + M_{pb_min3}} = 2.327 > 1.2 \text{ okay}$$

At **Joint 7:**

$$\frac{M_{pc7}}{M_{pb_max3}} = 2.177 > 1.2 \text{ okay}$$

At **Joint 8:**

$$\frac{M_{pc8}}{M_{pb_max3} + M_{pb_min3}} = 1.164 < 1.2 \text{ okay according to AISC for roof members.}$$

PANEL ZONE DESIGN-DOUBLER PLATE FOR SMF

$$\phi := 0.9$$

For 1st & 2nd stories:

Minimum thickness of doubler plate is:

$$t_{\min} := \frac{(d_{\text{col}} - 2 \cdot t_{f_{\text{col}}}) + (d_{\text{beam}} - 2 \cdot t_{f_{\text{beam}}})}{90} = 0.407 \cdot \text{in}$$

The expected flexural demands of the W21x83 beam at the column face are:

$$M_{f_{\max}} := M_{\text{pr}} + V_{H_{\max}} \cdot \left(\frac{d_{\text{beam}}}{2} \right) = 13541.788 \cdot \text{kip} \cdot \text{in}$$

$$M_{f_{\min}} := M_{\text{pr}} + V_{H_{\min}} \cdot \left(\frac{d_{\text{beam}}}{2} \right) = 12927.588 \cdot \text{kip} \cdot \text{in}$$

The shear forces at the column faces:

$$F_{f_{\max}} := \frac{M_{f_{\max}}}{(d_{\text{beam}} - t_{f_{\text{beam}}})} = 658.487 \cdot \text{kip} \quad F_{f_{\min}} := \frac{M_{f_{\min}}}{(d_{\text{beam}} - t_{f_{\text{beam}}})} = 628.621 \cdot \text{kip}$$

$$F_f := \max(F_{f_{\max}}, F_{f_{\min}}) = 658.487 \cdot \text{kip}$$

The available shear strength of the panel zone in joints with **one beam** is:

Column height: $h := 18\text{ft}$

$$V_{c_{\text{one}}} := \frac{M_{f_{\max}}}{h} = 62.693 \cdot \text{kip} \quad V_{u_{\text{one}}} := F_f - V_{c_{\text{one}}} = 595.794 \cdot \text{kip}$$

Capacity determined of the web panel zone:

$$R_{n_{\text{one}}} := \phi \cdot 0.6 \cdot f_y \cdot d_{\text{col}} \cdot t_{w_{\text{col}}} = 827.82 \cdot \text{kip} \quad \text{Since } R_n > V_u, \text{ doubler plate is not required}$$

The required column panel zone thickness is found as follows

$$t_{p_{\text{one}}} := \frac{V_{u_{\text{one}}}}{\phi \cdot 0.6 \cdot f_y \cdot d_{\text{col}}} = 1.008 \cdot \text{in} < t_{w_{\text{col}}} = 1.4 \cdot \text{in}$$

The available shear strength of the panel zone in joints with **two beams** is:

$$V_{e_two} := \frac{M_{f_max} + M_{f_min}}{h} = 122.543 \cdot \text{kip} \quad V_{u_two} := F_{f_max} + F_{f_min} - V_{e_two} = 1164.565 \cdot \text{kip}$$

Capacity determined of the web panel zone:

$$R_{n_two} := \phi \cdot 0.6 \cdot f_y \cdot d_{col} \cdot t_{w_col} = 827.82 \cdot \text{kip} \quad \text{Since } R_n < V_u, \text{ a doubler plate is required}$$

The required column panel zone thickness is found as follows

$$t_{p_two} := \frac{V_{u_two}}{\phi \cdot 0.6 \cdot f_y \cdot d_{col}} = 1.969 \cdot \text{in}$$

The extra thickness or the required thickness of the doubler plate is:

$$t_{dp_two} := t_{p_two} - t_{w_col} = 0.569 \cdot \text{in}$$

$$\text{or use } t_{dp_two} := \max(t_{dp_two}, t_{min}) = 0.569 \cdot \text{in}$$

For 3rd & 4th stories:

Minimum thickness of doubler plate is:

$$t_{min2} := \frac{(d_{col2} - 2 \cdot t_{f_col2}) + (d_{beam2} - 2 \cdot t_{f_beam2})}{90} = 0.407 \cdot \text{in}$$

The expected flexural demands of the W21x73 beam at the column face are:

$$M_{f_max2} := M_{pr_2} + V_{H_max2} \cdot \left(\frac{d_{beam2}}{2} \right) = 11909.219 \cdot \text{kip} \cdot \text{in}$$

$$M_{f_min2} := M_{pr_2} + V_{H_min2} \cdot \left(\frac{d_{beam2}}{2} \right) = 11297.493 \cdot \text{kip} \cdot \text{in}$$

The shear forces at the column faces:

$$F_{f_max2} := \frac{M_{f_max2}}{(d_{beam2} - t_{f_beam2})} = 582.073 \cdot \text{kip} \quad F_{f_min2} := \frac{M_{f_min2}}{(d_{beam2} - t_{f_beam2})} = 552.175 \cdot \text{kip}$$

$$F_{f2} := \max(F_{f_max2}, F_{f_min2}) = 582.073 \cdot \text{kip}$$

The available shear strength of the panel zone in joints with **one beam** is:

$$\text{Column height: } h_2 := 13 \text{ft}$$

$$V_{c_one2} := \frac{M_{f_max2}}{h_2} = 76.341 \cdot \text{kip} \quad V_{u_one2} := F_{f2} - V_{c_one2} = 505.732 \cdot \text{kip}$$

Capacity determined of the web panel zone:

$$R_{n_one2} := \phi \cdot 0.6 \cdot f_y \cdot d_{col2} \cdot t_{w_col2} = 528.768 \cdot \text{kip} \quad \text{Since } R_n > V_u, \text{ doubler plate is not required}$$

The required column panel zone thickness is found as follows

$$t_{p_one2} := \frac{V_{u_one2}}{\phi \cdot 0.6 \cdot f_y \cdot d_{col2}} = 0.918 \cdot \text{in} < t_{w_col2} = 0.96 \cdot \text{in}$$

The available shear strength of the panel zone in joints with **two beams** is:

$$V_{c_two2} := \frac{M_{f_max2} + M_{f_min2}}{h_2} = 148.761 \cdot \text{kip}$$

$$V_{u_two2} := F_{f_max2} + F_{f_min2} - V_{c_two2} = 985.487 \cdot \text{kip}$$

Capacity determined of the web panel zone:

$$R_{n_two2} := \phi \cdot 0.6 \cdot f_y \cdot d_{col2} \cdot t_{w_col2} = 528.768 \cdot \text{kip} \quad \text{Since } R_n < V_u, \text{ a doubler plate is required}$$

The required column panel zone thickness is found as follows

$$t_{p_two2} := \frac{V_{u_two2}}{\phi \cdot 0.6 \cdot f_y \cdot d_{col2}} = 1.789 \cdot \text{in}$$

The extra thickness or the required thickness of the doubler plate is:

$$t_{dp_two2} := t_{p_two2} - t_{w_col2} = 0.829 \cdot \text{in}$$

$$\text{or use } t_{dp_rwo2} := \max(t_{dp_two2}, t_{min2}) = 0.829 \cdot \text{in}$$

For 5th & 6th stories:

Minimum thickness of doubler plate is:

$$t_{min3} := \frac{(d_{col3} - 2 \cdot t_{f_col3}) + (d_{beam3} - 2 \cdot t_{f_beam3})}{90} = 0.408 \cdot \text{in}$$

The expected flexural demands of the W21x57 beam at the column face are:

$$M_{f_max3} := M_{pr_3} + V_{H_max3} \cdot \left(\frac{d_{beam3}}{2} \right) = 9004.3 \cdot \text{kip} \cdot \text{in}$$

$$M_{f_min3} := M_{pr_3} + V_{H_min3} \cdot \left(\frac{d_{beam3}}{2} \right) = 8395.268 \cdot \text{kip} \cdot \text{in}$$

The shear forces at the column faces:

$$F_{f_max3} := \frac{M_{f_max3}}{(d_{beam3} - t_{f_beam3})} = 440.308 \cdot \text{kip} \quad F_{f_min3} := \frac{M_{f_min3}}{(d_{beam3} - t_{f_beam3})} = 410.527 \cdot \text{kip}$$

$$F_{f3} := \max(F_{f_max3}, F_{f_min3}) = 440.308 \cdot \text{kip}$$

The available shear strength of the panel zone in joints 5 & 7 with **one beam** is:

Column height:

$$V_{c_one3} := \frac{M_{f_max3}}{h_2} = 57.72 \cdot \text{kip} \quad V_{u_one3} := F_{f3} - V_{c_one3} = 382.588 \cdot \text{kip}$$

Capacity determined of the web panel zone:

$$R_{n_one3} := \phi \cdot 0.6 \cdot f_y \cdot d_{col3} \cdot t_{w_col3} = 528.768 \cdot \text{kip} \quad \text{Since } R_n > V_u, \text{ doubler plate is not required}$$

The required column panel zone thickness is found as follows

$$t_{p_one3} := \frac{V_{u_one3}}{\phi \cdot 0.6 \cdot f_y \cdot d_{col3}} = 0.695 \cdot \text{in} < t_{w_col3} = 0.96 \cdot \text{in}$$

The available shear strength of the panel zone in joints 6 & 8 with **two beams** is:

$$V_{c_two3} := \frac{M_{f_max3} + M_{f_min3}}{h_2} = 111.536 \cdot \text{kip}$$

$$V_{u_two3} := F_{f_max3} + F_{f_min3} - V_{c_two3} = 739.299 \cdot \text{kip}$$

Capacity determined of the web panel zone:

$$R_{n_two3} := \phi \cdot 0.6 \cdot f_y \cdot d_{col3} \cdot t_{w_col3} = 528.768 \cdot \text{kip} \quad \text{Since } R_n < V_u, \text{ a doubler plate is required}$$

The required column panel zone thickness is found as follows

$$t_{p_two3} := \frac{V_{u_two3}}{\phi \cdot 0.6 \cdot f_y \cdot d_{col3}} = 1.342 \cdot \text{in}$$

The extra thickness or the required thickness of the doubler plate is:

$$t_{dp_two3} := t_{p_two3} - t_{w_col3} = 0.382 \cdot \text{in}$$

or use $t_{dp_two3} := \max(t_{dp_two3}, t_{min3}) = 0.408 \cdot \text{in}$

Panel-Zone Support Link Calculations by Using the Scissors Model:

Shear Modulus of steel: $G := 11500000 \text{ psi}$

For 1st story:

Calculate the ratios of the effective depth of the column to the span length and the effective depth of the beam to the column height, respectively:

$$\alpha := \frac{d_{col} - t_{f_col}}{L} = 0.054 \quad \beta := \frac{d_{beam} - t_{f_beam}}{h} = 0.095$$

For joints with one beam:

The volume of the panel zone is:

$$t_{p_one} := t_{w_col} + 0 = 1.4 \cdot \text{in}$$

$$V_{p_one} := \alpha \cdot L \cdot \beta \cdot h \cdot t_{p_one} = 558.545 \cdot \text{in}^3$$

The properties for the Scissors Model:

PANEL

$$K_{PS_one} := \frac{G \cdot V_{p_one}}{(1 - \alpha - \beta)^2} = 8.871 \times 10^6 \cdot \text{kip} \cdot \text{in}$$

$$M_{PS_one} := \frac{0.6 \cdot f_y \cdot V_{p_one}}{(1 - \alpha - \beta)} = 1.969 \times 10^4 \cdot \text{kip} \cdot \text{in}$$

$$\Theta_{PS_one} := \frac{M_{PS_one}}{K_{PS_one}} = 0.00222$$

FLANGES

$$K_{FS_one} := \frac{0.78 \cdot G \cdot b_{f_col} \cdot t_{f_col}^2}{(1 - \alpha - \beta)^2} = 9.214 \times 10^5 \cdot \text{kip} \cdot \text{in}$$

$$M_{FS_one} := \frac{1.87 \cdot f_y \cdot b_{f_col} \cdot t_{f_col}^2}{(1 - \alpha - \beta)} = 8172.57 \cdot \text{kip} \cdot \text{in}$$

$$\Theta_{FS_one} := \frac{M_{FS_one}}{K_{FS_one}} = 0.00887$$

TOTAL

$$M_{add_one} := \Theta_{PS_one} \cdot \frac{M_{FS_one}}{\Theta_{FS_one}} = 2.045 \times 10^3 \cdot \text{kip} \cdot \text{in}$$

$$K_{tot_one} := K_{PS_one} + K_{FS_one} = 9792911.4 \cdot \text{kip} \cdot \text{in}$$

$$M_{P_tot_one} := M_{PS_one} + M_{add_one} = 21737.78 \cdot \text{kip} \cdot \text{in} \quad \text{with } \Theta_{PS_one} = 0.00222$$

$$M_{F_tot_one} := M_{FS_one} + M_{PS_one} = 27865.022 \cdot \text{kip} \cdot \text{in} \quad \text{with } \Theta_{FS_one} = 0.00887 \quad \text{extend to } 10 \cdot \Theta_{PS_one} = 0.022$$

For joints with two beams:

The volume of the panel zone is:

$$t_{p_two} := t_{w_col} + t_{dp_two} = 1.969 \cdot \text{in}$$

$$V_{p_two} := \alpha \cdot L \cdot \beta \cdot h \cdot t_{p_two} = 785.753 \cdot \text{in}^3$$

The properties for the Scissors Model:

PANEL:

$$K_{PS_two} := \frac{G \cdot V_{p_two}}{(1 - \alpha - \beta)^2} = 1.248 \times 10^7 \cdot \text{kip} \cdot \text{in}$$

$$M_{PS_two} := \frac{0.6 \cdot f_y \cdot V_{p_two}}{(1 - \alpha - \beta)} = 27703.042 \cdot \text{kip} \cdot \text{in}$$

$$\Theta_{PS_two} := \frac{M_{PS_two}}{K_{PS_two}} = 0.00222$$

FLANGES:

$$K_{FS_two} := \frac{0.78 \cdot G \cdot b_{f_col} \cdot t_{f_col}^2}{(1 - \alpha - \beta)^2} = 9.214 \times 10^5 \cdot \text{kip} \cdot \text{in}$$

$$M_{FS_two} := \frac{1.87 \cdot f_y \cdot b_f \cdot t_{f_col} \cdot t_{f_col}^2}{(1 - \alpha - \beta)} = 8172.57 \cdot \text{kip} \cdot \text{in}$$

$$\Theta_{FS_two} := \frac{M_{FS_two}}{K_{FS_two}} = 0.00887$$

TOTAL

$$M_{add_two} := \Theta_{PS_two} \cdot \frac{M_{FS_two}}{\Theta_{FS_two}} = 2.045 \times 10^3 \cdot \text{kip} \cdot \text{in}$$

$$M_{P_tot_two} := M_{PS_two} + M_{add_two} = 29748.37 \cdot \text{kip} \cdot \text{in} \quad \text{with} \quad \Theta_{PS_two} = 0.00222$$

$$M_{F_tot_two} := M_{FS_two} + M_{PS_two} = 35875.612 \cdot \text{kip} \cdot \text{in} \quad \text{with} \quad \Theta_{FS_two} = 0.00887$$

$$\text{extend to } 10 \cdot \Theta_{PS_two} = 0.022$$

$$K_{tot_two} := K_{PS_two} + K_{FS_two} = 13401697.6 \cdot \text{kip} \cdot \text{in}$$

For 2nd story:

Calculate the ratios of the effective depth of the column to the span length and the effective depth of the beam to the column height, respectively:

$$\alpha := \frac{d_{col} - t_{f_col}}{L} = 0.054 \quad \beta := \frac{d_{beam} - t_{f_beam}}{h_2} = 0.132$$

For joints with one beam:

The volume of the panel zone is:

$$l_{p_zone} := t_{w_col} + 0 = 1.4 \cdot \text{in}$$

$$V_{p_zone} := \alpha \cdot L \cdot \beta \cdot h_2 \cdot t_{p_one} = 558.545 \cdot \text{in}^3$$

The properties for the Scissors Model:

PANEL

$$K_{PS_panel} := \frac{G \cdot V_{p_one}}{(1 - \alpha - \beta)^2} = 9.687 \times 10^6 \cdot \text{kip} \cdot \text{in}$$

$$M_{PS_panel} := \frac{0.6 \cdot f_y \cdot V_{p_one}}{(1 - \alpha - \beta)} = 2.058 \times 10^4 \cdot \text{kip} \cdot \text{in}$$

$$\Theta_{PS_panel} := \frac{M_{PS_panel}}{K_{PS_panel}} = 0.00212$$

FLANGES

$$K_{FS_one} := \frac{0.78 \cdot G \cdot b_{f_col} \cdot t_{f_col}^2}{(1 - \alpha - \beta)^2} = 1.006 \times 10^6 \cdot \text{kip} \cdot \text{in}$$

$$M_{FS_one} := \frac{1.87 \cdot f_y \cdot b_{f_col} \cdot t_{f_col}^2}{(1 - \alpha - \beta)} = 8540.093 \cdot \text{kip} \cdot \text{in}$$

$$\Theta_{FS_one} := \frac{M_{FS_one}}{K_{FS_one}} = 0.00849$$

TOTAL

$$M_{add_one} := \Theta_{PS_one} \cdot \frac{M_{FS_one}}{\Theta_{FS_one}} = 2.137 \times 10^3 \cdot \text{kip} \cdot \text{in}$$

$$M_{P_one} := M_{PS_one} + M_{add_one} = 22715.334 \cdot \text{kip} \cdot \text{in} \quad \text{with} \quad \Theta_{PS_one} = 0.00212$$

$$M_{F_one} := M_{FS_one} + M_{PS_one} = 29118.12 \cdot \text{kip} \cdot \text{in} \quad \text{with} \quad \Theta_{FS_one} = 0.00849 \quad \text{extend to}$$

$$K_{total_one} := K_{PS_one} + K_{FS_one} = 10693495.8 \cdot \text{kip} \cdot \text{in} \quad 10 \cdot \Theta_{PS_one} = 0.021$$

For joints with two beams:

The volume of the panel zone is:

$$t_{p_two} := t_{w_col} + t_{dp_two} = 1.969 \cdot \text{in}$$

$$V_{p_two} := \alpha \cdot L \cdot \beta \cdot h_2 \cdot t_{p_two} = 785.753 \cdot \text{in}^3$$

The properties for the Scissors Model:

PANEL:

$$K_{PS_two} := \frac{G \cdot V_{P_two}}{(1 - \alpha - \beta)^2} = 1.363 \times 10^7 \cdot \text{kip} \cdot \text{in}$$

$$M_{PS_two} := \frac{0.6 \cdot f_y \cdot V_{P_two}}{(1 - \alpha - \beta)} = 28948.856 \cdot \text{kip} \cdot \text{in}$$

$$\Theta_{PS_two} := \frac{M_{PS_two}}{K_{PS_two}} = 0.00212$$

FLANGES:

$$K_{FS_two} := \frac{0.78 \cdot G \cdot b_{f_col} \cdot t_{f_col}^2}{(1 - \alpha - \beta)^2} = 1.006 \times 10^6 \cdot \text{kip} \cdot \text{in}$$

$$M_{FS_two} := \frac{1.87 \cdot f_y \cdot b_{f_col} \cdot t_{f_col}^2}{(1 - \alpha - \beta)} = 8540.093 \cdot \text{kip} \cdot \text{in}$$

$$\Theta_{FS_two} := \frac{M_{FS_two}}{K_{FS_two}} = 0.00849$$

TOTAL

$$M_{add_two} := \Theta_{PS_two} \cdot \frac{M_{FS_two}}{\Theta_{FS_two}} = 2.137 \times 10^3 \cdot \text{kip} \cdot \text{in}$$

$$M_{p_two} := M_{PS_two} + M_{add_two} = 31086.162 \cdot \text{kip} \cdot \text{in} \quad \text{with} \quad \Theta_{PS_two} = 0.00212$$

$$M_{f_two} := M_{FS_two} + M_{PS_two} = 37488.948 \cdot \text{kip} \cdot \text{in} \quad \text{with} \quad \Theta_{FS_two} = 0.00849$$

$$K_{p_two} := K_{PS_two} + K_{FS_two} = 14634156.4 \cdot \text{kip} \cdot \text{in} \quad \text{extend to} \quad 10 \cdot \Theta_{PS_two} = 0.021$$

For 3rd & 4th stories:

Calculate the ratios of the effective depth of the column to the span length and the effective depth of the beam to the column height, respectively:

$$\alpha_2 := \frac{d_{col2} - t_{f_col2}}{L} = 0.052 \quad \beta_2 := \frac{d_{beam2} - t_{f_beam2}}{h_2} = 0.131$$

For joints with one beam:

The volume of the panel zone is:

$$t_{p_one2} := t_{w_col2} + 0 = 0.96 \cdot \text{in}$$

$$V_{p_one2} := \alpha_2 \cdot L \cdot \beta_2 \cdot h_2 \cdot t_{p_one2} = 366.316 \cdot \text{in}^3$$

The properties for the Scissors Model:

PANEL

$$K_{PS_one2} := \frac{G \cdot V_{P_one2}}{(1 - \alpha_2 - \beta_2)^2} = 6.311 \times 10^6 \cdot \text{kip} \cdot \text{in}$$

$$M_{PS_one2} := \frac{0.6 \cdot f_y \cdot V_{P_one2}}{(1 - \alpha_2 - \beta_2)} = 1.345 \times 10^4 \cdot \text{kip} \cdot \text{in}$$

$$\Theta_{PS_one2} := \frac{M_{PS_one2}}{K_{PS_one2}} = 0.00213$$

FLANGES

$$K_{FS_one2} := \frac{0.78 \cdot G \cdot b_f \cdot \text{col2} \cdot t_f \cdot \text{col2}^2}{(1 - \alpha_2 - \beta_2)^2} = 4.732 \times 10^5 \cdot \text{kip} \cdot \text{in}$$

$$M_{FS_one2} := \frac{1.87 \cdot f_y \cdot b_f \cdot \text{col2} \cdot t_f \cdot \text{col2}^2}{(1 - \alpha_2 - \beta_2)} = 4030.342 \cdot \text{kip} \cdot \text{in}$$

$$\Theta_{FS_one2} := \frac{M_{FS_one2}}{K_{FS_one2}} = 0.00852$$

TOTAL

$$M_{add_one2} := \Theta_{PS_one2} \cdot \frac{M_{FS_one2}}{\Theta_{FS_one2}} = 1.009 \times 10^3 \cdot \text{kip} \cdot \text{in}$$

$$M_{P_tot_one2} := M_{PS_one2} + M_{add_one2} = 14459.005 \cdot \text{kip} \cdot \text{in} \quad \text{with} \quad \Theta_{PS_one2} = 0.00213$$

$$M_{F_tot_one2} := M_{FS_one2} + M_{PS_one2} = 17480.684 \cdot \text{kip} \cdot \text{in} \quad \text{with} \quad \Theta_{FS_one2} = 0.00852 \quad \text{extend to}$$

$$K_{tot_one2} := K_{PS_one2} + K_{FS_one2} = 6783773.691 \cdot \text{kip} \cdot \text{in} \quad 10 \cdot \Theta_{PS_one2} = 0.021$$

For joints with two beams:

The volume of the panel zone is:

$$t_{p_two2} := t_w \cdot \text{col2} + t_{dp_two2} = 1.789 \cdot \text{in}$$

$$V_{P_two2} := \alpha_2 \cdot L \cdot \beta_2 \cdot h_2 \cdot t_{p_two2} = 682.718 \cdot \text{in}^3$$

The properties for the Scissors Model:

PANEL:

$$K_{PS_two2} := \frac{G \cdot V_{P_two2}}{(1 - \alpha_2 - \beta_2)^2} = 1.176 \times 10^7 \cdot \text{kip} \cdot \text{in}$$

$$M_{PS_two2} := \frac{0.6 \cdot f_y \cdot V_{P_two2}}{(1 - \alpha_2 - \beta_2)} = 25067.96 \cdot \text{kip} \cdot \text{in}$$

$$\Theta_{PS_two2} := \frac{M_{PS_two2}}{K_{PS_two2}} = 0.00213$$

FLANGES:

$$K_{FS_two2} := \frac{0.78 \cdot G \cdot b_{f_col2} \cdot t_{f_col2}^2}{(1 - \alpha_2 - \beta_2)^2} = 4.732 \times 10^5 \cdot \text{kip} \cdot \text{in}$$

$$M_{FS_two2} := \frac{1.87 \cdot f_y \cdot b_{f_col2} \cdot t_{f_col2}^2}{(1 - \alpha_2 - \beta_2)} = 4030.342 \cdot \text{kip} \cdot \text{in}$$

$$\Theta_{FS_two2} := \frac{M_{FS_two2}}{K_{FS_two2}} = 0.00852$$

TOTAL

$$M_{add_two2} := \Theta_{PS_two2} \cdot \frac{M_{FS_two2}}{\Theta_{FS_two2}} = 1.009 \times 10^3 \cdot \text{kip} \cdot \text{in}$$

$$M_{P_tot_two2} := M_{PS_two2} + M_{add_two2} = 26076.624 \cdot \text{kip} \cdot \text{in} \quad \text{with} \quad \Theta_{PS_two2} = 0.00213$$

$$M_{F_tot_two2} := M_{FS_two2} + M_{PS_two2} = 29098.303 \cdot \text{kip} \cdot \text{in} \quad \text{with} \quad \Theta_{FS_two2} = 0.00852$$

$$\text{extend to } 10 \cdot \Theta_{PS_two2} = 0.021$$

$$K_{tot_two2} := K_{PS_two2} + K_{FS_two2} = 12234445.947 \cdot \text{kip} \cdot \text{in}$$

For 5th & 6th stories:

Calculate the ratios of the effective depth of the column to the span length and the effective depth of the beam to the column height, respectively:

$$\alpha_3 := \frac{d_{col3} - t_{f_col3}}{L} = 0.052 \quad \beta_3 := \frac{d_{beam3} - t_{f_beam3}}{h_2} = 0.131$$

For joints with one beam:

The volume of the panel zone is:

$$t_{p_one3} := t_{w_col3} + 0 = 0.96 \cdot \text{in}$$

$$V_{P_one3} := \alpha_3 \cdot L \cdot \beta_3 \cdot h_2 \cdot t_{p_one3} = 366.137 \cdot \text{in}^3$$

The properties for the Scissors Model:

PANEL

$$K_{PS_one3} := \frac{G \cdot V_{P_one3}}{(1 - \alpha_3 - \beta_3)^2} = 6.306 \times 10^6 \cdot \text{kip} \cdot \text{in}$$

$$M_{PS_one3} := \frac{0.6 \cdot f_y \cdot V_{P_one3}}{(1 - \alpha_3 - \beta_3)} = 1.344 \times 10^4 \cdot \text{kip} \cdot \text{in}$$

$$\Theta_{PS_one3} := \frac{M_{PS_one3}}{K_{PS_one3}} = 0.00213$$

FLANGES

$$K_{FS_one3} := \frac{0.78 \cdot G \cdot b_f \cdot t_{f_col3}^2}{(1 - \alpha_3 - \beta_3)^2} = 4.732 \times 10^5 \cdot \text{kip} \cdot \text{in}$$

$$M_{FS_one3} := \frac{1.87 \cdot f_y \cdot b_f \cdot t_{f_col3}^2}{(1 - \alpha_3 - \beta_3)} = 4030.026 \cdot \text{kip} \cdot \text{in}$$

$$\Theta_{FS_one3} := \frac{M_{FS_one3}}{K_{FS_one3}} = 0.00852$$

TOTAL

$$M_{add_one3} := \Theta_{PS_one3} \cdot \frac{M_{FS_one3}}{\Theta_{FS_one3}} = 1.009 \times 10^3 \cdot \text{kip} \cdot \text{in}$$

$$M_{P_tot_one3} := M_{PS_one3} + M_{add_one3} = 14451.297 \cdot \text{kip} \cdot \text{in} \quad \text{with} \quad \Theta_{PS_one3} = 0.00213$$

$$M_{F_tot_one3} := M_{FS_one3} + M_{PS_one3} = 17472.739 \cdot \text{kip} \cdot \text{in} \quad \text{with} \quad \Theta_{FS_one3} = 0.00852 \quad \text{extend to}$$

$$K_{tot_one3} := K_{PS_one3} + K_{FS_one3} = 6779625.502 \cdot \text{kip} \cdot \text{in} \quad 10 \cdot \Theta_{PS_one3} = 0.021$$

For joints with two beams:

The volume of the panel zone is:

$$t_{p_two3} := t_{w_col3} + t_{dp_two3} = 1.368 \cdot \text{in}$$

$$V_{P_two3} := \alpha_3 \cdot L \cdot \beta_3 \cdot h_2 \cdot t_{p_two3} = 521.66 \cdot \text{in}^3$$

The properties for the Scissors Model:

PANEL:

$$K_{PS_two3} := \frac{G \cdot V_{P_two3}}{(1 - \alpha_3 - \beta_3)^2} = 8.985 \times 10^6 \cdot \text{kip} \cdot \text{in}$$

$$M_{PS_two3} := \frac{0.6 \cdot f_y \cdot V_{P_two3}}{(1 - \alpha_3 - \beta_3)} = 19152.754 \cdot \text{kip} \cdot \text{in}$$

$$\Theta_{PS_two3} := \frac{M_{PS_two3}}{K_{PS_two3}} = 0.00213$$

FLANGES:

$$K_{FS_two3} := \frac{0.78 \cdot G \cdot b_{f_col3} \cdot t_{f_col3}^2}{(1 - \alpha_3 - \beta_3)^2} = 4.732 \times 10^5 \cdot \text{kip} \cdot \text{in}$$

$$M_{FS_two3} := \frac{1.87 \cdot f_y \cdot b_{f_col3} \cdot t_{f_col3}^2}{(1 - \alpha_3 - \beta_3)} = 4030.026 \cdot \text{kip} \cdot \text{in}$$

$$\Theta_{FS_two3} := \frac{M_{FS_two3}}{K_{FS_two3}} = 0.00852$$

TOTAL

$$M_{add_two3} := \Theta_{PS_two3} \cdot \frac{M_{FS_two3}}{\Theta_{FS_two3}} = 1.009 \times 10^3 \cdot \text{kip} \cdot \text{in}$$

$$M_{P_tot_two3} := M_{PS_two3} + M_{add_two3} = 20161.338 \cdot \text{kip} \cdot \text{in} \quad \text{with } \Theta_{PS_two3} = 0.00213$$

$$M_{F_tot_two3} := M_{FS_two3} + M_{PS_two3} = 23182.78 \cdot \text{kip} \cdot \text{in} \quad \text{with } \Theta_{FS_two3} = 0.00852$$

$$\text{extend to } 10 \cdot \Theta_{PS_two3} = 0.021$$

$$K_{tot_two3} := K_{PS_two3} + K_{FS_two3} = 9458412.15 \cdot \text{kip} \cdot \text{in}$$

BEAM HINGES:

For 1st & 2nd stories:

Add hinges for each beam at the locations below:

$$\text{RelativeDistance}_1 := \frac{d_{\text{beam}} + d_{\text{col}}}{L} = 0.12$$

$$\text{RelativeDistance}_2 := 1 - \text{RelativeDistance}_1 = 0.88$$

For 3rd & 4th stories:

Add hinges for each beam at the locations below:

$$\text{RelativeDistance}_1 := \frac{d_{\text{beam2}} + d_{\text{col2}}}{L} = 0.116$$

$$\text{RelativeDistance}_2 := 1 - \text{RelativeDistance}_1 = 0.884$$

For 6th & 5th stories:

Add hinges for each beam at the locations below:

$$\text{RelativeDistance}_1 := \frac{d_{\text{beam3}} + d_{\text{col3}}}{L} = 0.115$$

$$\text{RelativeDistance}_2 := 1 - \text{RelativeDistance}_1 = 0.885$$

Gap Elements' Backbone Curve Calculations for 3 Different Gap Sizes:

$$k_{\text{initial}} := 0.5 \frac{\text{kip}}{\text{in}}$$

For 1st Story:

$$\text{Gap}_{1\text{st}} := 0.0045 \cdot h = 0.97 \cdot \text{in} \quad \text{-Less than brace frame yielding limit}=0.005 \cdot h$$

$$\delta_{g_{1\text{st}}} := \text{Gap}_{1\text{st}} = 0.972 \cdot \text{in}$$

$$P_{gt_{1\text{st}}} := \begin{pmatrix} -k_{\text{initial}} \cdot \text{Gap}_{1\text{st}} \\ -1.25 \cdot P_{yt} \end{pmatrix} = \begin{pmatrix} -0.486 \\ -920.27 \end{pmatrix} \cdot \text{kip} \quad P_{gc_{1\text{st}}} := \begin{pmatrix} k_{\text{initial}} \cdot \text{Gap}_{1\text{st}} \\ 1.25 \cdot P_{yc} \end{pmatrix} = \begin{pmatrix} 0.486 \\ 984.689 \end{pmatrix} \cdot \text{kip}$$

For all other stories:

$$\text{Gap} := 0.0045 \cdot h_2 = 0.7 \cdot \text{in}$$

$$\delta_g := \text{Gap} = 0.7 \cdot \text{in}$$

$$P_{gt} := \begin{pmatrix} -k_{\text{initial}} \cdot \text{Gap} \\ -1.25 \cdot P_{yt1_2} \end{pmatrix} = \begin{pmatrix} -0.351 \\ -850.298 \end{pmatrix} \cdot \text{kip} \quad P_{gc} := \begin{pmatrix} k_{\text{initial}} \cdot \text{Gap} \\ 1.25 \cdot P_{yc1_2} \end{pmatrix} = \begin{pmatrix} 0.351 \\ 909.818 \end{pmatrix} \cdot \text{kip}$$

For 1st Story:

$$\text{Gap}_{1st2} := 0.003 \cdot h = 0.65 \cdot \text{in}$$

$$\delta_{g_{1st2}} := \text{Gap}_{1st2} = 0.648 \cdot \text{in}$$

$$P_{gt_{1st2}} := \begin{pmatrix} -k_{\text{initial}} \cdot \text{Gap}_{1st2} \\ -1.25 \cdot P_{yt} \end{pmatrix} = \begin{pmatrix} -0.324 \\ -920.27 \end{pmatrix} \cdot \text{kip} \quad P_{gc_{1st2}} := \begin{pmatrix} k_{\text{initial}} \cdot \text{Gap}_{1st2} \\ 1.25 \cdot P_{yc} \end{pmatrix} = \begin{pmatrix} 0.324 \\ 984.689 \end{pmatrix} \cdot \text{kip}$$

For all other stories:

$$\text{Gap2} := 0.003 \cdot h_2 = 0.47 \cdot \text{in}$$

$$\delta_{g2} := \text{Gap2} = 0.47 \cdot \text{in}$$

$$P_{gt2} := \begin{pmatrix} -k_{\text{initial}} \cdot \text{Gap2} \\ -1.25 \cdot P_{yt1_2} \end{pmatrix} = \begin{pmatrix} -0.234 \\ -850.298 \end{pmatrix} \cdot \text{kip} \quad P_{gc2} := \begin{pmatrix} k_{\text{initial}} \cdot \text{Gap2} \\ 1.25 \cdot P_{yc1_2} \end{pmatrix} = \begin{pmatrix} 0.234 \\ 909.818 \end{pmatrix} \cdot \text{kip}$$

For 1st Story:

$$\text{Gap}_{1st3} := 0.0015 \cdot h = 0.32 \cdot \text{in}$$

$$\delta_{g_{1st3}} := \text{Gap}_{1st3} = 0.324 \cdot \text{in}$$

$$P_{gt_{1st3}} := \begin{pmatrix} -k_{\text{initial}} \cdot \text{Gap}_{1st3} \\ -1.25 \cdot P_{yt} \end{pmatrix} = \begin{pmatrix} -0.162 \\ -920.27 \end{pmatrix} \cdot \text{kip} \quad P_{gc_{1st3}} := \begin{pmatrix} k_{\text{initial}} \cdot \text{Gap}_{1st3} \\ 1.25 \cdot P_{yc} \end{pmatrix} = \begin{pmatrix} 0.162 \\ 984.689 \end{pmatrix} \cdot \text{kip}$$

For all other stories:

$$\text{Gap3} := 0.0015 \cdot h_2 = 0.23 \cdot \text{in}$$

$$\delta_{g3} := \text{Gap3} = 0.23 \cdot \text{in}$$

$$P_{gt3} := \begin{pmatrix} -k_{\text{initial}} \cdot \text{Gap3} \\ -1.25 \cdot P_{yt1_2} \end{pmatrix} = \begin{pmatrix} -0.117 \\ -850.298 \end{pmatrix} \cdot \text{kip} \quad P_{gc3} := \begin{pmatrix} k_{\text{initial}} \cdot \text{Gap3} \\ 1.25 \cdot P_{yc1_2} \end{pmatrix} = \begin{pmatrix} 0.117 \\ 909.818 \end{pmatrix} \cdot \text{kip}$$

Appendix B: Analysis Results of Perform 3D

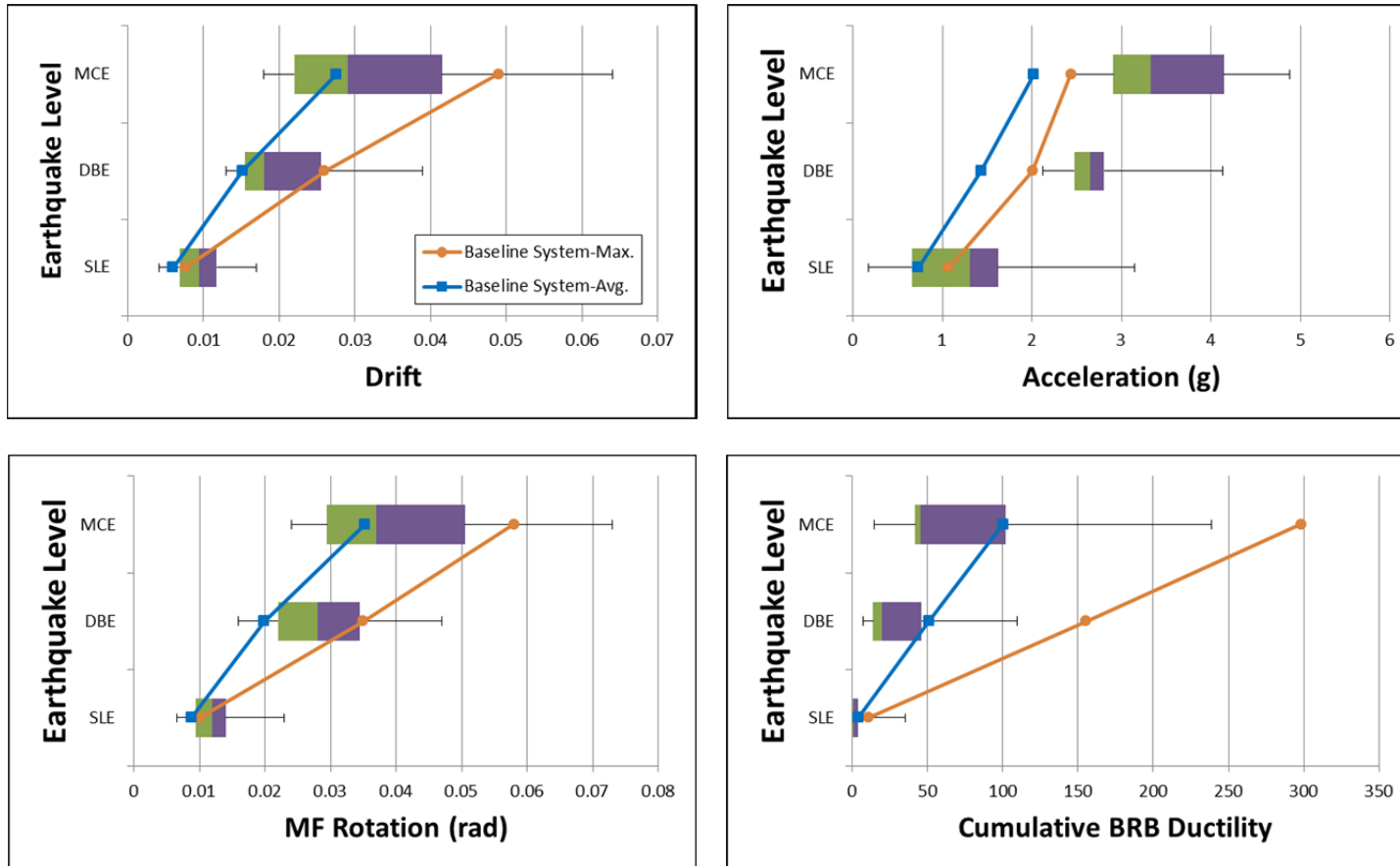


Figure B-1: 3-Story_50M50B_Gap0.45% with Baseline System

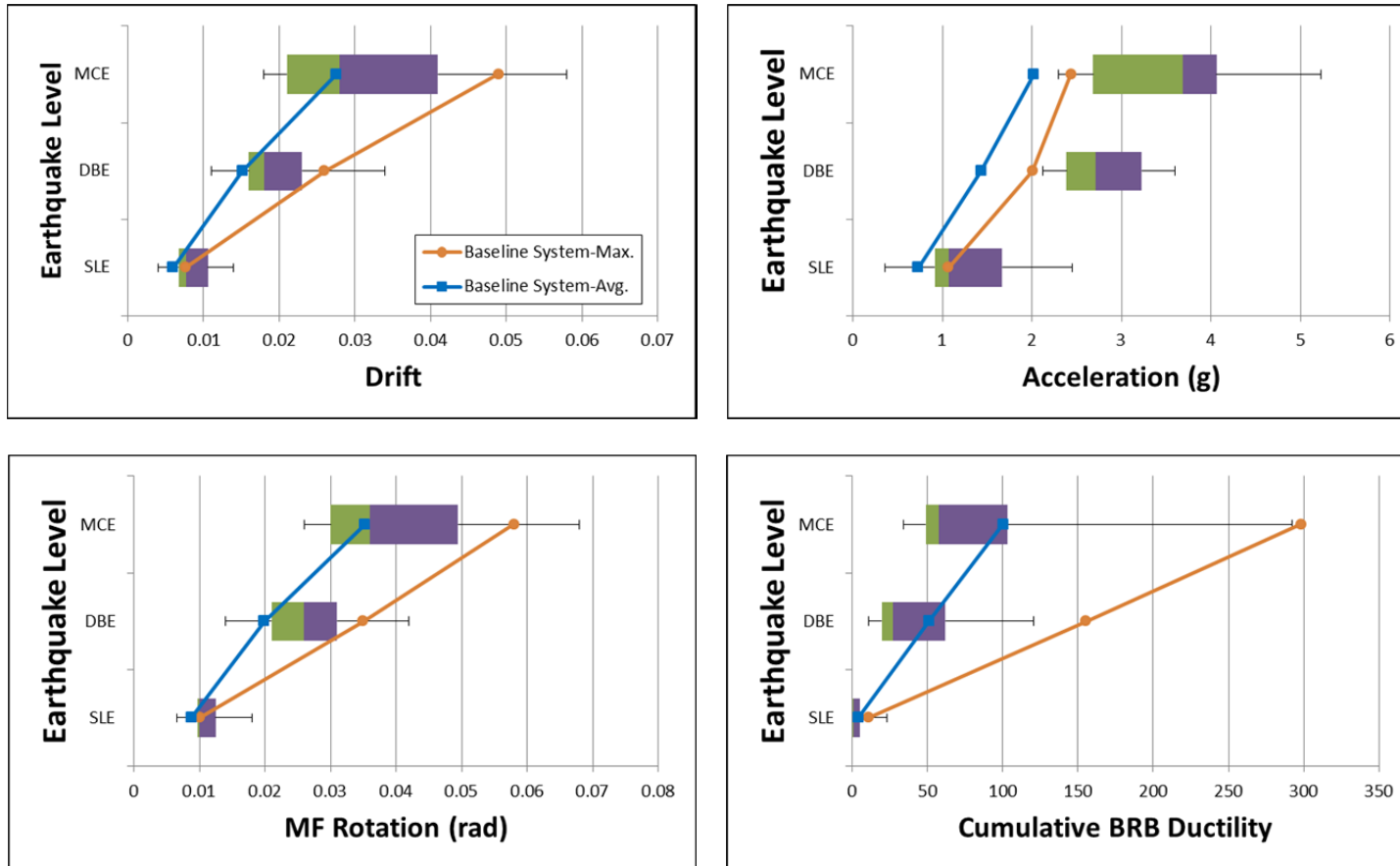


Figure B-2: 3-Story_50M50B_Gap0.30% with Baseline System

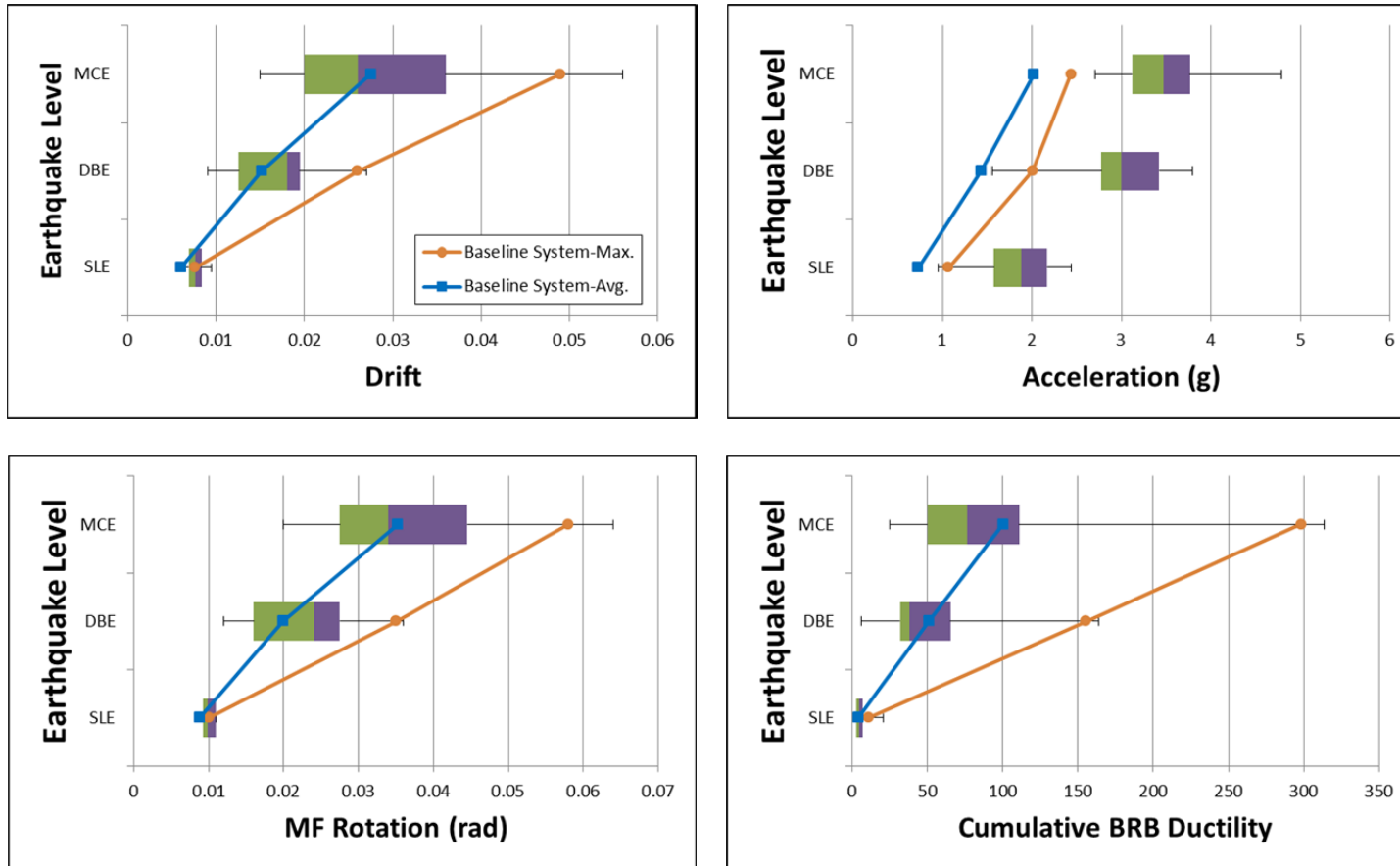


Figure B-3: 3-Story_50M50B_Gap0.15% with Baseline System

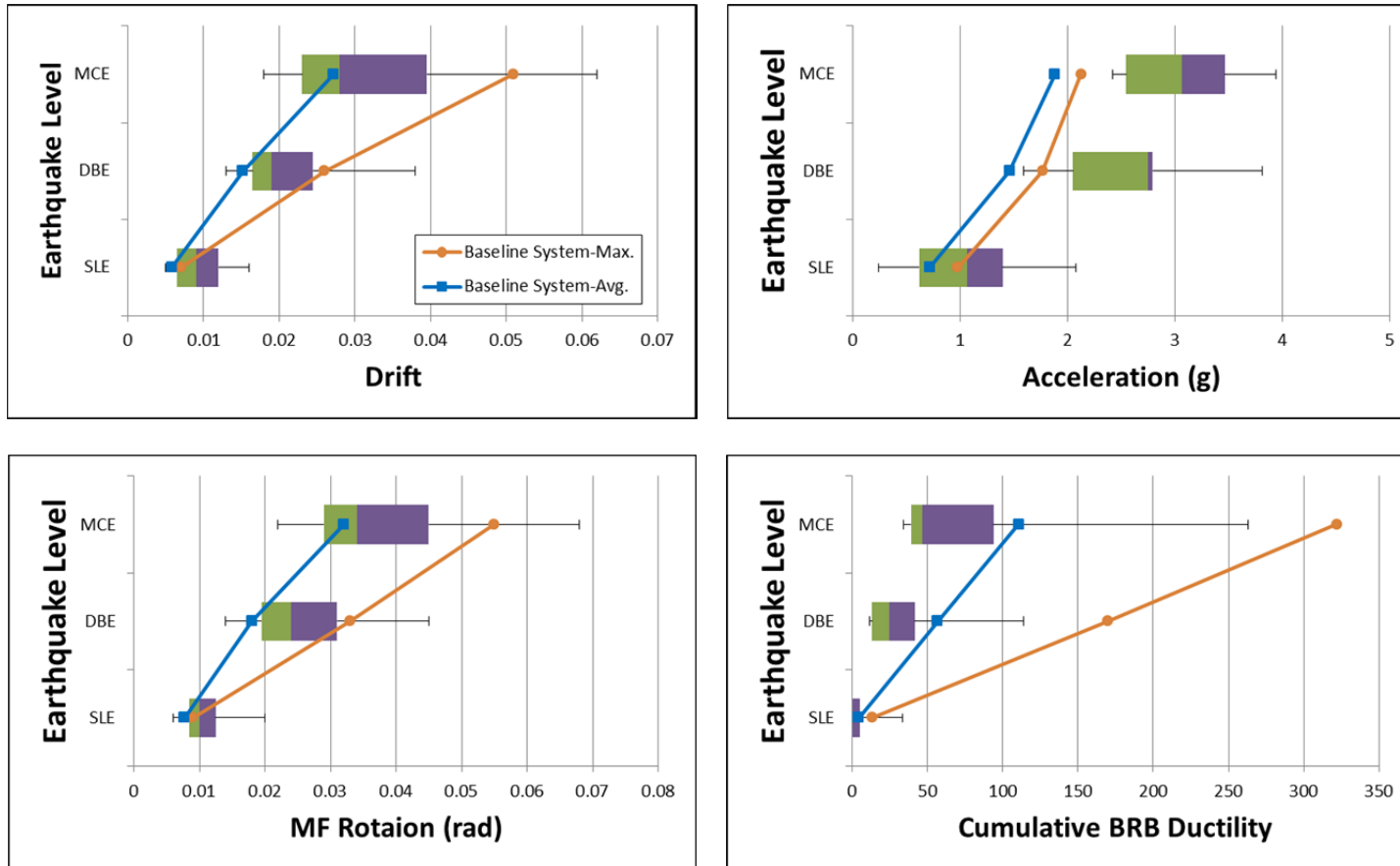


Figure B-4: 3-Story_60M40B_Gap0.45% with Baseline System

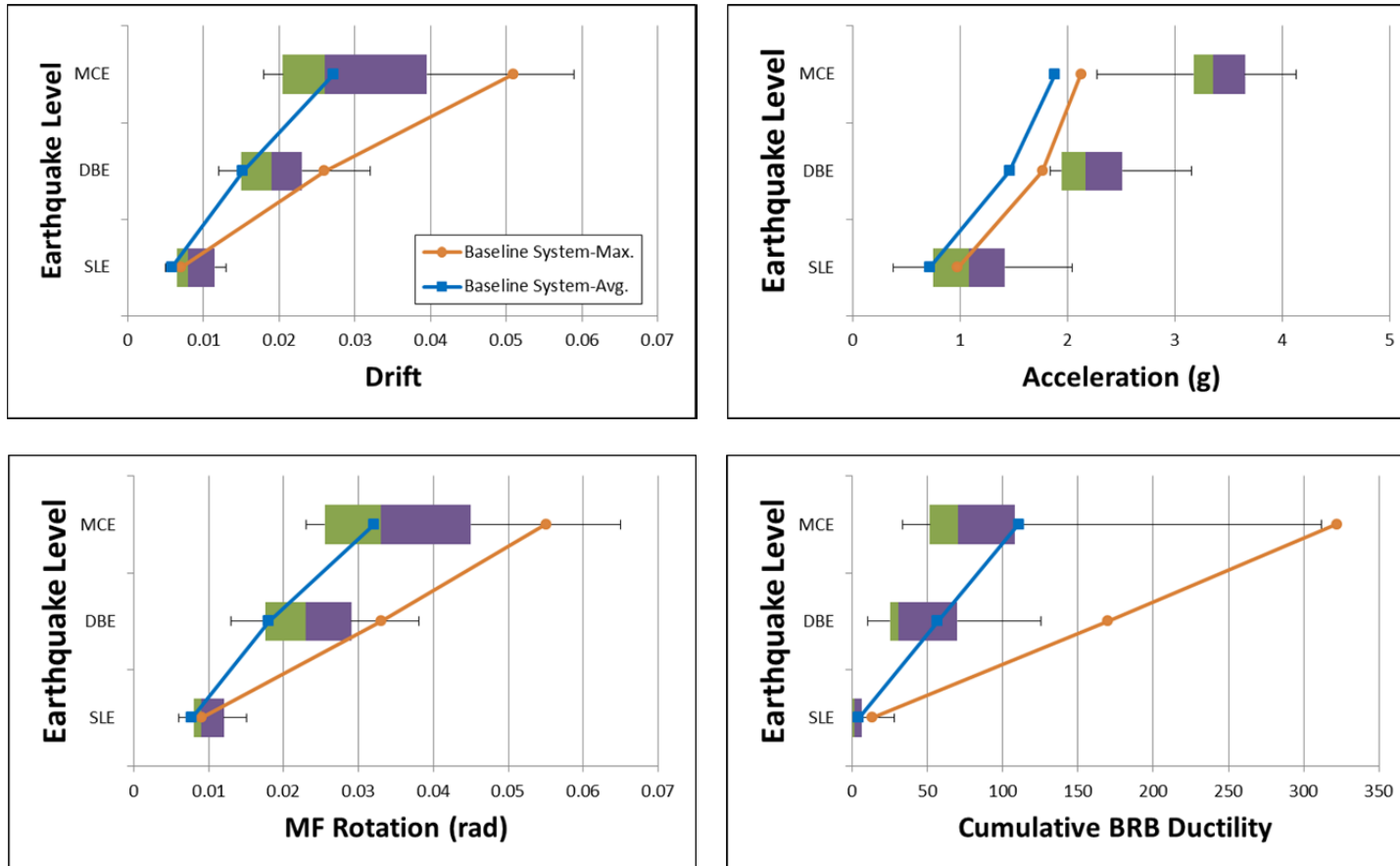


Figure B-5: 3-Story_60M40B_Gap0.30% with Baseline System

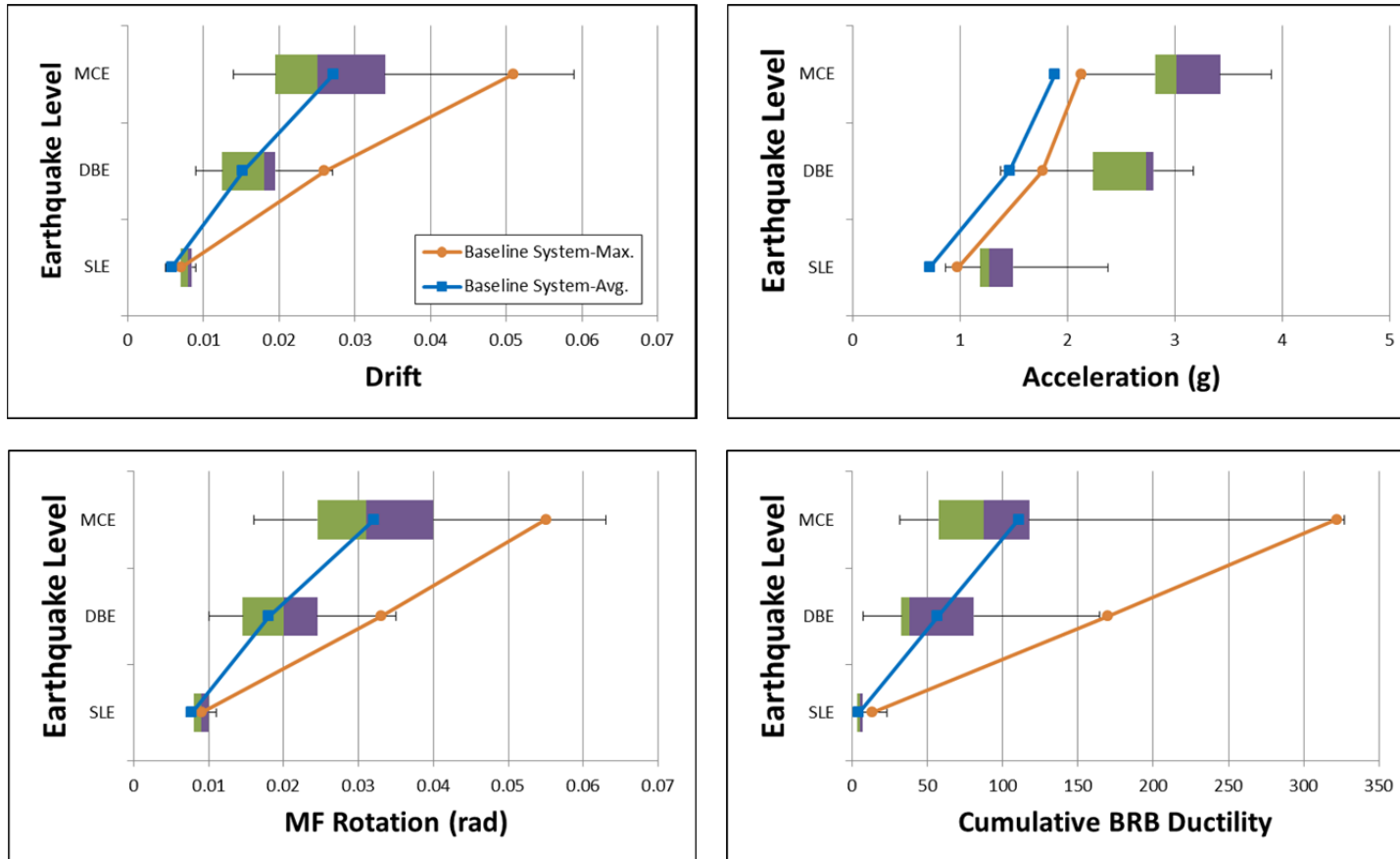


Figure B-6: 3-Story_60M40B_Gap0.15% with Baseline System

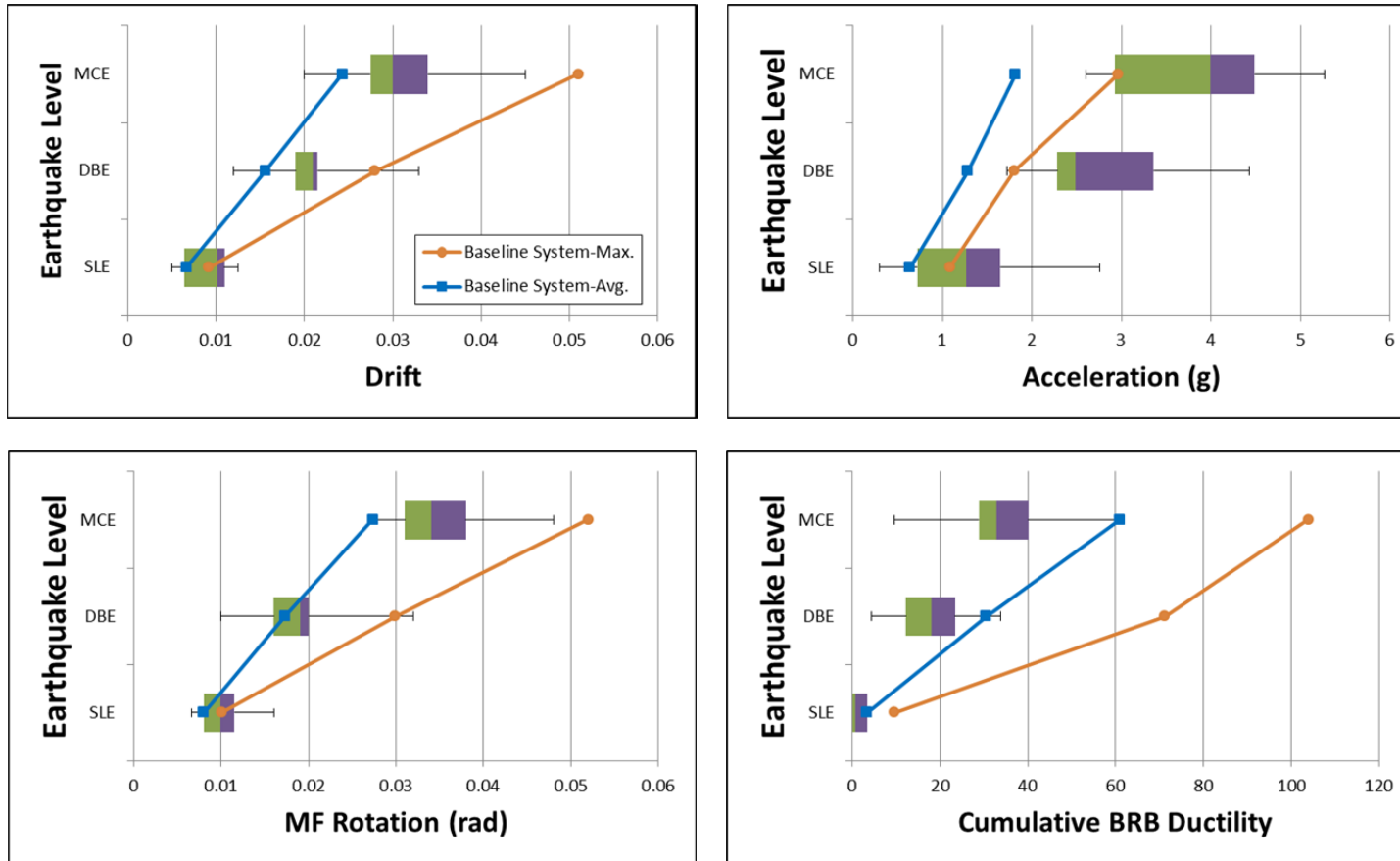


Figure B-7: 6-Story_50M50B_Gap0.45% with Baseline System

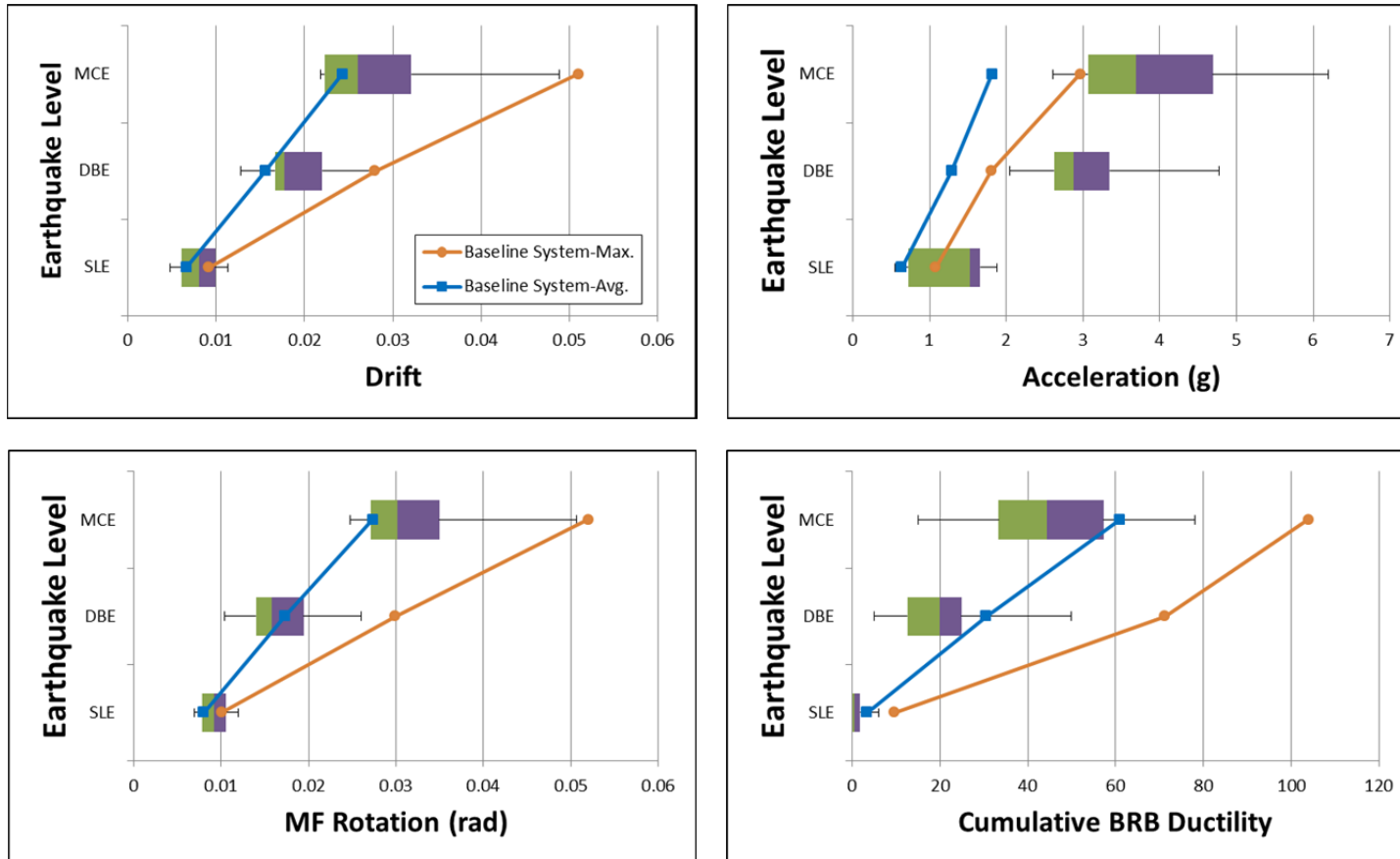


Figure B-8: 6-Story_50M50B_Gap0.30% with Baseline System

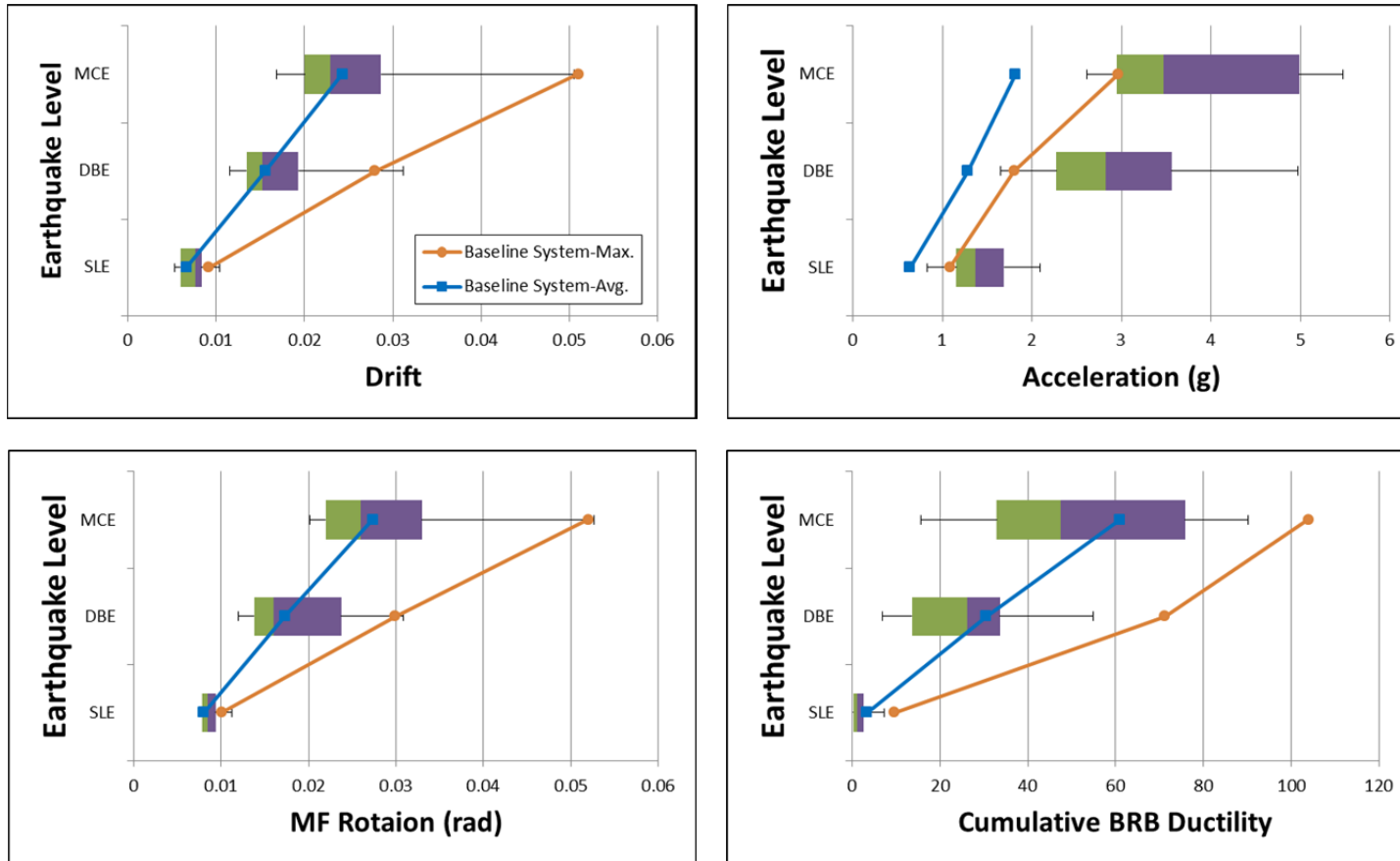


Figure B-9: 6-Story_50M50B_Gap0.15% with Baseline System

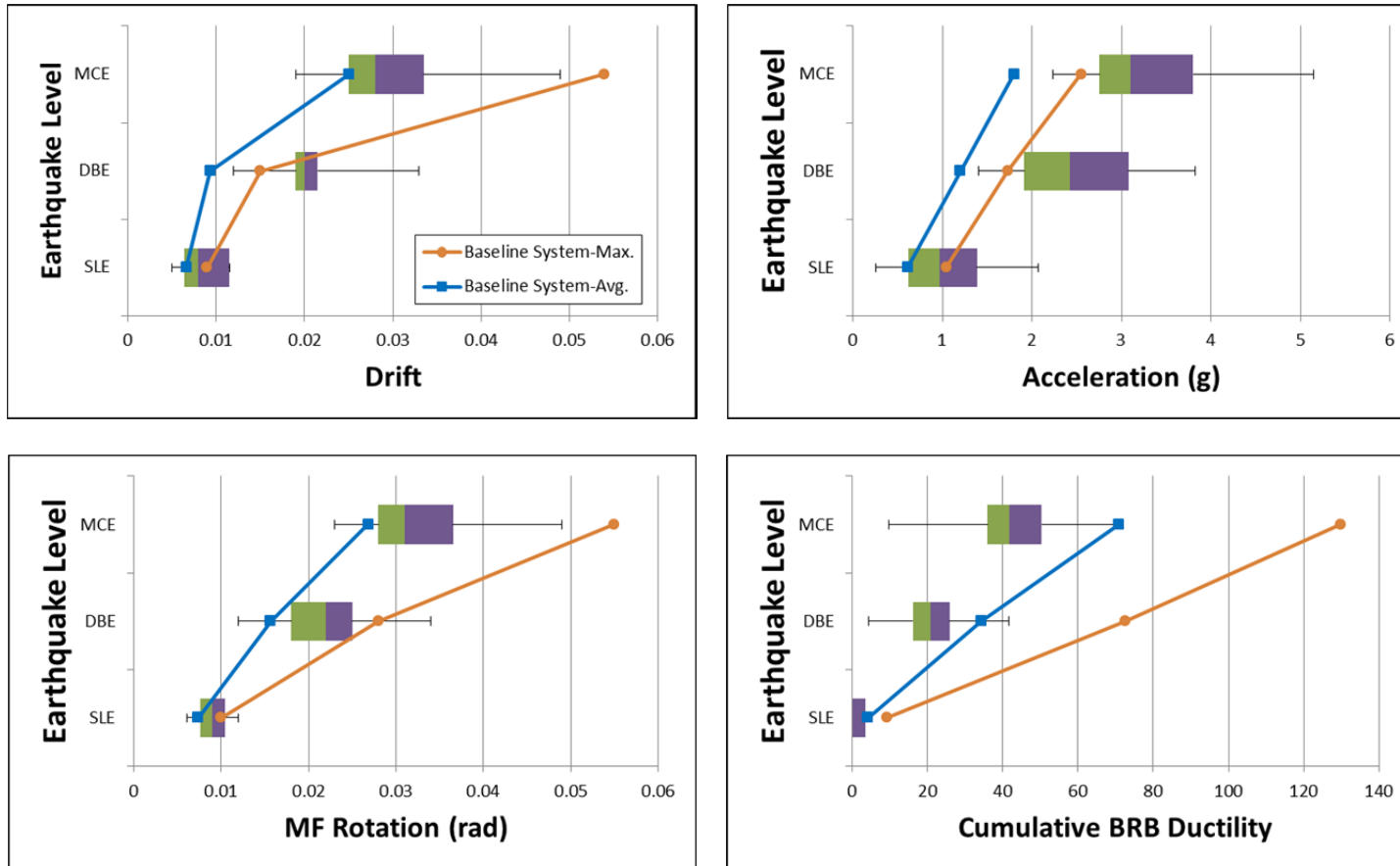


Figure B-10: 6-Story_60M40B_Gap0.45% with Baseline System

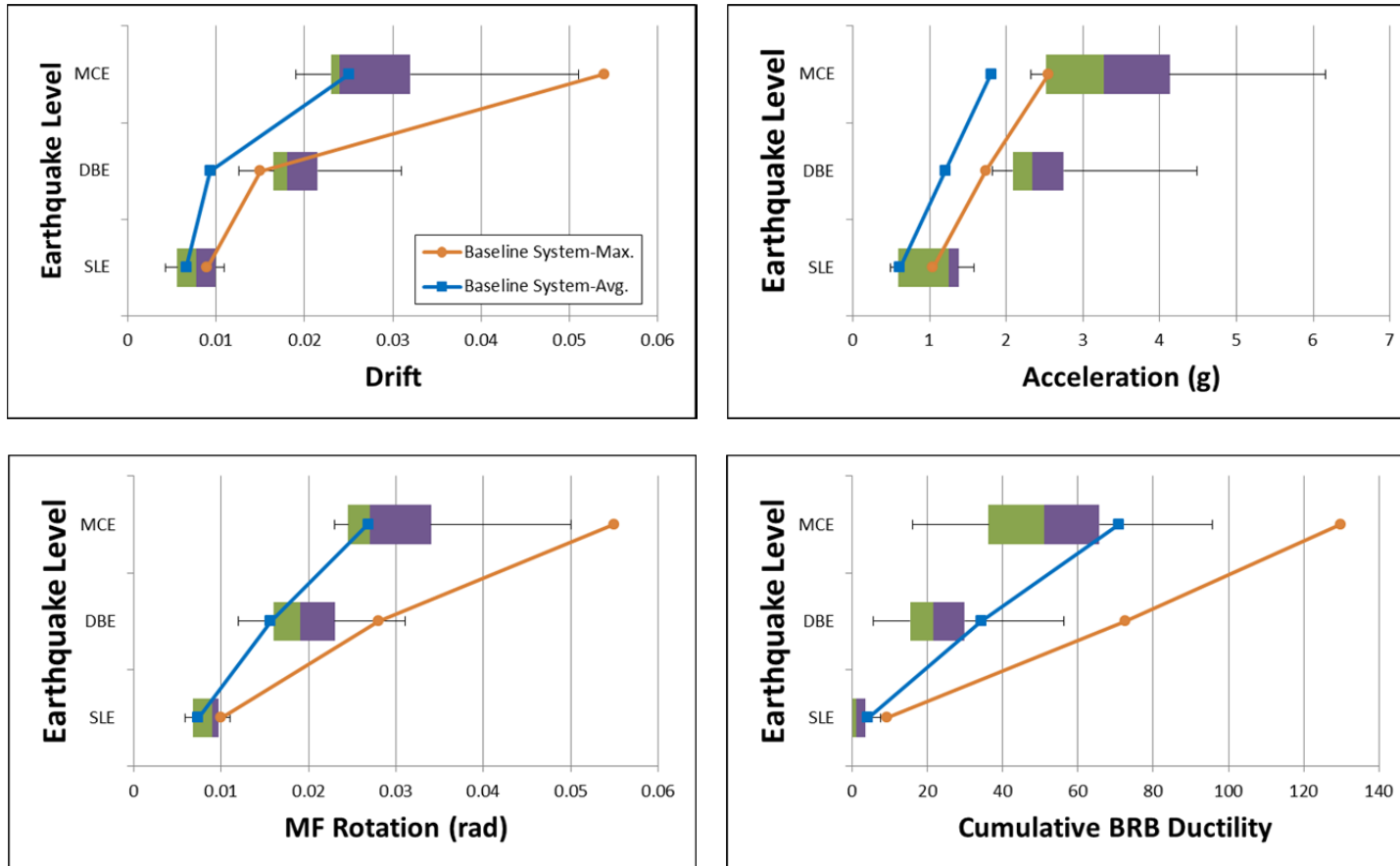


Figure B-11: 6-Story_60M40B_Gap0.30% with Baseline System

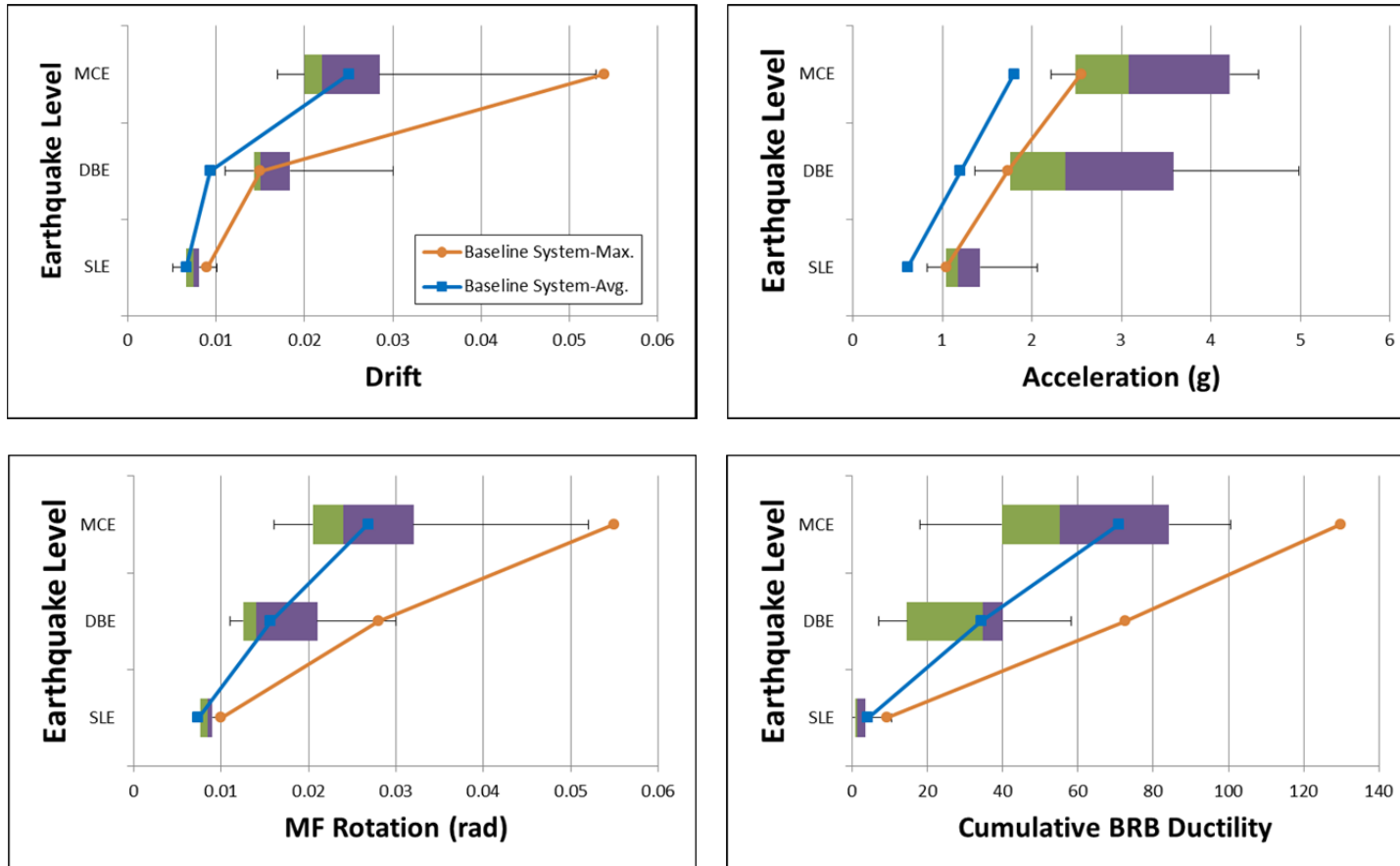


Figure B-12: 6-Story_60M40B_Gap0.15% with Baseline System